INVESTIGATION OF DEGRADATION OF NBR AND HNBR ELASTOMERS BY LIGHT SCATTERING RHEOLOGY AND MOLECULAR DYNAMICS TECHNIQUES

BY

Rehan Anwar Chaudry

A Thesis Presented to the

DEANSHIP OF GRADUATE STUDIES

KING FAHD UNIVERSITY OF PETROLEUM & MINERALS

DHAHRAN, SAUDI ARABIA

In Partial Fulfillment of the
Requirements for the Degree of

MASTER OF SCIENCE

In

CHEMICAL ENGINEERING

December, 2003

KING FAHD UNIVERSITY OF PETROLEUM & MINERALS

DHAHRAN 31261, SAUDI ARABIA

DEANSHIP OF GRADUATE STUDIES

This thesis, written by **REHAN ANWAR CHAUDRY** under the direction of his thesis advisor and approved by his thesis committee, has been presented to and accepted by the Dean of Graduate Studies, in partial fulfillment of the requirements for the degree of MASTER OF SCIENCE IN CHEMICAL ENGINEERING.

Thesis Committee

Dr. Basel Abu Sharkh
(Thesis Advisor)

Dr. Ibnelwaleed A. Hussein
(Co-Advisor)

Dr. Ramazan Kahraman
(Member)

Dr. Usamah A. Al-Mubaiyedh
(Member)

Dr. Mohamed B. Amin
(Member)

Prof. Mohamed B. Amin
(Department Chairman)

Prof. Osama Ahmed Jannadi
(Dean of Graduate Studies)

17-03-2004

Date

DEDICATION

To My Great Grandmother

ACKNOWLEDGEMENTS

I am extremely grateful to Almighty Allah who alone made this accomplishment possible. Research is basically unveiling the mysteries of the universe by trying to understand the laws of nature as set by the Creator.

I would like to express my gratitude to my thesis advisor Dr. Basel Abu Sharkh for his constant help and inspirational guidance, throughout this work. Working with him was indeed a wonderful and learning experience. I am also very indebted to my thesis co-advisor Dr. Ibnelwaleed A Hussein for his tremendous help. His continuous encouragement and numerous discussions helped enormously during experimental part and thesis writeup. My deep thanks are offered to my thesis committee members Dr. Ramazan Kahraman, Dr Dr. Usamah A. Al-Mubaiyedh and Dr. Mohamed B. Amin for their contribution and their critical review of this thesis.

I am thankful to the chairman of the Chemical Engineering Department, Dr. Mohamed B. Amin for all the facilities and cooperation extended to me during my stay. Many thanks to the staff members, especially Mr. Riyasat for whose kind personality, and timely advices, I,ll remain thankful for ever. I would also like to thank all my collegues and friends especially Mr Tayeb Hamid whom I owe a lot.

Finally, I am grateful to my parents and all family members for their extreme moral support, encouragement and patience during the course of my studies here.

TABLE OF CONTENTS

LIST OF TABLES

LIST OF FIGURES

THESIS ABSTRACT

Name: REHAN ANWAR CHAUDRY

Title: Investigation of Degradation of NBR and HNBR Elastomers by Light Scattering, Rheology and Molecular Dynamics Techniques

Degree: Master of Science

Major Field: Chemical Engineering

Date of Degree: December 2003

In this study, the Degradation and Miscibility of raw, uncured Nitrile Rubbers, (NBR & HNBR) has been investigated. The ACN (Acrylonitrile Content), Mooney Viscosity and % Hydrogenation are the primary criteria defining each specific brand of these rubbers. Degradation behavior as a function of these parameters was studied. The objective was to assess whether thermomechanical degradation of these rubbers is occurring during the "conditioning" process and if so, to characterize its nature and sort means to prevent it. It was found that thermomechanical treatment does affect these rubbers and that degradation is a combination of chain scission and cross-linking. Molecular parameters were found to effect selection of dominating degradation mechanism. Molecular weight measurements were carried out using light scattering technique. The rheological and light scattering results of the conditioned samples with and without antioxidants were compared to the properties of as received samples. Results were supported by variations in $\overline{M_w}$ *(weight-average molecular weight) by light scattering. FTIR was applied as an additional complementary Investigation technique to shed some light on the different functionalities generated during the "conditioning" process.*

The miscibility study of the two rubbers was performed using a variety of techniques such as rheology, DSC, SEM, Mechanical testing, and Molecular Dynamics. The different techniques agreed in suggesting that the structurally similar HNBR and NBR are mechanically compatible. Molecular Simulation studies showed that these rubbers are not only mechanically but thermodynamically compatible, however due to the nature of these materials segmental miscibility is hard to achieve by conventional methods.

Master of Science Degree

King Fahd University of Petroleum and Minerals

Dhahran, Saudi Arabia

December 2003

ملخص الرسالة

الإسم: ريحان أنور شودري

العنوان: دراسة تحلل مطاط النيتريل بيوتادايين باستخدام تشتت الضوء، الريولوجيا والمحاكاة الجزيئية

الدرجة: ماجستير في العلوم

التخصص: الهندسة الكيميائية

التاريخ: ديسمبر ٢٠٠٣م

في هذه الدراسة تم اختبار انحلال واندماج أنواع مختلفة من مطاط النيتريل بيوتادايين. العوامل التي تحدد نوعية المطاط تتمثل في كمية الأكريلونايترايل واللزوجة ونسبة الهيدرجة. كما تم دراسة تأثير هذه العوامل على عملية الإنحلال. هدف هذه الدراسة كان لتقييم ماإذا كان الإنحلال الثرموميكانيكي لهذا المطاط يحدث عند التحضير واذا كان كذلك فسيتم دراسة طبيعته والطرق المانعة لحدوثه. لقد وجد أن المعالجة الثرموميكانيكية تؤثر على خصائص المطاط كما ان الخصائص الجزيئية تؤثر على طريقة الإنحلال. تم عمل قياسات الأوزان الجزيئية بواسطة طريقة استطارة الضوء.

ولإتمام دراسة الاندماج استخدمت عدة طرق منها: الرويولوجيا و الكالوميتري و (المجهر الإلكتروني) والإختبارات الميكانيكية والديناميكية الجزيئية. كل الطرق اثبتت ان نوعي المطاط منسجمان ميكانيكيا بينما ان دراسات النمذجة الجزيئية اثبتت ان نوعي المطاط منسجمان ميكانيكيا وثرموديناميكيا.

Chapter 1

INTRODUCTION

1.1 Brief History of Polymers

Polymers have existed in natural form since life began and those such as DNA, RNA, proteins and polysaccharides play crucial roles in plant and animal life. From the earliest times man has exploited naturally occurring polymers as materials for providing clothing, decoration, shelter, tools, weapons, writing materials and other requirements. However, the origin of today's polymer industry commonly is accepted as being in the nineteenth century when important discoveries were made concerning the modification of certain natural polymers.

In 1820 Thomas Hancock discovered that when masticated (i.e. subjected to high shear forces repeatedly), natural rubber becomes more fluid, making it easier to blend with additives and to mould. Some years later, in 1839, Charles Goodyear found that the elastic properties of natural rubber could be improved, and its thickness eliminated, by heating with sulphur. Patents for this discovery were issued in 1844 to Goodyear, and slightly earlier to Hancock, who christened the process of vulcanisation. In 1851 Nelson Goodyear, Charles brother, patented the vulcanisation of natural rubber with large amounts of sulphur to produce a hard material more commonly known as hard rubber, ebonite or vulcanite. Polymer science is concerned with the composition and properties of

a large number of substances classed as 'Polymers', which include rubbers, Plastics and fibers.

1.2 Basic Definitions and Nomenclature

In strict terms, *polymer* is a *substance* composed of molecules which have long sequence of one or more species of atoms or groups of atoms linked to each other by primary, usually covalent bonds. The emphasis upon substance in this definition is to highlight that although the words polymer and *macromolecule* are used interchangeably, the latter strictly defines the molecules of which the former is composed.

Linking together monomer molecules through chemical reactions forms macromolecules, the process by which this is achieved is known as *polymerization*. For instance, cellulose is the basic fibrous material, which comprises wood, paper, cotton, linen, and other fibers. Chemists knew long ago that cellulose has the formula $C_6H_{10}O_5$, as shown by chemical analysis, yet their measurements did not indicate that the molecule of cellulose existed in the form shown by the formula. Instead they found evidence that cellulose molecule was unbelievably large. Hence they did not really believe it was a molecule, but considered the true molecule to be $C_6H_{10}O_5$, and that hundreds of such molecules were bunched together in aggregates.

Over 150 years ago, the formula for rubber was established as C_5H_8, but here again the evidence indicated that the molecule was much larger than shown by the formula. It was only as recently as 1920's that Staudinger advanced the revolutionary idea that the rubber molecule was indeed a giant molecule or *macromolecule*. Today it is generally accepted that the class of materials that form these fibers, plastics and rubbers are all composed of

such macromolecules. Hence the formula for cellulose, if it is to represent one molecule, should more accurately be written as $(C_6H_{10}O_5)_{2000}$, while rubber should be represented as $(C_5H_8)_{20,000}$.

1.3 Skeletal Structure and type of Polymers

The structure of Macromolecules is not limited to linear geometry represented by two ends, while this is true for macromolecules, there are also non linear structures of branched and network type. Branched Polymers have side chains, or branches, of significant length. These polymers are characterized by number and size of their branches. Network Polymer has three-dimensional structures in which each chain is connected to all others by a sequence of junction points and other chains. Such Polymers are said to be *crosslinked* and are characterized by their *crosslink density*, or degree of crosslinking. Variations in skeletal structure give rise to major differences in properties. Unlike linear and branched polymers, network polymers do not melt easily and will not dissolve in ordinary solvents, though they may swell considerably in compatible solvents. The importance of crosslink density has already been encountered in terms of vulcanisation (i.e. sulphur-crosslinking) of natural rubber. With low crosslink densities the product is a flexible elastomer, whereas it is a rigid material when the crosslink density is high.

Polymers can be classified on different basis. One being the type of monomer they are made of. On this basis two main divisions are *homopolymer* and *copolymers*, as evident from the name, the former one is type of polymer that is derived from one species of

monomer, or whose structure can be represented by multiple repetition of a single type of repeat unit.

The formal definition of a *copolymer* is, a polymer derived from more than one species of monomer or whose molecule contain two or more different type of repeat units. But the most common classification classifies them into three groups: *thermoplastics, elastomers* and *thermostes.* As our material falls in the category of elastomers, so we focus on that. *Elastomers* are crosslinked rubbery polymers (i.e. rubbery networks) that can be stretched easily to high extensions and which rapidly recover their original dimensions when the applied stress is released. This extremely important and useful property is a reflection of their molecular structure in which the network is of low crosslink density.

1.4. Rubbers

The main three structural requirements that are needed of a polymer before it can have elastomeric properties are listed below.

Polymer must be above its glass transition temperature, Tg

The polymer must have a very low degree of crystallinity ($\varnothing_c \rightarrow 0$).

The polymer should be lightly crosslinked.

Although many polymers have some of these characteristics there are only few, which display true elastomeric behavior. As discussed earlier that natural rubber (Polyisoprene) has a formula C_5H_8. Nearly 2000 species of trees, shrubs, or vines of the tropical and temperate regions produce latex from which natural rubber or a closely related substance can be obtained. It was introduced to the western world in early nineteenth century, but it

was not until 1839 when Charles Goodyear discovered the process of vulcanisation that a variety of rubber articles started to come into the market.

Although the polymerization of isoprene dates back over 100 years, all attempts to synthesize the exact structure of natural rubber were unsuccessful until the advent of the "stereospecific" catalyst during the decade of the 1950's. This was due to the fact that isoprene exists in four possible isomeric structures and one of which is cis-1, 4. Which means that carbon atom 1 and 4 are joined in forming the chain, and cis means that these carbon atoms 1 and 4 are both on the same side of double bond. It also turns out that natural rubber consists of polymer chains all having an almost perfect cis-1,4 structure, or in technical terms the polymer molecule was *stereoregular.* Development of *stereospecific* catalyst brought a revolution in the field of synthetic rubber development, and opened a window towards development of large number of synthetic elastomers. During the past 25 years a number of general and special purpose synthetic rubbers have been developed, mainly *Polybutadiene and Polyisoprene, Styrene-Butadiene, Ethylene-Propylene, Butyl* and *Halobutyl. Neoprene and Hypalon, Nitrile* and *Polyacrylic rubber*

Rubbers are complex materials; In general they exhibit a unique combination of physical properties whilst at the same time a virtually infinite number of vulcanized rubber compounds is possible, yielding a very wide range of properties. It differs very considerably from other engineering materials; for example it is the most highly deformable material, exhibiting virtually complete recovery, and it is virtually incompressible with a bulk modulus some thousand time greater than its shear or Young's modulus.

1.5 NBR & HNBR

Nitrile Rubber (NBR) is commonly considered the workhorse of the industrial and automotive rubber products industries. NBR is actually a complex family of unsaturated copolymers of acrylonitrile and butadiene. Nitrile elastomers offer a broad balance of low temperature, oil, fuel, and solvent resistance as related to *acrylonitrile content*. These characteristics, combined with their good abrasion and water-resistant qualities, make them suitable for use in a wide variety of applications with heat resistance requirements to 149° C. NBR materials can withstand all but the most severe automotive applications. On the industrial side NBR finds uses in roll covers, hydraulic hoses, conveyor belting, graphic arts, oil field packers and sealed for all kinds of plumbing and appliance applications.

Nitrile rubber is defined as a *copolymer* of a diene and an unsaturated nitrile. The majority of the nitrile elastomers produced today are copolymers of acrylonitrile and butadiene.

$$\underset{\text{Butadien}}{CH_2 = CH - CH = CH_2} \quad + \quad \underset{\text{Acrylonitrile}}{CH_2 = \underset{\displaystyle CN}{\underset{|}{CH}}}$$

$$\underset{\text{Copolymer unit}}{\left(CH_2 - CH = CH - CH_2 - CH_2 - \underset{\displaystyle CN}{\underset{|}{CH}}\right)_n}$$

The development of high performance special purpose elastomer has become increasingly important in recent years, because the environmental conditions in many industrial applications have become more severe and specification limits have been

tightened. The acrylonitrile content decides the ultimate properties of the nitrile rubber elastomer. In spite of possessing a favorable combination of physical properties, there has been a continuous demand to improve the aging resistance of NBR due to tougher requirements as fore mentioned.

HNBR: Hydrogenated nitrile rubber is the latest high –performance elastomer that has emerged as an important product since some past decades. The double bond present in the diene part of the elastomer is generally more susceptible to thermal and oxidative degradation. The selective hydrogenation of olefinic unsaturation in NBR imparts significant improvements in resistance to degradation, and other properties.

The principal driving force behind the development of HNBR is the increasing performance demanded of elastomer by the automotive and oil drilling industries. Even the conventional oil-resistant rubbers, namely nitrile rubber, chloroprene rubber, and chlorinated polyethylene are reaching their performance limits. Fluoroelastomers, which are the possible substitutes in these applications, are very expensive and possess processing difficulties. Hence HNBR has been developed to bridge the gap between general-purpose oil-resistant rubbers and fluoroelastomers. Typical applications include, hose beltings, cables, O-rings, seals, hoses, tubing, electrical jacketing, gaskets, shoe products, coated fabrics, flooring, adhesives, cements, PVC additive etc. Some typical uses are depicted in the figures.

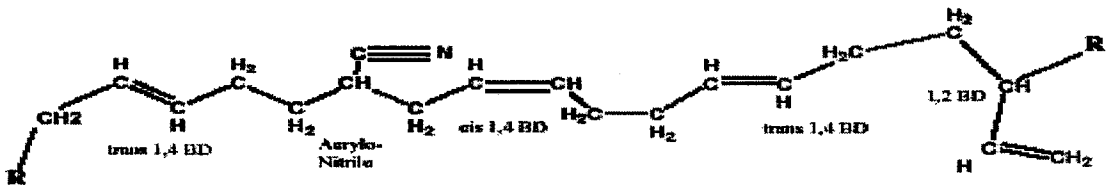

Figure (1.1) Structure of NBR

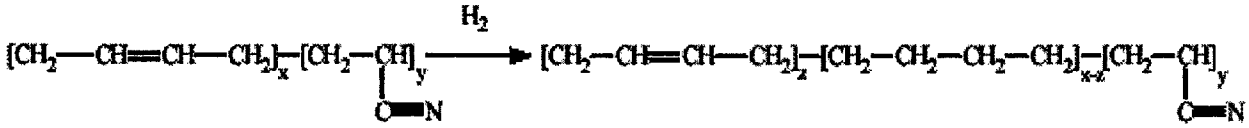

Figure (1.2) Hydrogenation of NBR

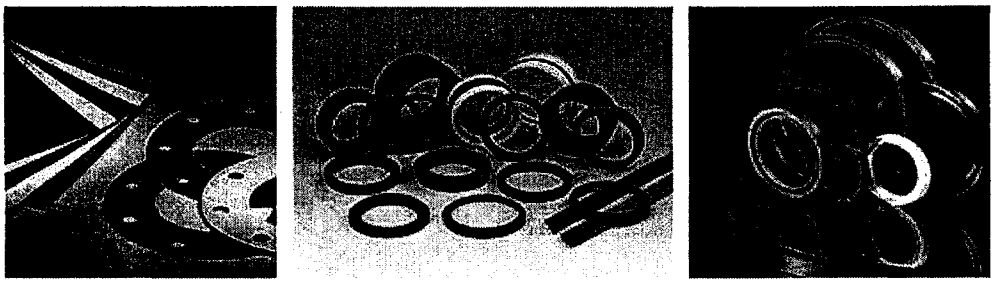

Figure (1.3) Typical finished rubber articles

1.6 Objectives and Scope of this Research

It is a well accepted fact that polymers are susceptible to attack by a wide variety of naturally occurring and man made agents. On this basis the degradation could be classified in to different types such as, organic solvent, moisture, Mechanical, thermal and biodegradation etc. This degradation will limit the lifetime of the material and could cause catastrophic failure. In some cases, degradation may be a desirable goal. For example, in designing plastic bottles or packaging material so that they rapidly degrade into environmentally safe by-products. In any case the study of the degradation is a study of prime importance in the life of a polymer. Elastomers as other polymers are processed above their softening temperature. These conditions such as high temperature, presence of oxygen, and substantial shear stresses can cause chemical reactions to occur, which is essentially the onset of degradation. The result of these chemical reactions is the build-up or breakdown of polymer chain that considerably influence the liquid and solid-state properties of the polymer. Hence, in all studies that involve melt conditioning (either in melt blender or in the extruder) care should be given to prevent degradation of polymer during the conditioning process. The objective of this study is to make sure that the degradation of these rubbers was prevented during the conditioning process.

The most common types of degradation occur through chemical reactions at the molecular level. Degradation resulting from various reactions with oxygen (especially at high temperatures) is the most important mechanism that influences the liquid and solid-state properties of the polymer. Even during processing in enclosed equipment, sufficient oxygen is still present for oxidation reactions to take place. Degradation by heat alone

(thermal degradation or thermolysis) is important, however, since in a restricted –oxygen atmosphere these reactions may take place simultaneously with thermal oxidation.

The existing literature reveals that the studies on degradation have been concentrated mostly on natural rubber, and the mechanism of degradation has demonstrated how it might be prevented. Although there have been studies made on thermal, mechanical, irradiative and other types of degradation concerning nitrile rubbers, but the literature was limited to rubber/rubber and rubber/plastic blends there has been no investigation on raw and uncured rubber. In the present study, HNBR has been degraded thermo mechanically in atmosphere of air, with or without oxidants. Effect of parameters such as ACN content, % Hydrogenation and Mooney Viscosity along with processing parameters (temperature, mixing speed) on degradation will be studied. The conditioned samples will be characterized mainly by Rheology and light scattering and will be compared with as received samples. Other techniques such as FTIR and SEM will be used to analyse the results to develop a better understanding of the mechanism.

NOTE: This thesis is written in "paper format". Hence, the reader can skip the initial three chapters and go directly to the results and discussion part given in chapter 4. the first paper is entitled " Influence of Molecular Parameters and Processing Conditions on the Degradation of Hydrogenated Nitrile Butadiene rubbers". The second paper is entitled "Study of Miscibility and Mechanical properties of NBR & HNBR blends". The third paper carries the title " Miscibility of NBR and HNBR rubber Blends: A molecular Dynamics Investigation".

Chapter 2

LITERATURE REVIEW

Extensive studies regarding nitrile rubbers have been found in the literature during past two decades. Stability of nitrile rubber and modified nitrile rubber has been investigated under different operating conditions and numerous techniques such as thermogravimetry, DSC, FTIR, SEM, Rheology and light scattering are employed for this purpose. However most of the studies on degradation have been made on rubber/rubber & rubber/plastic blends. Studies on degradation and its mechanism of pure raw rubber have been limited to natural rubber. Very few studies raised the question of degradation of raw, uncured Nitrile rubber.

Bhattacharjee et al [1990] studied the low temperature degradation of NBR and HNBR rubbers thermogravimetrically and found that the mol wt in case of NBR first increased and then decreased after prolonged aging. In case of HNBR it first decreased then there was in increase in mol wt. They attributed these results to the formation of carbonyl and carboxylic functionalities. ESCA studies on highly saturated rubbers showed that oxidation in HSN took place through -C≡N, which was converted to –C=NH.

A. K. Bhomick et al [1997] studied degradation of SBR (Styrene butadiene rubber) at high temperatures having different levels of unsaturation under anaerobic and aerobic conditions using thermogravimetry (TGA), DSC,IR and NMR spectroscopy. The

results were anomalous in nature in presence of air due to crosslinking and oxidation of rubber. Isothermal data, IR and NMR results revealed thermal isomerization, cyclization, oxidation, depolymerization and chain scission processes occurred during the course of degradation. Stephen et al (2002) characterized the aged nitrile rubber by NMR spectroscopy and proposed that measurements of relaxation time show that aging proceeds mainly via additional crosslinking. Scission (shortening) of the polymer chains does not appear to contribute much to aging.

Morgan studied the stability of different rubbers under operating conditions encountered in the oil industry (Morgan, 2000). Budrugeac (1995) studied the influence of air pressure on the mechanical degradation of NBR at different temperatures and found that higher air pressures accelerate the degradation process. The thermal degradation of a commercial, stabilized, unfilled nitrile (Buna-N) rubber material was investigated at temperatures in the range 85-140°C (Celina et al., 1998). The resulting heterogeneous oxidation, due to diffusion limitations in oxygen availability, was studied using infrared microscopy and modulus profiling. These chemical oxidation profiles (carbonyl formation) were correlated with mechanical modulus (hardness) profiles. Degradation of the sample was found to proceed via a linear increase in the carbonyl concentration, but an exponential increase in the modulus with time was observed. It is concluded that the profile development and aging behavior can be described by a diffusion-limited autoxidation mechanism, which can be modeled computationally. Thermomechanical degradation of nitrile rubber blends with other polymers has also been investigated. Manoj and De (1998) studied the self-crosslinking of poly (vinyl chloride)-nitrile rubber

blends during processing at elevated temperatures. The extent of the reaction depends on the blend composition, processing temperature, shear rates, fill factor and the presence of a PVC stabilizer. The reaction was found to involve hydrolysis of the nitrile group by HCl liberated during the degradation of PVC. Dynamic mechanical analysis (DMA) and solid-state NMR were used to investigate the changes in the structure and the morphology of the binary blends PVC/NBR and PVC/ENR, and the PVC/ENR/NBR ternary blend during thermal aging (Perera et al., 2000a&b). Samples were prepared by mechanical blending at 150°C. Thermal aging was carried out at 80°C for 7 days and at 140°C for 2 days. The effect of the change in the tan δ peak position, the tan δ peak width and the tan δ_{max} were used to understand the miscibility and damping properties. Solid-state ^{13}C NMR measurements were carried out using high power decoupling cross polarization and magic angle spinning. Observation of new peaks and changes in the peak widths were used to understand the possible degradation mechanism and changes of the dynamics due to these reactions. Proton relaxation times were interpreted based on the heterogeneity of the matrix. Results show that there is a change in the morphology during thermal aging at lower temperature. Budrugeac and Segal (1998) investigated thermoxidative degradation of NBR and estimated the activation energy of the reaction.

DSC was used to investigate the melting behavior for the binary blends. The crystallinity of the blends decreased with increase in NBR content. The thermal behavior of another blend; nitrile rubber (NBR)/poly (ethylene-co-vinyl acetate) (EVA) blends was studied by thermogravimetry (Varghese et al., 2001). The effects of blend ratio, different crosslinking systems (sulphur, peroxide and mixed), various fillers (silica, clay and carbon

black) and filler loading on the thermal properties were evaluated. It was found that the initial decomposition temperature increased with the addition of NBR to EVA. Among the various crosslinking systems studied, the peroxide cured system showed the highest initial decomposition temperature. This is associated with the high bond dissociation energy of C–C linkages. The addition of fillers improved the thermal stability of the blend. The thermal ageing of these blends was carried out at 50° and 100°C for 72 h. It was seen that the properties are not affected by the mild ageing condition.

Hydrogenated acrylonitrile-butadiene rubber (HNBR)/chlorosulfonated polyethylene (CSPE) blends were investigated (Giurgina and Zaharescu, 2000). The changes in crosslinking, chlorine and sulfur content and unsaturation were determined for three compositions (25:75, 50:50 and 75:25wt %). Thermal degradation was carried out over the temperature range from 150° up to 190°C; radiation exposure was performed at three irradiation doses: 100, 200 and 300 kGy. Mechanistic aspects of thermal and radiation ageing are pointed out. It was found that the high activation energy required during the thermal degradation of the studied polymer systems is a consequence of the interaction of mixed components.

Swapan Saha et al (1999) investigated the rheological and morphological characteristics of polychloroprene/PVC blends. The effect of temperature and mixing speed were studied. The results showed that there exited specific interaction between polar groups of PVC and PCP. This does not help in mixing and in forming a single phase. Temperature and rpm contribute to the formation and perfection of a PCP network structure. Grassie and Heaney (1974) showed that nitrile rubber in absence of air is

completely unchanged after 40 hours at 160 C. This work bears out the observations of Lee and Morell (1973) found that in gum and black vulcanizates of NBR, continuous stress relaxation was negligible at 150 C^{o} in the absence of air. It must be concluded that if nitrile vulcanizates could be completely protected from degradation by oxygen they would be long lived at temperatures of at least 160 C^{o}.

Takashi et al (1983) studied blends of PVC and poly Acrylonitrile-co-butadiene by x-ray diffraction, light scattering, DSC, and RTL (radiothermoluminescence) and concluded that the blends were two-phase systems. No evidence was found for molecular miscibility. The two-phase structure was maintained at temperature up to 150 C^{o}. K.H Lee (2000) studied physical properties and morphology of SAN/NBR blends as a function of AN content. They showed that the miscibility increased as the AN content in NBR was increased upto 50 wt %. Blend miscibility of HNBR was studied by J.L White and G.Severe (2000). The study indicated that the glass transition temperature behavior in HNBR was typical of ethylene copolymer. HNBR had tendency to crystallize in the outstretched and stretched state. HNBR had a Newtonian type viscosity at low shear rate and a non-Newtonian behavior at high shear rate.

A relationship between blending conditions and size of dispersed phase of NBR/ HNBR blends was studied by C. S. Sirisinha et al (2000). Rheology and DSC made the study. It was found that Mooney viscosity of the blends more depend on the blending time rather than rotor speed. It was observed the smaller the size of NR dispersed phase, the higher the blend resistance to oil. A.Y. Corn (1999) studied the parameters that affect the rheology of tire compounds. Effects of storage temperature and storage time on the

rheological properties of model tire compounds were characterized. Results of the work suggest that the filler particles and bound rubber domains form a network structure, which leads to an increase in peak start up stress and a drop of extrudate quality.

A. K. Bhowmick et al (1993) studied rheological behavior and processability of Neoprene and Acrylic rubbers. It was found that these systems show pseudoplastic flow behavior. C-M-Chan et al (1999) used NBR as a compatiblising agent for PVC/SBR rubber blends. A sulphur curing system was employed to cross link the rubber of the blends. A significant improvement in the mechanical properties was observed.

In short, extensive studies on the miscibility degradation of Nitrile rubbers and HNBR's blends have been made and very useful information has been drawn from these studies as aforementioned. However degradation study of NBR and HNBR raw and uncured rubber has remained a neglected issue and especially investigation under Thermomechanical conditions was not found extensively. Neither Rheology nor Dynamic laser light Scattering was found in the published literature by degradation point of view.

Chapter 3

EXPERIMENTAL TECHNIQUES

3.1 RHEOLOGY AND DEGRADATION

3.1.1 Introduction to Rheology

Rheology (from the Greek, *panta rhei = all things flows*) is the science of the deformation and flow of matter. Deformation is defined as the relative displacement of points in a body and it can be divided into two types:

1. *Flow* is the irreversible part of the deformation: when the stress is removed the material does not revert into its original configuration. Hence, work is converted into heat.

2. *Elasticity* is the reversible part of deformation: removing the stress the applied work is largely recovered and the body retains its original configuration.

Rheology embodies three main concepts such as *force*, *deformation* and *time*. Irreversible flows, reversible elastic deformations or their combination (viscoelasticity) can therefore model and describe a rheological phenomenon under certain assumptions.

Dynamic Mechanical Analysis (DMA) is a method that measures the stiffness and mechanical damping (i.e., the internal friction and thermal dissipation) of a cyclically deformed material as a function of time. The combination of stiffness and damping properties is a reflection of the unique viscoelastic nature of polymers. Or in other words term dynamic test is used to describe the type of mechanical test in which the rubber is subjected to a deformation pattern from which the cyclic stress/strain behavior is

calculated. The objective of the test is not to fatigue the rubber as those tests fall into a different category of tests. Dynamic properties are important in a large number of engineering applications of rubber including springs and dampers and are generally much more useful from design point of view than the results of many 'static' tests.

The dynamic tests are basically of two kinds depending on the type of dynamic motion. One is free vibration in which the test piece is set into oscillation and the amplitude is allowed to decay due to damping in the system. The other is forced vibration in which the oscillation is maintained by external means. These are illustrated in the figure. Elastomers are infect viscoelastic materials and hence their response to dynamic stressing is a combination of an elastic response and a viscous response, and energy is lost in each cycle. A simple model to represent this behavior is a spring and a dashpot in parallel for sinusoidal strain the motion is described by: $\gamma = \gamma_o \sin \omega t$

Where

$\gamma = strain$
$\gamma_o = \max imum\ strain\ amplitude$
$\omega = angular\ frequency, and$
$t = time$

If the rubber were a perfect spring the stress (τ) would be similarly sinusoidal and in phase with the strain. However because the rubber is a viscoelastic the stress will not be in phase with the strain but can be considered to precede it by the phase angle (δ) so that:

$$\tau = \tau_o \sin(\omega t + \delta) \qquad (3.1)$$

It is convenient to consider the stress as a vector having two components, one in phase with the displacement (τ') and one 90° out of phase(τ''). The sinusoidal motion is illustrated in the fig 3.1

The vector moduli in shear are defined by:

$$E^* = E' + iE'' \tag{3.2}$$

Where

$$E^* = complex\,(resul\tan t)\,\mathrm{mod}\,ulus$$
$$E' = in-phase\,or\,storage\,\mathrm{mod}\,ulus$$
$$E'' = out-of-phase\,or\,loss\,\mathrm{mod}\,ulus$$

Because of the dynamic nature of the test, material response is composed of two elements. The first the storage modulus, or elastic modulus, denoted as E' or G', is the in-phase portion of the response. It represents the purely elastic component of the material's behavior. Likewise, the out-of-phase component of the material's behavior is called the loss modulus, denoted as G". It represents the energy that is lost to viscous dissipation or internal friction between the molecules- that is, the portion of the viscoelastic response that dissipates energy like a viscous fluid. The ratio G"/ G' is the loss tangent (tan δ). The quantity G"/ω is called the dynamic viscosity, η'.

3.1.2 Rubber Rheology and Degradation

Dynamic mechanical analysis is a valuable technique for the rubber industry. It has been used extensively to solve numerous problems, such as understanding the mechanism of carbon black reinforcement, curing kinetics, aging characteristics, processability, and end use performance.

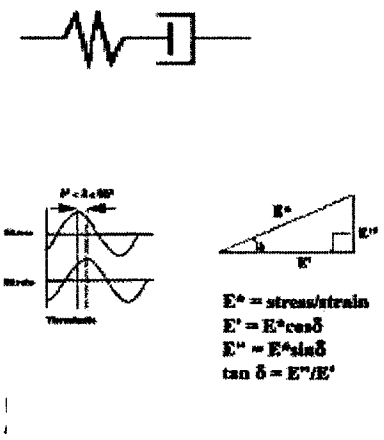

Figure (3.1) Maxwell model, Viscoelasticity and Complex Modulus

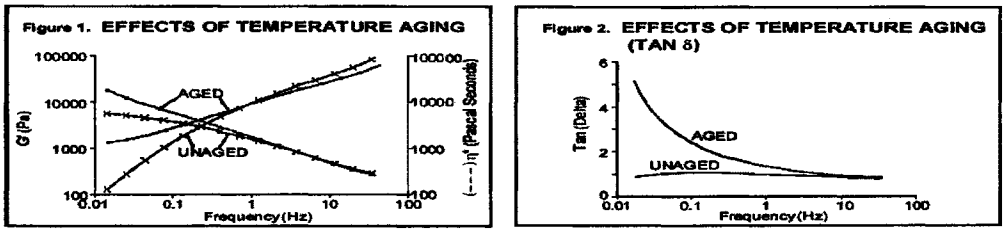

Figure (3.2) Effect of Temperature on Aging

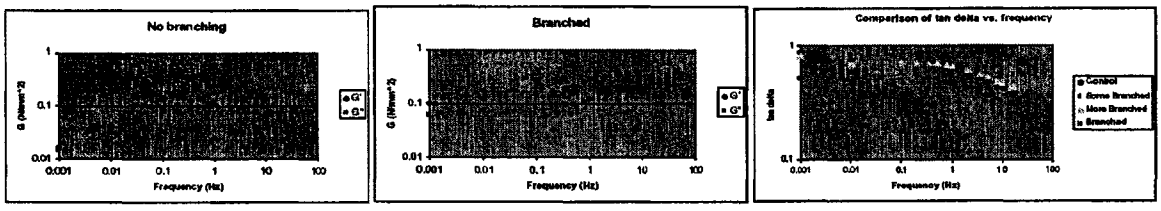

Figure (3.3) Sample Cole Cole Plot

The molecular weight, Mw distribution, and long chain branching of raw rubber can quickly and accurately are determined using dynamic mechanical analysis. This is accomplished by measuring its melt rheology as a function of frequency (range from 0.1 to 100 rad /s. samples about 1mm thick and 25mm in diameter are placed between two parallel plates. The sample is sinusoidally stained at a controlled frequency. A torque transducer measures the resulting sinusoidal force that is transmitted through the sample. These oscillations are analyzed by electronics. When the two waves superimpose the material is purely elastic; when they are displaced by 90° (which is called the phase angle) the material is purely viscous. Most materials are viscoelastic and have a phase angle between zero and 90°. In general rheological properties may vary with amplitude, rate, and temperature. Rheological parameters, such as complex viscosity (η^*). Storage modulus (G'), loss modulus (G") are measured simultaneously. They describe the viscosity, elasticity and damping of the material. The dependence of viscosity on frequency characterizes molecular weight and molecular weight distribution. Rheology has been employed in studying different phenomenon related to elastomers, such as compounding, molding curing and degradation. As mentioned earlier that rheological studies for degradation have been made for different materials including rubber/rubber and rubber/plastic blends. [Hussain and Willaimas, 2000] Hussain et al carried out more or less the similar investigation on Polyethylene's. A typical aging (degradation) study is shown in the figure 3.2. First figure illustrates the storage modulus ($G^{'}$) and complex viscosity (η^*) results for the two materials. The samples appear to be similar at the higher frequencies, which are not very sensitive to molecular structure. At the lower frequencies there is a divergence between the materials. The η^* value for the unaged (as received)

sample appears to be obtaining a plateau representative of its molecular weight. The η^* value for the aged sample continues to rise suggesting that the molecular weight has increased. The latter result may be due to cross-linking, which can occur during thermal treatment. The differences in G' values are consistent with the η^* results. The second figure provides information on tan delta (ratio of G" the loss modulus, to G'). These results show that a structural change could result in a non-homogeneous melt and eventually result in poorly fabricated products. Similarly degradation would have influenced the branched content of the rubber. We can determine the level of branching in the uncured rubber. The compound with little or no branching exhibits a crossover of G' and G" when plotted s a function of frequency. There is no crossover in the data from the highly branched one as shown in the figure 3.3.

3.2 LIGHT SCATTERING

3.2.1 Light Scattering Methods

The scattering of light by small particles is a familiar phenomenon as, for example, the appearance of dust particles in a beam of light. Similarly if polymer molecules are dissolved in a solvent, the light scattered by the polymer far exceeds that scattered by the solvent, and it is an absolute measure of molecular weight.

The 1940s became a kind of "Golden Age" of polymer investigation. Bruno Zimm, Walter Stockmayer, Peter Debye and others played large roles in creating characterization apparatus as well as novel polymers as the supplies of natural rubber were cut off due to Second World War. Because these new synthetic elastomers depended

heavily on their molecular weight distribution to give them the rheological properties that were desired, light scattering instrument were invented to determine the molar masses. The weight-average molecular weight can be obtained directly only by light scattering experiments. The most commonly used technique is light scattering from dilute polymer solution. Light scattering is classified into two types, Static and Dynamic Light scattering also known as Quasi Elastic Light Scattering (QELS).

3.2.2 Static Light Scattering and determination of Molar mass and size.

Light scattering provides the absolute molecular weight and size (radius of gyration $<s^2>$) of macromolecules in solution. The amount of light scattered is directly proportional to the product of the weight-average molar mass and the concentration of the macromolecule

Based on Zimm's formalism, the Rayleigh-Debye-Gans light scattering model for dilute polymer solutions can be expressed as

$$\frac{K^* c}{R(\theta)} = \frac{1}{\overline{M}_w P(\theta)} + 2A_2 c + \ldots \qquad (3.3)$$

Where:

$R(\theta)$ is the excess intensity of scattered light at angle Q

c is the sample concentration

$\overline{M}_w$ is the weight-average molecular weight (molar mass)

A_2 is a second viral coefficient

K* is an optical parameter equal to $\frac{4\pi^2 n_\circ^2}{N_A \lambda^4}\left[\frac{dn}{dc}\right]^2$

n is the solvent refractive index and dn/dc is the refractive index increment

N_A is Avogadro's number

$\lambda_\circ$ is the wavelength of the scattered light in vacuum.

The term $R(\theta)$ is called Rayleigh ratio, which is defined as

$$R(\theta) = \frac{i(\theta) r^2}{I_\circ V} \tag{3.4}$$

In this equation, Io is the intensity of the incident light beam and $i(\theta)$ is the intensity of the scattered light measured at a distance of r from the scattered volume. The parameter $P(\theta)$ appearing in the main equation is called the particle scattering function, which incorporates the effect of chain size and conformation on the angular dependence of the scattered light intensity. Debye showed that the functional form of $P(\theta)$ depends upon the shape of the scatterers and derived the following expression for monodisperse Gaussian coils.

$$P(\theta) = \frac{2}{v^2}\left[v - 1 + e^{-v}\right] \tag{3.5}$$

where $v^2 = q^2\langle s^2 \rangle$ in which $\langle s^2 \rangle$ is the mean-square radius of gyration of the coil and q is the scattering vector, which for dilute solutions is given by

$$q = \frac{4\pi n_\circ \sin(\theta/2)}{\lambda} \qquad \text{and} \qquad \langle s^2 \rangle = \frac{\langle r^2 \rangle}{6}$$

Basic instrumentation for light-scattering measurements is illustrated in the fig. Light from a high intensity mercury lamp (or laser) is polarized and filtered before passing through a glass sample cell that contains a filtered, dilute polymer solution. Scattered light intensity at an angle θ is recorded as a signal from a movable high-voltage photomultiplier tube. Alternatively multiple detectors can be located at several fixed location.

Eq. 3.3 is the basis of the calculation for most of the light scattering instruments. The equation assumes vertically polarized incident light. The task is now to determine, the molar mass and mean square radius. It is possible to solve the Eq 3.3 in a variety of ways, leading to a number of different fit methods. However we shall consider Zimm fit method, as that will be used in our further study.

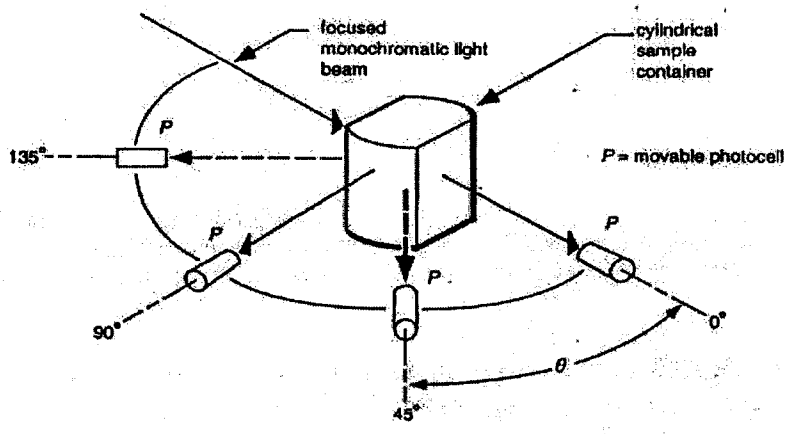

Figure 3.4 Principle of Light Scattering machine

3.2.3 ZIMM Method

To perform calculations with the Zimm fit method, which is a fit to $K^*c/R(\theta)$ vs $\sin^2(\theta/2)$, we need to expand the reciprocal of our main eq, to first order in c. in this method $\overline{M}_w$ is obtained by means of *Zimm Plot*. Zimm plots require tedious measurements of scattered light intensity at many angles, then a double extrapolation to both zero concentration and zero angle is used to obtain information concerning molecular weight and second-virial coefficient.

In the limit of small angles where $P(\theta)$ approaches unity, it can be shown by means of a series expansion of $1/P(\theta)$, then Eq 3.3 becomes

$$\boxed{\frac{Kc}{R(\theta)} = \frac{1}{M_w}\left[1 + \frac{16}{3}\left(\frac{\pi n}{\lambda}\right)^2 \langle s^2 \rangle \sin^2\left(\frac{\theta}{2}\right)\right] + 2A_2 c} \qquad (3.6)$$

Plots of $Kc/R(\theta)$ versus $\langle s^2 \rangle \sin^2(\theta/2)$ for different angles and concentrations are shown in the figure. The term k in the abscissa is an arbitrary constant that is added to provide spacing between each curve. A double extrapolation to $\theta = 0^\circ$ and c = 0, for which the second and third term in the above equation become zero yields $\overline{M}_w$ as the reciprocal of the intercept.

In recent years, helium- neon (He-Ne) lasers ($\lambda = 6328\,A^\circ$) have replaced conventional light-sources in some commercial light scattering instruments. The high intensity of these light sources permits scattering measurements at much smaller angles

(2o to 10o) than possible with conventional light sources. A Typical Zimm plot is shown in Figure 3.5.

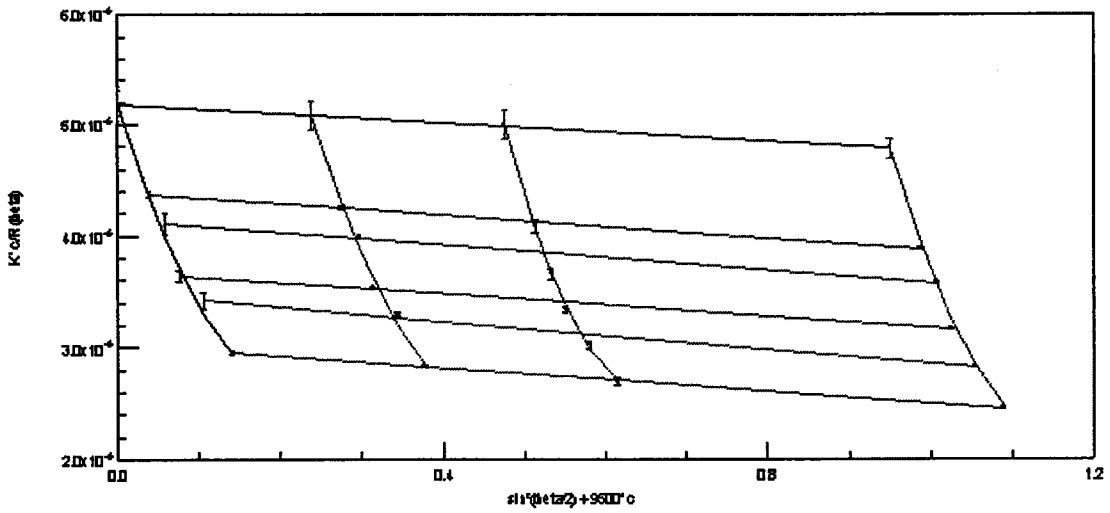

Figure (3.5) Typical Zimm Plot

3.2.4 Quasi Elastic Light Scattering (QELS)

The Brownian movement is the random motion of large particles due to the collision with relatively small ones. Macromolecules in solution experience the same motion. The result is a random motion caused by the constant collision of solvent molecules from all sides. When the light scatters from these moving molecules, this imparts randomness to the phase of the scattered light. Now a comparison of the scattered light from two or more particles is added together, there will be a changing destructive or constructive interference. This leads to time-dependent fluctuations in the intensity of the scattered light.

In a QELS experiment, the time averaged fluctuations in the scattered light are measured by a fast proton counter. These fluctuations in scattered light are directly proportional to the rate of diffusion of the molecule through the solvent and can be analyzed to determine a quantity called hydrodynamic radius for the sample. The QELS data is in the form of Correlation function, as these fluctuations are quantified via a second order correlation function given by

$$g^2(\tau) = \frac{\langle I_{(t)} I_{(t+\tau)} \rangle}{\langle I_{(t)} \rangle^2} \tag{3.7}$$

where $I(t)$ is the intensity of the scattered light at time t, and the brackets indicate averaging over all t. The correlation function depends on the delay τ, that is, the amount that a duplicate intensity trace is shifted from the original before the averaging is performed, is also called as the shift time.

3.2.5. Hydrodynamic Radius (R_H)

By definition then, the DLS measured radius is the radius of a hypothetical hard sphere that diffuses with the same speed as the particle under examination. Analysis of the correlation function yields the hydrodynamic radius. In dynamic light scattering experiments, the radius (R) of the particle is calculated from the diffusion coefficient (D) via the Stokes-Einstein equation, given by

$$D = \frac{kT}{f} = \frac{kT}{6\pi\eta R} \tag{3.8}$$

Where k is the Boltzmann constant, T is the temperature, η is the solvent viscosity and $f = 6\pi\eta R$ is the frictional coefficient for a compact sphere in a viscous medium. Now By definition then, the DLS measured radius is the radius of a hypothetical hard sphere

that diffuses with the same speed as the particle under examination, since hypothetical hard spheres are non-existent. In practice, macromolecules in solution are non-spherical, dynamic (tumbling), and solvated. As such, the radius calculated from the diffusional properties of the particle is indicative of the apparent size of the dynamic hydrated/solvated particle. Hence the terminology, 'hydrodynamic' radius.

3.2.6 Correlation Curve

Dynamic Light Scattering (DLS), also known as Photon Correlation Spectroscopy (PCS), is concerned with the investigation of correlation of photons. In a typical light scattering experiment, single photons are detected with a single photon counting device. This detector converts the signal from a single photon into an electronic signal, basically a '1' or a '0', depending on whether a photon was detected or not, in a certain time interval. The objective of PCS is to find any peculiar properties of the scattered signal that can be used to characterize and describe the seemingly random "noise" of the signal, and the correlation curve is used to achieve this objective. A typical way to describe a signal is by way of its 'autocorrelation'. The autocorrelation function of the signal from the scattered intensity is the convolution of the intensity signal as a function of time with itself. In more abstract terms, if the detected intensity is described as a function I(t), then the autocorrelation function of this signal is given by the following expression, where τ is the shift time.

$$G(\tau) = \int I_{(t)} . I_{(t+\tau)} dt \qquad (3.8)$$

The above function is also called the intensity correlation function, and it is used to describe the correlation between the scattering intensities measured at t = 0 and some later time ($t_n = t_0 + \tau$).

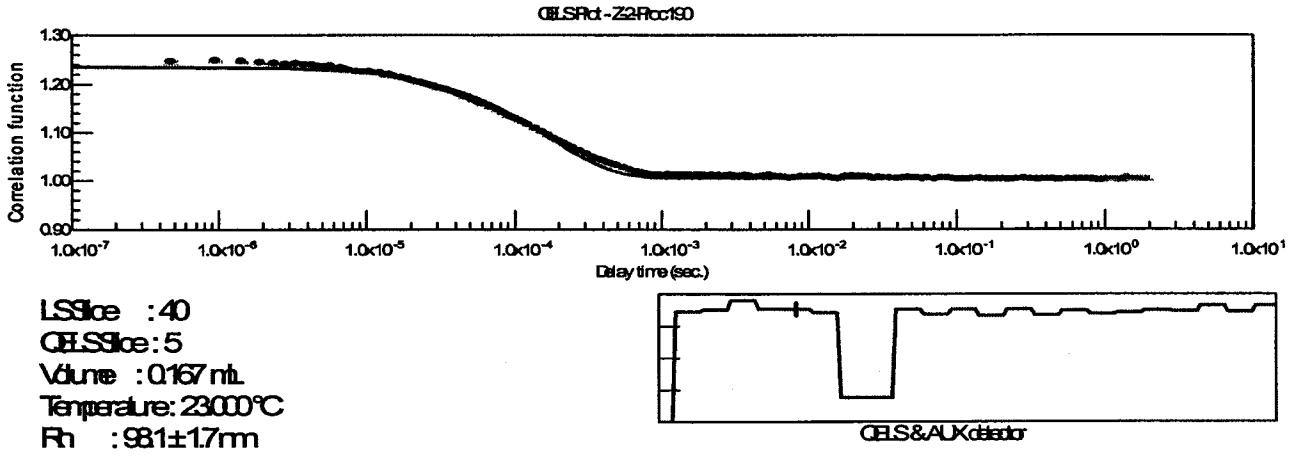

Figure (3.6) Typical Correlation Function

3.3 MOLECULAR SIMULATION

3.3.1 Introduction to Molecular Chemistry

Computational chemistry is relatively a new discipline. Its advent and popularity have paralleled improvements in computing power during the last several decades. As with other disciplines in chemistry, computational chemistry uses tools to understand chemical reactions and processes. Scientists use computer software to gain insight into chemical processes. Although computational chemists frequently develop and refine

software tools, their primary interest is in applying software tools to enhance chemical knowledge.

The challenges for computational chemistry are to characterize and predict the structure and stability of chemical systems, to estimate energy differences between different states, and to explain reaction pathways and mechanisms at the atomic level. Meeting these challenges could eliminate time-consuming experiments. Software tools for computational chemistry are often based on empirical information.

Further, the computer-aided chemistry approach often provides new insights into the mechanism of thermal decomposition and formation of breakdown products that are unavailable by experimental techniques. This ability to explore the relationship between a molecule's structure and its chemical and physical properties allows for a more systematic approach to the design of new polymers and processes.

With the advent of modern experimental techniques, researchers have been able to draw more and more information of systems at molecular level. The most important information of a molecular system in statistical mechanics is its energy levels. Once energy levels and distributions are known, the total energy of the system can be calculated using statistical mechanical theories. This, in turn, can be used to derive many thermodynamic properties. The total energy of a molecular system (including kinetic and potential energies of the motions and interactions of the molecules) is referred to as the internal energy of the system. Individual molecular velocities determine the kinetic energy. Contrary to the kinetic energy, potential energy is not a property of a single molecule; rather, it is a property of the collection of molecules representing the whole system. Molecules interact with each other and the molecular interaction gives rise to

most of the important macroscopic behavior, like phase equilibrium. The knowledge of molecular interactions is the key to understanding of the quantitative thermodynamic behavior of a real system.

Usually, the principal theory behind any computational chemistry software is the concept of a potential energy surface and the distinction between classical and quantum energies, kinetic and potential energies, energies of electrons versus energies of nuclei, etc. A potential energy surface is simply a specification of the classical potential energy, V, as a function of molecular structure. For example, the potential surface (in this case a potential curve) for a diatomic molecule is sketched qualitatively in the following illustration. The potential energy curve shows the potential energy of the molecule as a function of the internuclear distance R. Now, in fact, there are six degrees of freedom on which the energy might depend—for instance the X, Y, and Z coordinates of each of the two atoms. However, five of these degrees of freedom correspond to translations (3) and

rotations (2) of the rigid molecule and do not affect the energy of the system. This leaves only the internuclear distance as the variable upon which the potential energy depends as shown in the figure 3.7.

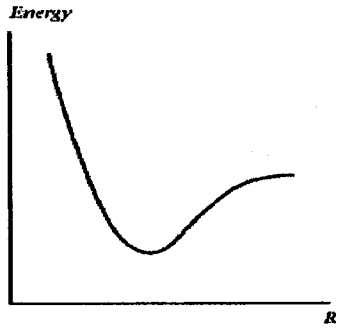

Figure (3.7) Potential Energy Curve

The semi-empirical methods of computational are quantum mechanical methods that can describe the breaking and formation of chemical bonds, as well as provide information about the distribution of electrons in the system. For example the possible energy states of a molecular system can be calculated from the solution of the Schrodinger wave equation, i.e., so-called "ab initio" calculation in quantum mechanics. However, these kinds of solutions are rarely available or practical for a real system. Thus, in order to get molecular information (microstate energies) of a system, one needs a molecular model or molecular theory. The molecular model provides us necessary equivalent information representing the real system. Once the model is set up, one can use statistical thermodynamics to relate the thermodynamic properties with microstate information through statistical mechanics ensemble theory. The molecular information about the systems is contained in the partition function that gives the energy distribution of a system. However, the microstate energy levels are usually not available for most systems except for very simple cases due to our inability to solve the Schrodinger equation. Most of the time, the energy levels are evaluated numerically through applied statistical thermodynamics. The calculation of thermodynamic properties within technical accuracy by molecular simulation becomes possible nowadays because of the availability of high-speed computers.

3.3.2. Geometry Optimizations

A geometry optimization samples single points on the potential surface, searching for a minimum. At a potential minimum, any small change in geometry causes the potential energy to rise. The technique used to search for the minimum is called the optimization algorithm, and several of these are available in the literature. Energy

minimization alters molecular geometry to lower the energy of the system, and yields a more stable conformation. As the minimization progresses, it searches for a molecular structure in which the energy does not change with infinitesimal changes in geometry. This means that the derivative of the energy with respect to all Cartesian coordinates, called the *gradient*, is near zero. This is known as a *stationary point* on the potential energy surface.

If small changes in geometric parameters raise the energy of the molecule, the conformation is relatively stable, and is referred to as a *minimum*. If the energy lowers by small changes in one or more dimensions, but not in all dimensions, it is a *saddle point*.

Unfortunately, there is no well-accepted theory that allows accurate evaluation of expressions for the thermodynamic properties in terms of an intermolecular force model for condensed state. The only available method for essentially accurate evaluation for that is provided by molecular simulation, based on a specific molecular model, i.e. force-field-based computer simulation.

3.3.3 Molecular Dynamics

Molecular dynamics involves the addition of kinetic energy to the above potential energy surface description and the subsequent motion of the molecular system over the potential surface. This motion follows the laws of classical mechanics according to Newton normally, the classical total energy (sum of kinetic energy and potential energy) is conserved and the motion is faster (larger kinetic energy) near minima in the potential surface (smaller potential energy). If a set of initial conditions is defined (initial velocities and a particular point on the potential surface), then Newton's laws cause the molecular

system to evolve along a path that is referred to as the molecular dynamics trajectory. This trajectory traverses the potential surface in ways that are of considerable interest to explore. Both the end point of a trajectory and the path taken to get there are of interest in molecular modeling.

3.4 FTIR SPECTROSCOPY

The Infra Red spectra arise from the molecular transitions between quantum states of differing internal energies. Frequency of the emitted or absorbed radiation is a direct measure of energy differences and is associated with molecular vibrations and rotations characteristics of a chemical group, e.g alkyl, carbonyl etc. Fourier Transform Infrared spectrophotometeric (FTIR) analyses were carried out in chemistry department for the determination of molecular structure of as received and the processed samples. As degradation is a destructive process, so a variety of new functionalities were expected to be generated during the course. FTIR was used to identify these functionalities. FTIR study was performed using FTIR 16FPC (Perkin Elmer). For this purpose very thin membranes of the rubber samples were prepared in the Carver Press and subsequently used in the spectrophotometer. The objective was to have a qualitative idea of different functionalities generated in the samples after the degradation.

3.5 DSC ANALYSIS

The thermal properties of the blends (NBR/HNBR) were measured calorimetrically. A TA Instruments DSC 2910 equipped with Thermal Analyst 2200

software was used for this purpose. A blanket of nitrogen was maintained. Samples from the Carver press were used in this study

3.6 MECHANICAL TESTING

For the tensile properties, of the blends (NBR/HNBR) dumbbell shaped specimens were stamped out according to ASTM standards. The tensile tests were performed in an Instron 5567 tensile testing machine at room temperature to investigate mechanical properties of the blends.

3.7 SEM STUDY

The degradation process being a destructive process will affect the morphology of the samples. Micrographs of the processed samples will reveal the extent of degradation

Chapter 4

RESULTS AND DISCUSSION

4.1 Influence of Molecular Parameters and Processing Conditions on the Degradation of Hydrogenated Nitrile Butadiene rubbers

4.1.1 ABSTRACT

Thermomechanical modification of hydrogenated nitrile butadiene rubbers (HNBR) of different molecular parameters was investigated by rheological Light scattering and FTIR techniques. The influences of acrylonitrile content, degrees of hydrogenation and Mooney viscosity were examined. A Haake melt blender with Banbury-type mixing blades was used to condition the as-received rubber samples in the temperature range from 190° to 260°C. The objective was to assess whether thermomechanical degradation of these uncured rubbers take place during the "conditioning" process, and if so to characterize its nature. Both the dynamic viscosity, η' and the storage modulus G', were measured for as-received and conditioned samples in an ARES rheometer. Experimental results showed that degradation in these rubbers occurred through chain scission and cross-linking. Depending on the molecular parameter, it was found that one of these two mechanisms dominated the degradation process in most brands. Addition of adequate amounts of antioxidant (Irganox 1010 and Irgafos 168) was only successful in preventing degradation by cross-linking. FTIR analysis used as a

qualitative technique, showed generation of carbonyl functionalities in the degraded samples. Light scattering results of change in molecular weight and size, resulting from processing were in agreement with rheological findings.

4.1.2 INTRODUCTION

Rubber articles are formed using conventional techniques such as injection molding, extrusion etc. The conditions at which the material is processed in these techniques, namely elevated temperature, presence of oxygen, closed environment and mechanical stresses can cause chemical changes to occur [1]. Even a small extent of reaction can have immense effects on the physical properties of the polymer. These chemical changes can cause "self-vulcanization" [2]. In the case of elastomers, the process of vulcanization is mandatory before the material could be shaped into products.

Structural modifications during processing of rubbers is a complex phenomenon that involves multiple reactions occurring at the same time, with individual mechanisms, such as, isomerization, cyclization, oxidation, cross-linking, chain scission etc[3]. On the molecular level, two competing processes dominate degradation: molecular scission, which results in shorter chains, and cross-linking, which gives a more tightly networked structure[4].

Nitrile elastomers, the materials investigated in our present study are produced by emulsion polymerization of butadiene rubber (BR) and acrylonitrile (ACN). The properties of the resulting elastomer are dependent on the acrylonitrile/butadiene ratio. A review of the structure of the elastomer points out that its structure is very complex [5]. The butadiene copolymerizes into three different structures: trans, cis and 1,2-. The trans

configuration dominates (~78%) in a typical sample. The cis configuration (~12%) serves to break up substantial crystallinity since it enters in a statistical pattern. The 1,2- sites (~10%) are free vinyl groups typically causing branching and often gel formation. The ACN groups are inserted in a statistical pattern ranging from head-tale, head-head, and tail-tail [5].

In copolymers of such nature, different parts of the copolymer should differ greatly in thermal stability. The double bond present in the diene part of the elastomer is generally more susceptible to thermal and oxidative degradation, and shows two stages of degradation [3]. Selective hydrogenation of this olefinic unsaturation in NBR imparts significant improvements in resistance to degradation and other properties [6,7]. The ACN content ultimately determines the resistive nature of a typical brand and usually an increase in ACN content results in an increase in oil, fuel, abrasion, and heat resistance as well as an increase in hardness and tensile strength [7]. Extensive studies regarding nitrile butadiene rubber (NBR) are available in the literature where stabilities of NBR and hydrogenated NBR (HNBR) have been investigated under different operating conditions and numerous techniques such as thermogravimetry, IR, DSC, FTIR, SEM, and rheology were employed for this purpose [8,3]. However, most of the studies on degradation have focused on rubber/rubber and rubber/plastic blends[9-14].

Studies on degradation of pure raw rubber have been limited to natural rubber. Very few studies raised the question of influence of molecular structure and processing conditions of raw, uncured NBR[3,8]. For example, Bhattacharjee et al. used TGA to investigate low (75°-150°C) and high temp (800°C) degradation of HNBR's and reported generation of ester (-COOR) and carbonyl groups (-C=O)[8]. For highly saturated nitrile

rubber, increase in Mw was observed, while a decrease in Mw was reported for NBR. The increase in Mw of saturated nitrile rubbers was suggested to be due to the conversion of the (-C≡N) group to (-C=NH).

The degradation of NBR occurs through attack of the double bond, whereas that of highly saturated HNBR is likely to occur through the (-C≡N) functionalities and free radical decomposition[8]. Sarkar et al. investigated the degradation of hydrogenated Styrene butadiene rubber (HSBR) using TGA analysis, DSC, IR, and NMR spectroscopy[3]. HSBR was found to be more stable in nitrogen atmosphere than SBR. Garbarczyk et al. characterized nitrile rubber by NMR spectroscopy and microimaging and reported that ageing proceeds mainly via additional cross-linking[4]. Scission of the polymer chain does not appear to contribute to ageing.

Batch blenders are widely used in polymer research laboratories, yet not much consideration has been given to thermomechanical structural modification of polymers in these blenders. Survey of the existing literature reveals that only few articles raised the topic of degradation during processing of raw Nitrile rubbers. It is interesting to note that melt blending was used to prepare samples for miscibility and other studies involving different elastomers [15-22]. However, the possibility of thermomechanical degradation during the blending process was not examined in detail. Thermomechanical degradation renders inconclusive results with regard to polymer-polymer miscibility [23]. Similarly, for all such studies in which blends are prepared in these internal mixers, the possibility of polymer modification during melt blending should be examined and adequate amounts of antioxidant should be added [23]. Among many different techniques such as NMR, DSC, GPC, HPLC and light scattering, rheology was found to be one of the most sensitive

techniques in detecting polymer degradation [23]. IR spectroscopy has been used since 1950 in the study of oxidative degradation[27] .FTIR is a rapidly expanding area in the field of polymer miscibility and degradation[28-30] Previous literature also showed a number of investigations made on rubber and rubber blends, by using the technique of light scattering[23-26]. In addition, practical applications of HNBR in the oil and other industries involve subjecting these rubbers to both thermal and mechanical stresses[5]. Hence, such studies of thermomechanical degradation of HNBRs are important.

In this study, rheology is used to study the influence of processing conditions on the thermomechanical degradation of pure HNBR elastomers. Rheology is a technique that is very sensitive to molecular level changes for example, molecular weight, crosslinking, chain scission and branching etc. The technique is convenient and relatively fast, and requires little sample preparation. Light scattering, (static and dynamic) and FTIR are used to confirm the findings of the rheology and to validate the ability of rheology to detect structural changes in HNBR resulting from thermomechanical degradation. In addition the influence of molecular parameters such as ACN content, degree of hydrogenation and Mooney viscosity (Mw) on degradation are investigated.

4.1.3 EXPERIMENTAL

4.1.3.1 Materials

The commercial HNBRs and NBR used in this study were obtained from Zeon Chemicals, USA. The characterization data such as ACN content, specific gravity, Mooney viscosity, and degree of hydrogenation as obtained from the manufacturer are

reported in Table 4.1.1. For convenience, the HNBRs are designated as Z-1 to Z-7 similarly NBR as N-1. The polymers were selected from a wide range of brands in a way so that they could be paired to study the influence of the above molecular parameters one at a time. For example, Z-6 and Z-7 have the same or close values of ACN and density but vary in the degree of unsaturation. Hence, the comparison of Z-6 vs Z-7 will disclose the effect of the degree of hydrogenation on degradation. Similarly, comparison of Z-4 vs Z-7 could reveal the effect of Mooney viscosity (Mw). For comparison purposes an NBR was also studied.

A mixture of antioxidants (AO), which mainly consists of 50/50 blend of the primary AO Irganox 1010 {Phenol B, tetrakis [methlene 3-(3',5'-di-t-butylphenol) propionate] methane, Mw=1178} and a secondary AO Irgafos 168 {P-1, tris[2,4-di-t-butylphenol] phosphite, Mw=646} was used in this study. These AO's were supplied by Ciba Specialty Chemicals.

4.1.3.2 Blender Conditioning and Sample Preparation

All as-received rubbers were cut into small pieces and then ground in a Fritsch Grinding mill. Then, the rubbers were conditioned in the Haake PolyDrive mix blender for 10 minutes at 50 rpm using Banbury type internal mixing blades at different temperatures. The samples were then pressed in a Carver press to form the disks to be inserted between the ARES platens as described in a previous publication [23]. Tests for degradation of all samples during the conditioning process at different temperatures (190°, 250°, 260°C) were performed and compared with rheology of as-received samples, to determine the extent of degradation each rubber was undergoing

Table 4.1.1: Characterization Data of Elastomers

Designation	% ACN	Specific Gravity	% Hyd	Mooney Visc.	Brand Name
Z-1	44	0.98	98	63-77	Zetpol-1000L
Z-2	17	0.98	95	60-100	Zetpol-4310
Z-3	44	0.98	91	71-85	Zetpol-1020
Z-4	36	0.95	96	120>	Zetpol-2010H
Z-5	50	1	91	58-72	Zetpol-0020
Z-6	36	0.95	85	50-65	Zetpol-2030L
Z-7	36	0.95	96	50-65	Zetpol-2010L
N-1	45	1	--	48-63	Nipol-DN4555

4.1.3.3 Measurements in ARES

All rheological tests of the conditioned and as-received samples were carried out using parallel plate geometry, with 25 mm diameter platens. A gap of 1.5 mm was used for all studies, and a strain amplitude, γ^{o}, of 15 % was used for all polymers. The 15% strain was selected following a strain sweep test. The frequency, ω, sweep testing was employed in the range ω=0.01-100 rad/s. All measurements were conducted using nitrogen as a convective heating medium to avoid any possible oxidation during the sweep tests. In this study, degradation is assessed through measurements of dynamic viscosity, η', and elastic modulus, G'. Reproducibility tests were performed for sample Z-6 (see Figure 4.1.1a). The agreement of both viscous and elastic properties shows the excellent reproducibility of the rheological measurements.

To rule out the possibility of degradation occurring in the grinding process, a study of the as received and the just ground sample (unconditioned) was performed on a representative sample (Z-6). In Figure 4.1.1b, viscoelastic properties of as-received and ground Z-6 are shown. The excellent agreement between the two sets of data clearly indicates the absence of any measurable degradation during the grinding process.

4.1.3.4 Solution Preparation for Light Scattering

Stock solutions were prepared by dissolving the rubber samples in pure 99.9 % solvent grade Acetone (Fluka, Germany). The solutions were left over night for proper dissolution. Stock solutions were further diluted to obtain proper concentrations (1.0e-4, 5.0e-5,2.5e-5 g/ml) for the static light scattering (SLS) experiments. Samples were filtered

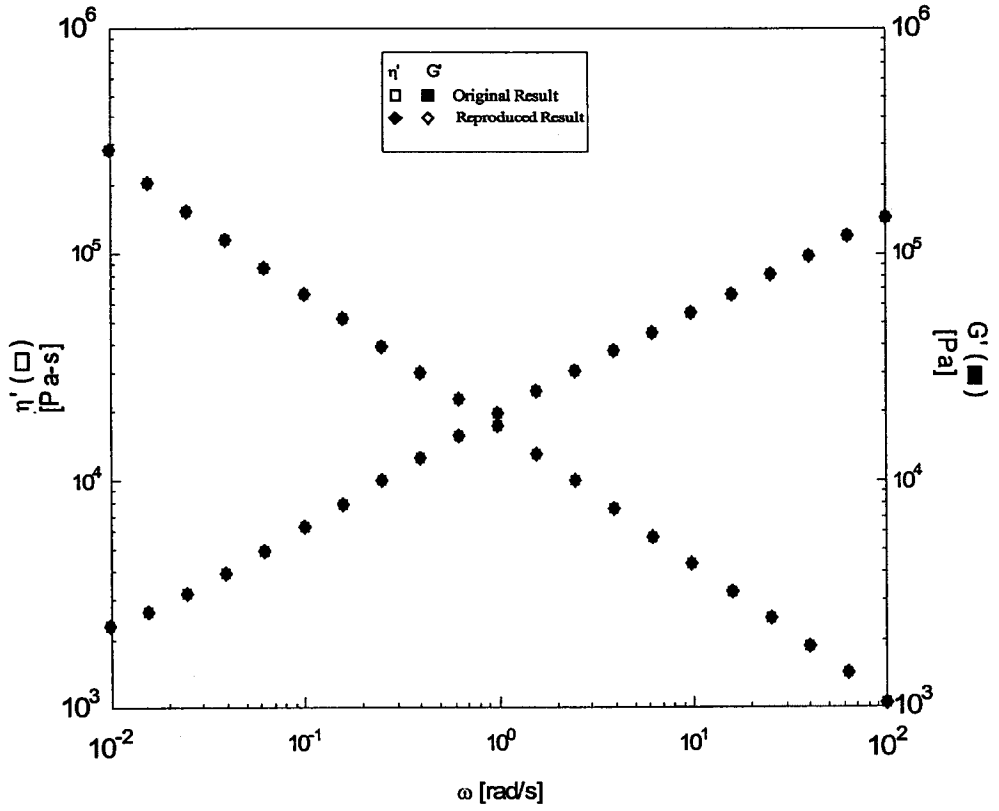

Figure (4.1.1a) Reproducibility Test (sample Z-6)

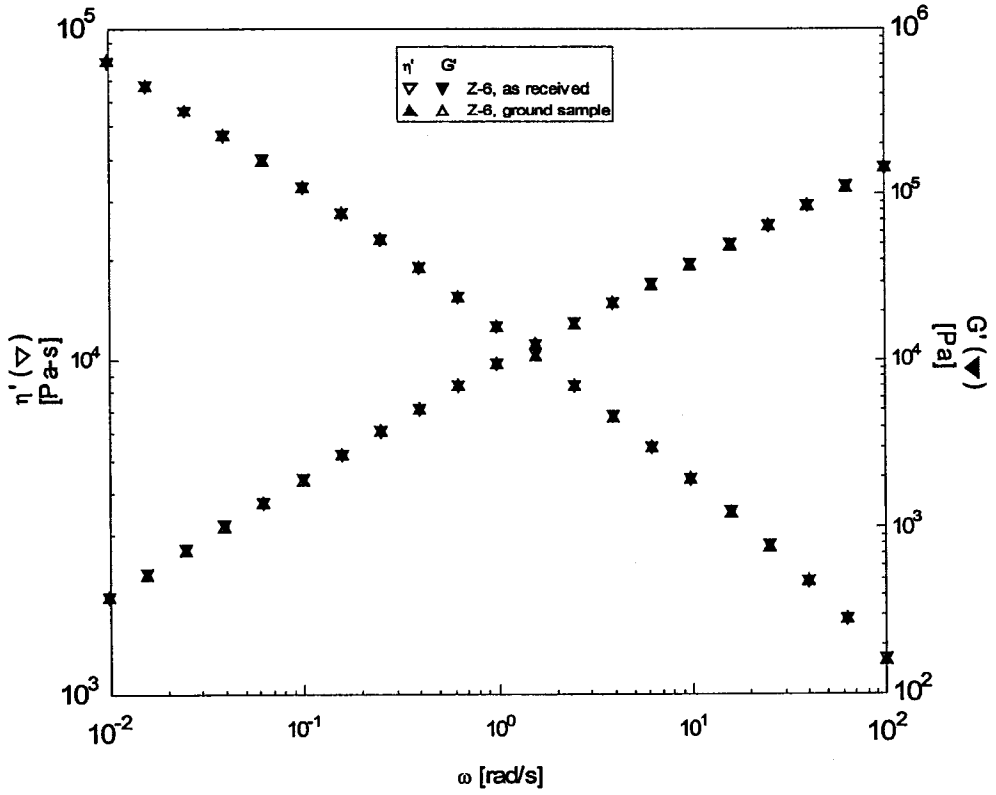

Figure (4.1.1 b) Effect of Grinding Mill on the degradation of Z-6.

twice to obtain dust free solutions using 0.22 μm Millipore filters.

4.1.3.5 Static and Dynamic Light Scattering

SLS measurements were made using a fully computerized DAWN-EOS laser light scattering instrument (Wyatt Technologies, USA) with ASTRA software. The refractive index increment (dn/dc) was measured using an RFM-340 Refractometer (Bellingham & Stanley, UK). The laser source for the light scattering instrument is a HeNe laser (λ_0=690 nm). For Dynamic Light Scattering studies, a Wyatt QELS instrument was used in combination with the DAWN-EOS instrument. The system was used in micro-batch mode. QELSbatch software was used in addition to ASTRA to determine the average value of the hydrodynamic radius.

4.1.4 RESULTS AND DISCUSSION

4.1.4.1 Extent of Degradation in each Sample.

In this section, the degradation of pure samples Z-1 to Z-7 (see Table 4.1.1) is discussed. In all of these results changes in η' and G′ are monitored. Usually cross-linking leads to increase in both η' and G′ while chain scission results in a decrease in both. In Figure 4.1.2, results of η' and G′ for Z1 are given. Very little degradation was observed in this sample. There was almost no degradation up to a temperature of 250°C, indicating the high stability of the sample. Further elevating the temperature to 260°C leads to slight increase in viscoelastic properties at low ω (sensitive to structural changes). The extraordinary stability (up to 250°C) can be attributed to the excellent proportion of ACN

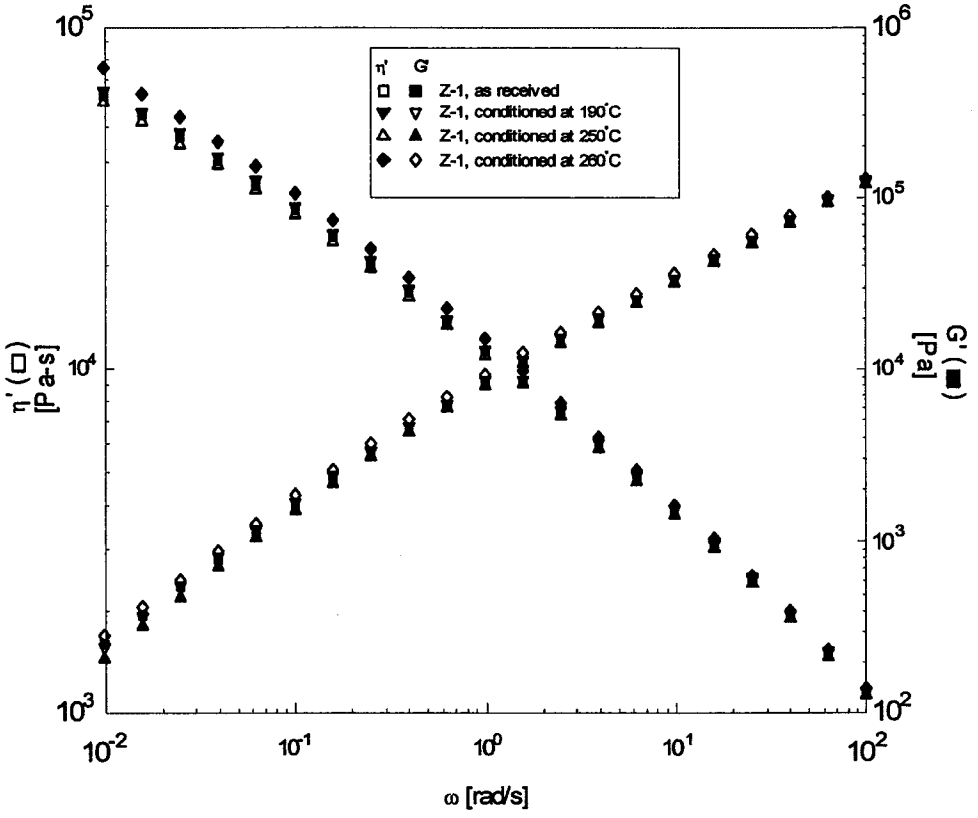

Figure (4.1.2) Thermomechanical Degradation of Z-1 (T_{test}=190°C, γ^{o}=15%).

content and high level of saturation. ACN content usually varies between 15 to 50 %, and this sample contained 44%, which is high enough to resist any thermal degradation[6]. Also, it is known that the main susceptible part for degradation is the butadiene portion (which contains the double bond). Now, high ACN means low % of butadiene and with 98 % degree of hydrogenation there is a minor chance for heat to be absorbed at the double bond. The small increase in Mw at 260°C might have been caused by cross-linking at the (-C≡N) group, which was suggested to be converted to (-C=NH)[8]. Cross-linking can also take place due to oxidative addition reaction at the double bond of the diene part. However, this increase is negligible and this sample can generally be considered stable. This is expected for a sample with high ACN content and high degree of hydrogenation.

For Z-2, results of $\eta'(\omega)$ and $G'(\omega)$ as a function of ω are given in Figure 4.1.3. A marked decrease in viscosity was observed. The Mw decreased as the material was progressively conditioned at high temperatures. This decrease in viscosity is attributed to the decrease in Mw (chain scission). This sample has quite a low ACN level (17 %); hence, butadiene is abundant in the sample. But, most of the unsaturation is removed since the percentage hydrogenation for Z-2 is 95% (see Table 4.1.1). It is likely that the absence of double bond sites in the butadiene part forces the thermomechanical degradation to proceed via chain scission and in fact, a decrease in Mw was observed.

Also, Z-3 was examined under the same conditions to study influence of the degree of hydrogenation on degradation. Z-3 has an ACN content and Mooney viscosity (Mw) that are almost the same as Z-1. However, the only major difference between the two HNBRs is the degree of hydrogenation. The degree of hydrogenation for Z-1 is 98% while that for Z-3 is only 91%. As shown in Figure 4.1.4, conditioning of Z-1 and Z-3 at

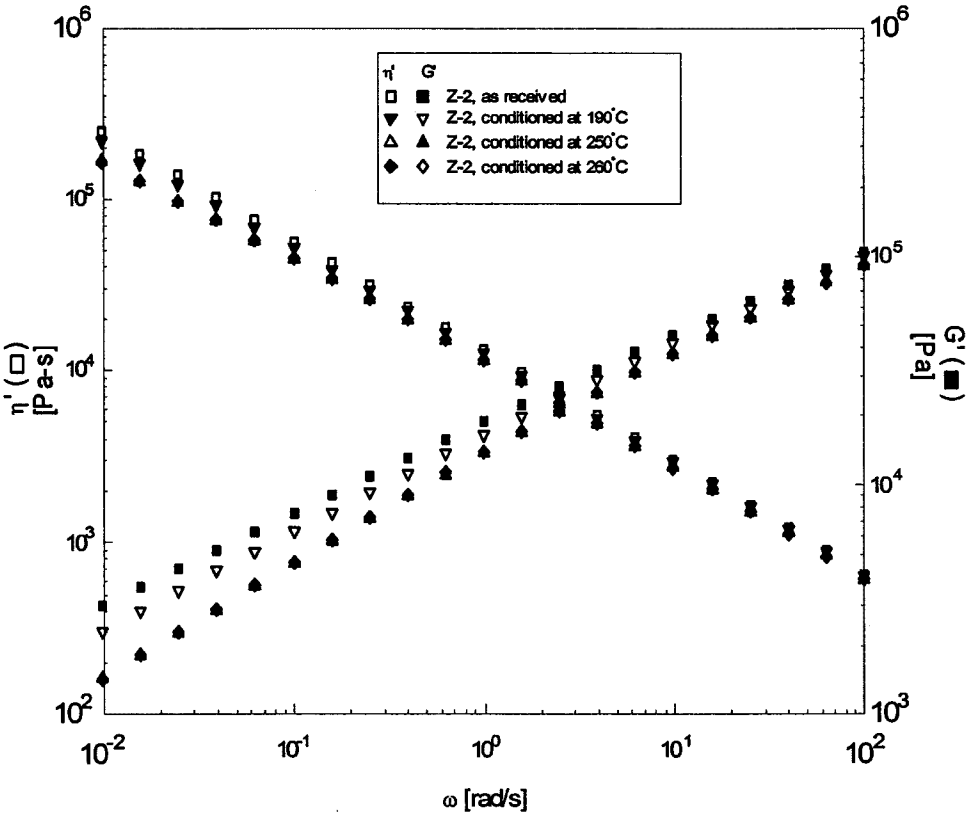

Figure (4.1.3) Thermomechanical Degradation of Z-2 (T_{test}=190°C, γ^o=15%).

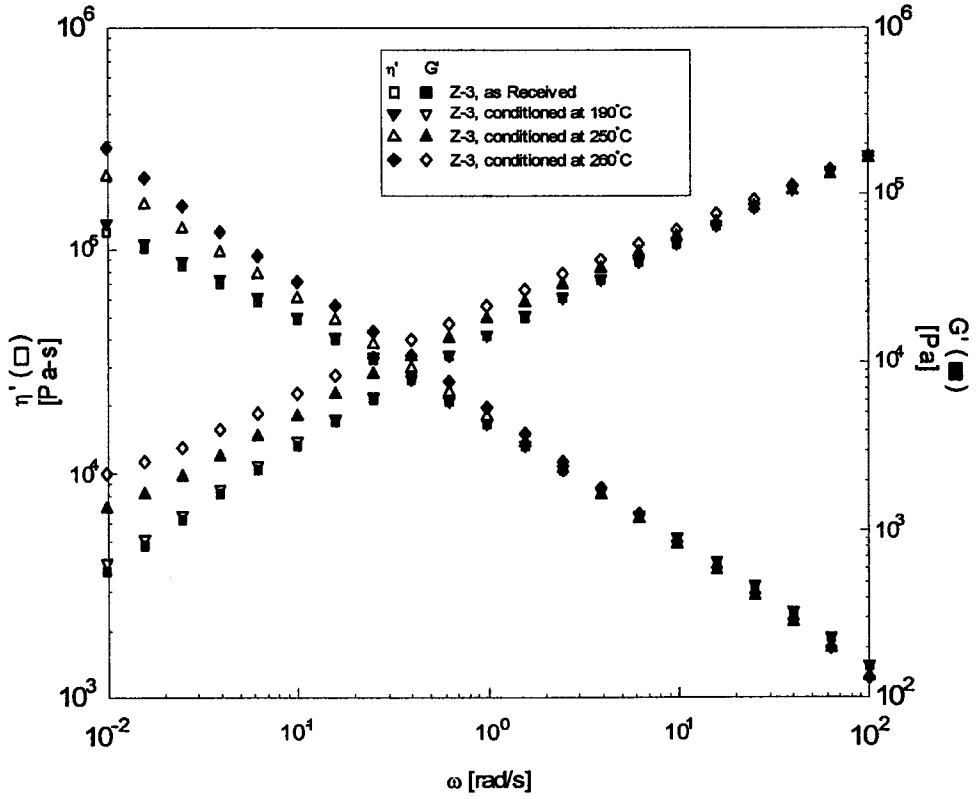

Figure (4.1.4) Thermomechanical Degradation of Z-3 (Ttest =190°C, γ^{o}=15%).

190°C did not result in measurable degradation. However, increase in both viscous and elastic components of Z-3 was observed at 250°C and 260°C. This suggests that the degradation of these rubbers is temperature sensitive. Comparison of Z-1 and Z-3 suggests that the more probable mechanism of cross-linking is oxidative addition at the double bonds. An overall comparison of degradation results of the three rubbers (Z-1,Z-2 and Z-3) indicates that the stability of HNBR could be extended to higher temperatures by increasing the ACN content and the degree of hydrogenation.

In Figure 4.1.5, results for Z-4 are displayed. A very different behavior was observed for this sample. Here, a decrease in both η' and G' was detected at low ω as well as at high ω. This suggests major changes in Z-4 structure due to thermomechanical degradation. This drop in viscoelastic properties is observed at all test temperatures and it increases at high temperatures. Here, chain scission is suggested as the dominant mechanism for degradation. As shown in Table 4.1.1 , Z-4 has somewhat high ACN content (36%), high degree of hydrogenation (96%) and has the highest Mooney viscosity (Mw). The drop in viscoelastic properties is likely a result of high mechanical stresses that developed during processing due to high viscosity of this brand of HNBR. This result indicates that mechanical stresses have a major contribution to overall degradation. This contribution increases with increasing Mw (viscosity) of the brand.

In Figure 4.1.6, the trend of Z-5 degradation is almost similar to that of Z-3. Again, cross-linking is suggested. The structural parameters of the two HNBRs are very similar; hence, their degradation behavior. The high ACN content is likely behind the stability at the low temperatures (190°C). However, cross-linking occurs at high temperatures.

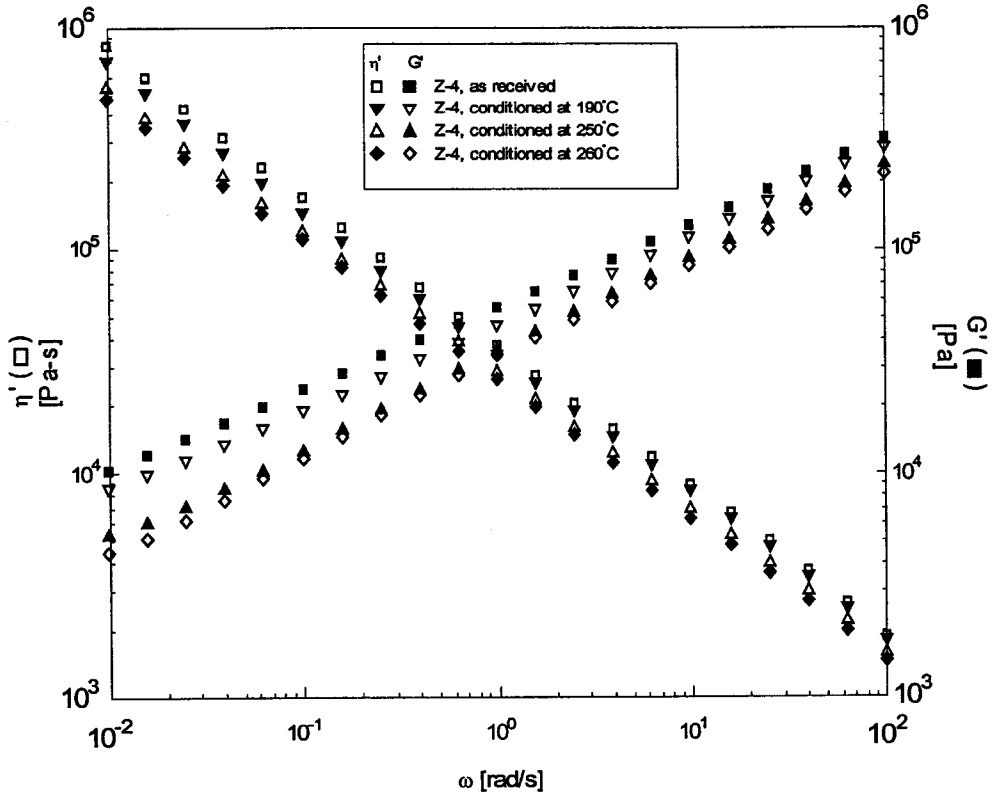

Figure (4.1.5) Thermomechanical Degradation of Z-4 (T_{test}=190°C, γ^o=15%).

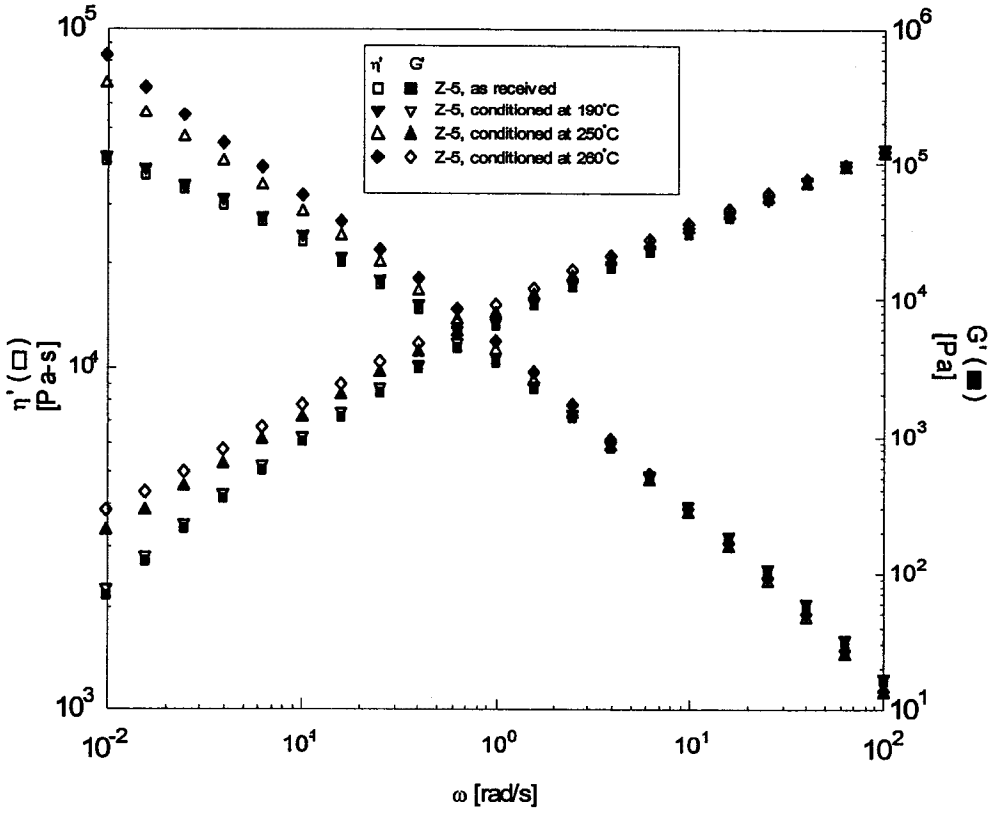

Figure (4.1.6) Thermomechanical Degradation of Z-5 (Ttest =190°C, γ^{o}=15%).

The effect of the degree of hydrogenation on degradation of HNBR with high ACN content was examined by comparing the results for Z-6 and Z-7. The results are shown in Figure 4.1.7 and Figure 4.1.8, respectively. The two HNBRs have the same ACN content (36%) and Mooney viscosity (50-65). But, the degree of hydrogenation is 85% for Z-6 and 96% for Z-7. The results for Z-6 suggest polymer stability at 190°C, but extensive cross- linking is observed at 250°C and 260°C. The large extent of cross linking observed in the relatively unsaturated Z-6 is likely to take place at the butadiene double bonds via oxidative addition reactions as suggested previously

As shown in Figure 4.1.8, Z-7 is very stable with only minor decrease in η' and G′ at elevated temperature. A comparison of Z-6 and Z-7 indicates that the chain scission mechanism of degradation dominates at high saturation levels. On the other hand cross-linking dominates at low saturation levels.

A comparison of Z-4 and Z-7, with the same ACN and level of hydrogenation and different Mooney viscosity, reveals the effect of Mw. The extensive chain scission that was observed in the high Mw HNBR, Z-4, is absent in Z-7. This result again indicates that mechanical stresses have a major effect on degradation of these rubbers during processing. Figure 4.1.9 shows rheological results for one of the NBR (N-1). As expected in case of NBR large amount of degradation was found. The extent was more than, found in any of the HNBR's. This was due to the unsaturation present in the backbone of NBR.

Further, quantitative measures were used to assess the degradation of the above HNBRs. Enhancement of the dynamic viscosity, η', of the conditioned HNBR over that of the as-received (AR) one is calculated. The same definition is applied to the ratio of G′.

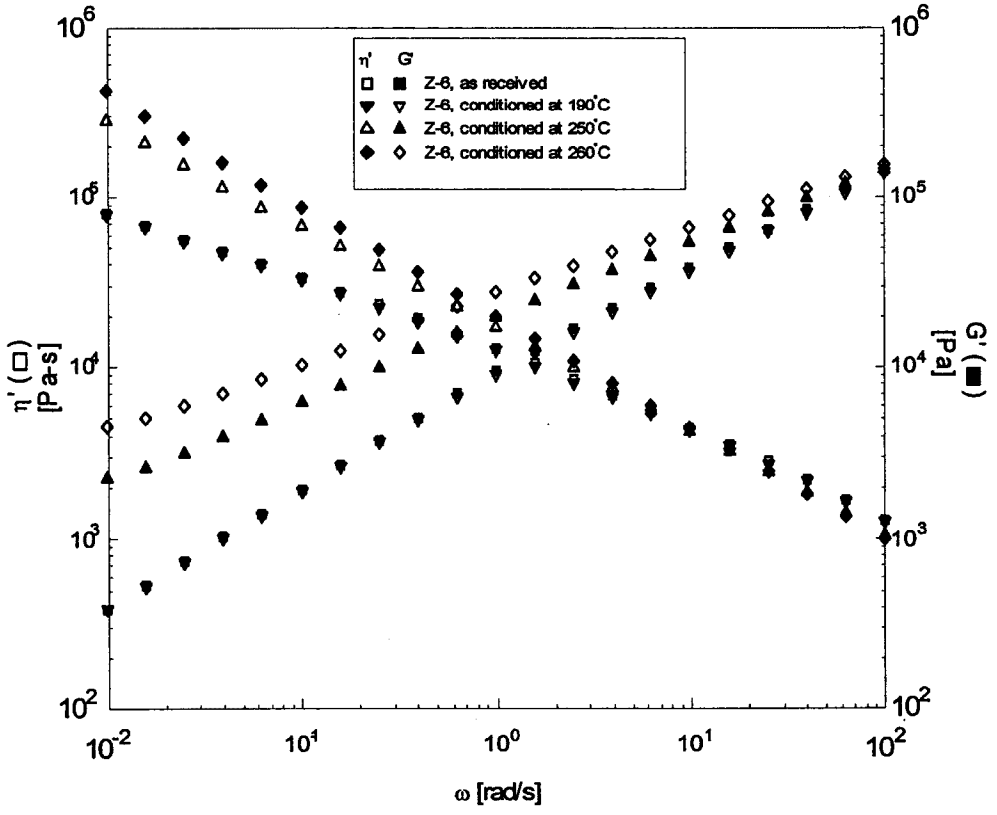

Figure (4.1.7) Thermomechanical Degradation of Z-6 (Ttest =190°C, γ^{o}=15%).

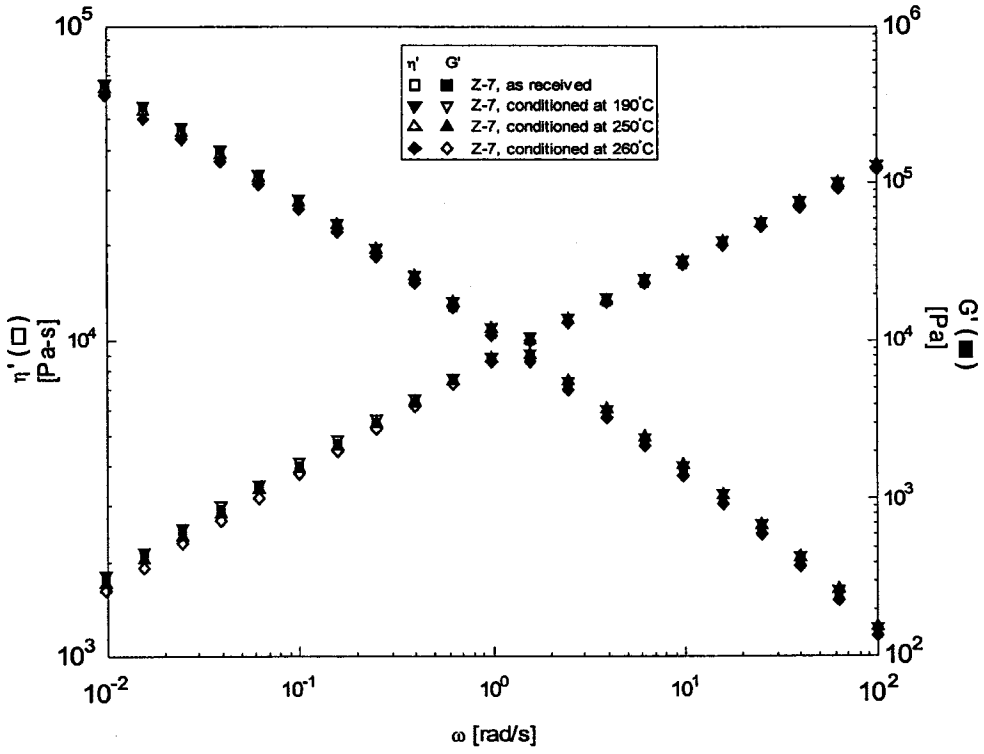

Figure (4.1.8) Thermomechanical Degradation of Z-7 (T_{test}=190°C, γ^o=15%).

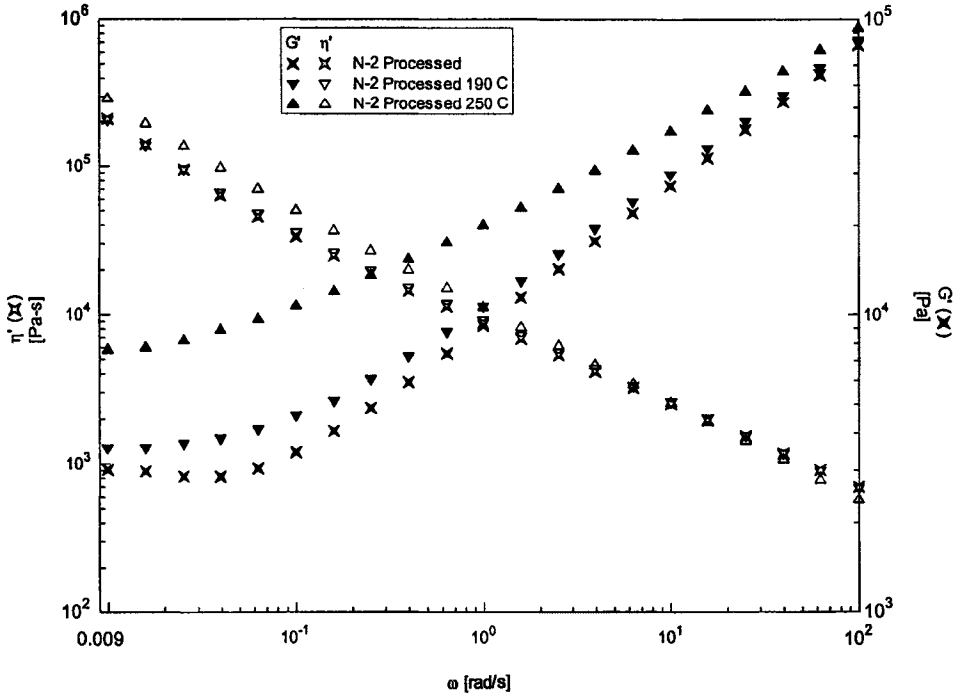

Figure (4.1.9) Thermomechanical Degradation of NBR (N-1)(T_{test}=190°C, γ^{o}=15%).

This ratio is calculated at the same ω for all HNBRs (ω=0.025 rad/s). Results for relative change factors (η'_{cond}/η'_{AR}, G'_{cond}/G'_{AR}) as a function of temperature are given in Figures 4.1.10a and 4.1.10b respectively. As expected, G′ was found to be more sensitive than η'. The trends of the two curves are similar. The relatively unsaturated resin, Z-6, showed the highest degree of degradation and its high temperature sensitivity is obvious. Enhancement factors that are less than 1 (chain scission) were obtained for Z-2 and Z-4 at all temperatures. Also, a factor of ~1 was obtained for Z-1 and Z-7 at 190°C; however, minor degradation is observed at higher temperatures. For Z-3 and Z-5, degradation was detected at 250°C and 260°C.

4.1.4.2 Light Scattering

The molecular weight and hydrodynamic radius results obtained by static and dynamic light scattering of a selected group of samples, are depicted in Table 4.1.2 . The thermomechanically degraded samples at different temperatures (190°C, 250°C) showed variations in M_w in accord with the predictions made by rheology. A typical Zimm-Plot is shown in Figure 4.1.11(a) The molecular weight of Z-3 showed an increase from $3x10^5$ to $6.31x10^5$ upon increasing the processing temperature from 190 to 250 °C. This result corresponds with the rheology results that indicated an increase in molecular weight caused by crosslinking. The hydrodynamic radius of Z-3 determined by dynamic light scattering showed a similar trend. Z-4 was found to have the highest molecular weight (4.5 E+06) among the three elastomers shown in Table 4.1.2. This result is expected because of its high Mooney viscosity (>120). Unlike Z-3, Z-4 showed a decrease in

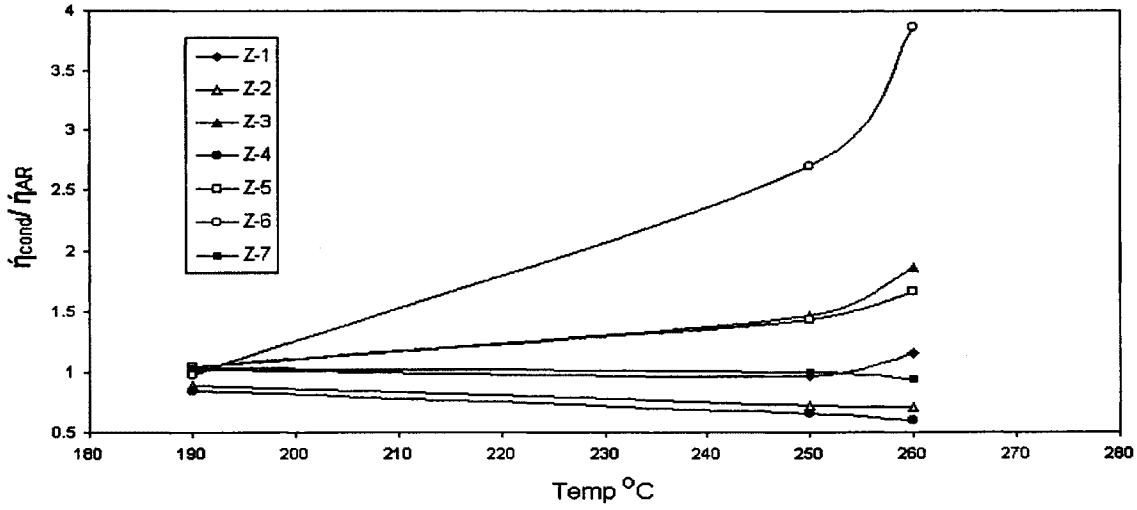

Figure (4.1.10a) Enhancement of Viscosity of HNBRs at different Temperatures

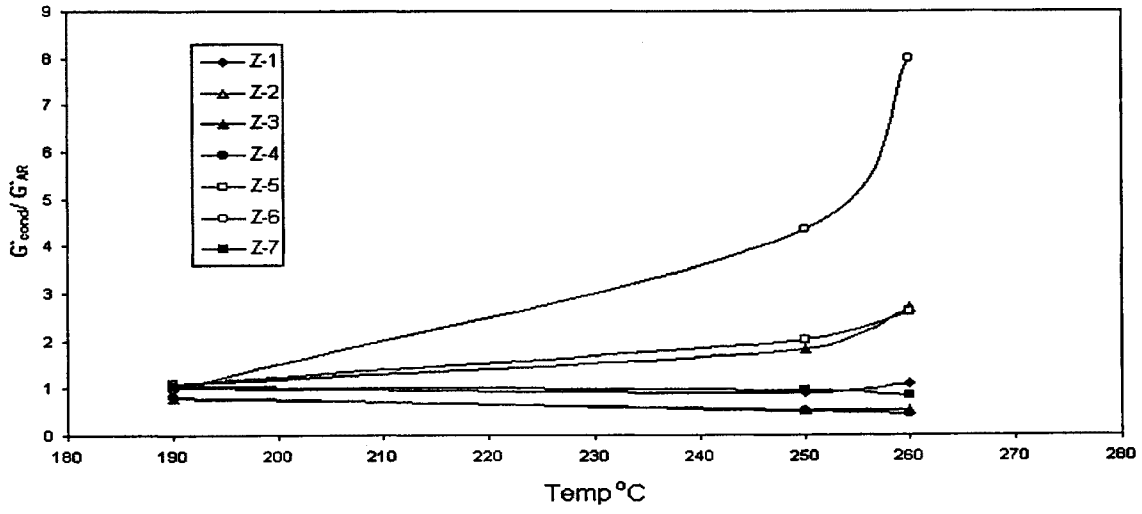

Figure (4.1.10b) Enhancement of Elastic Modulus of HNBRs at different Temperatures

Table 4.1.2 Light Scattering results for selected samples

Sample	Conditioned at 190 °C		Conditioned at 250 °C	
	Molecular Wt (M_w) g/mol	Hydrodynamic radius (R_h) nm	Molecular Wt (M_w) g/mol	Hydrodynamic radius (R_h) nm
Z-3	3.045±0.277 E05	98.5±56.8	6.312±0.708 E05	120±22.6
Z-4	4.510±1.041 E06	163±55.6	1.772±0.168 E06	125±57.3
Z-6	1.928±0.069 E05	82.7±21.1	6.214±1.177 E05	130.5±56.8

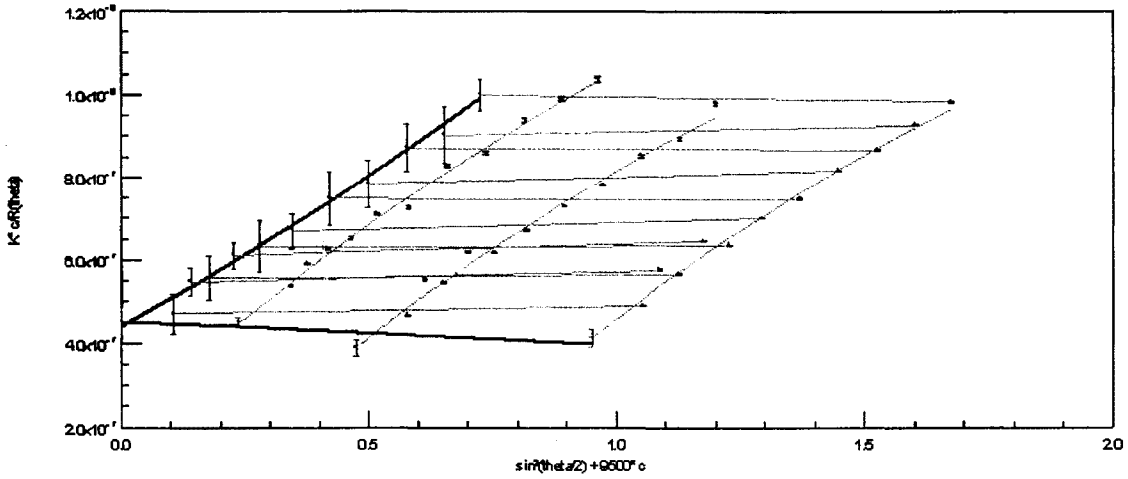

Figure (4.1.11a) A typical Zimm plot of static light-scattering

Molecular weight and hydrodynamic radius upon increasing the processing temperature from 190 to 250 °C. Again, these results correspond with the rheology results that indicated a decrease in molecular weight cause by chain session at the higher processing temperature.

The relatively unsaturated Z-6 that showed maximum increase in molecular weight due to cross linking in rheological results showed a three times increase in molecular weight (from 1.928 E05 to 6.214 E05). The values of molecular weights were found to be close to those reported for Nitrile rubbers in the literature[24] .

4.1.4.3 FTIR Analysis

Typical transmission and absorption spectra for one of the sample are shown in the figure 4.1.11(b) and 4.1.11(c) respectively. The two strong peaks in the left half, are characteristic of these rubbers and there occurrence is due to the stretching of C-H and C≡N bonds at wave numbers 2235.30 cm-1 and 2896.06 cm-1 respectively. The peak corresponding to C=C appears at 1632.63 cm-1 which is relatively a medium peak. Booth end of the spectra is occupied by clusters of numerous peaks; however our focus is at the region of interest i.e carbonyl region containing the peaks called degradation peaks (1650-1850 cm-1). Carbonyl functionalities were already found present in the as received samples. This could be due to a number of reasons such as, catalytic oxidation caused by some catalyst Particles left in the material, some initial processing, aging, weathering etc. In the Fig 4.1.12 overlay spectrums of Z-1 are shown .The three spectrums are generally similar to each other and do not show any major changes, or new peaks that shows the stable nature of Z-1 brand as seen earlier (rheology). The peak at 1736 cm^{-1} attributes to

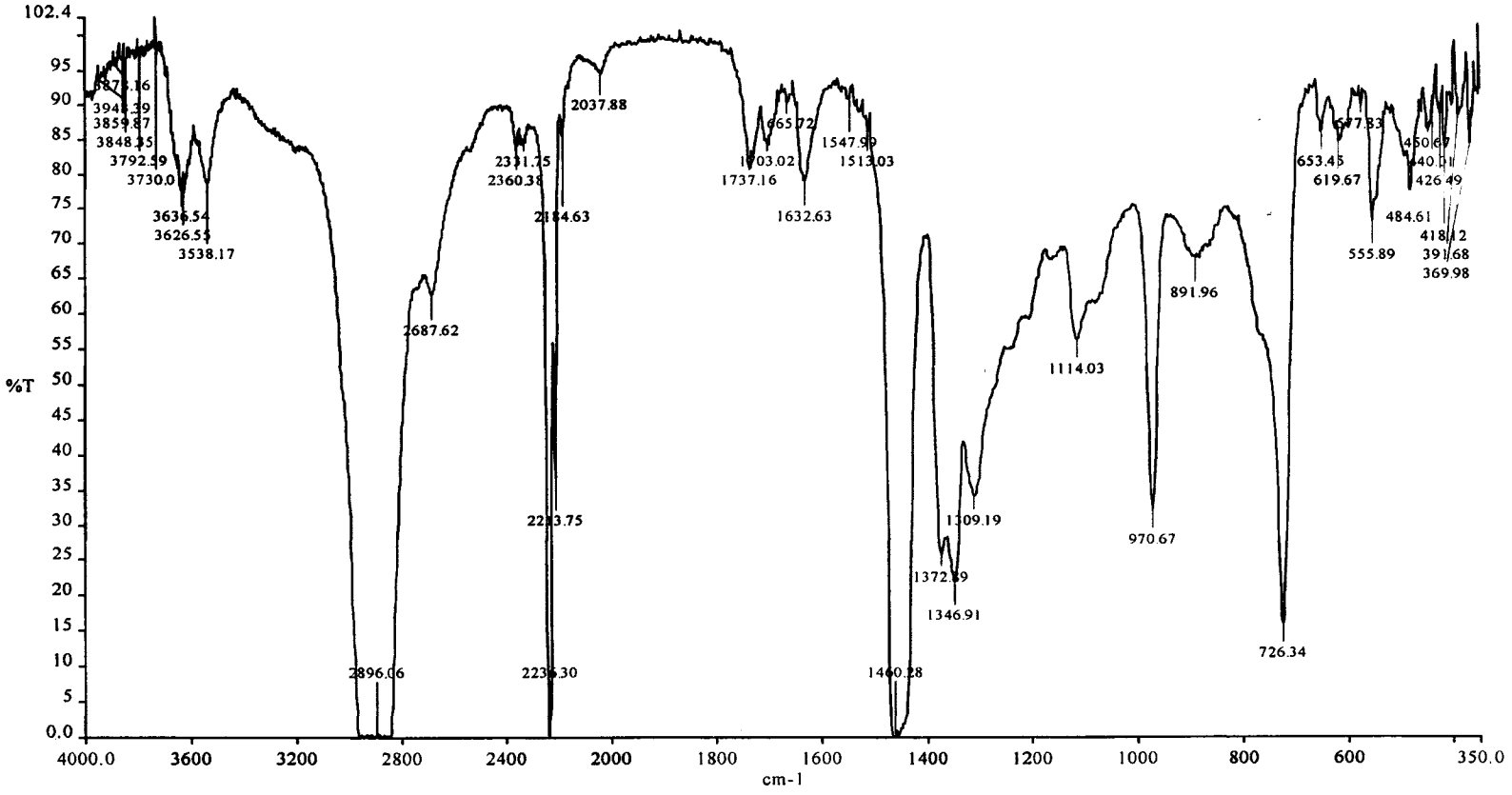

Figure (4.1.11b) Typical transmission spectra for the Hydrogenated-Butadiene-Acrylonitrile copolymer

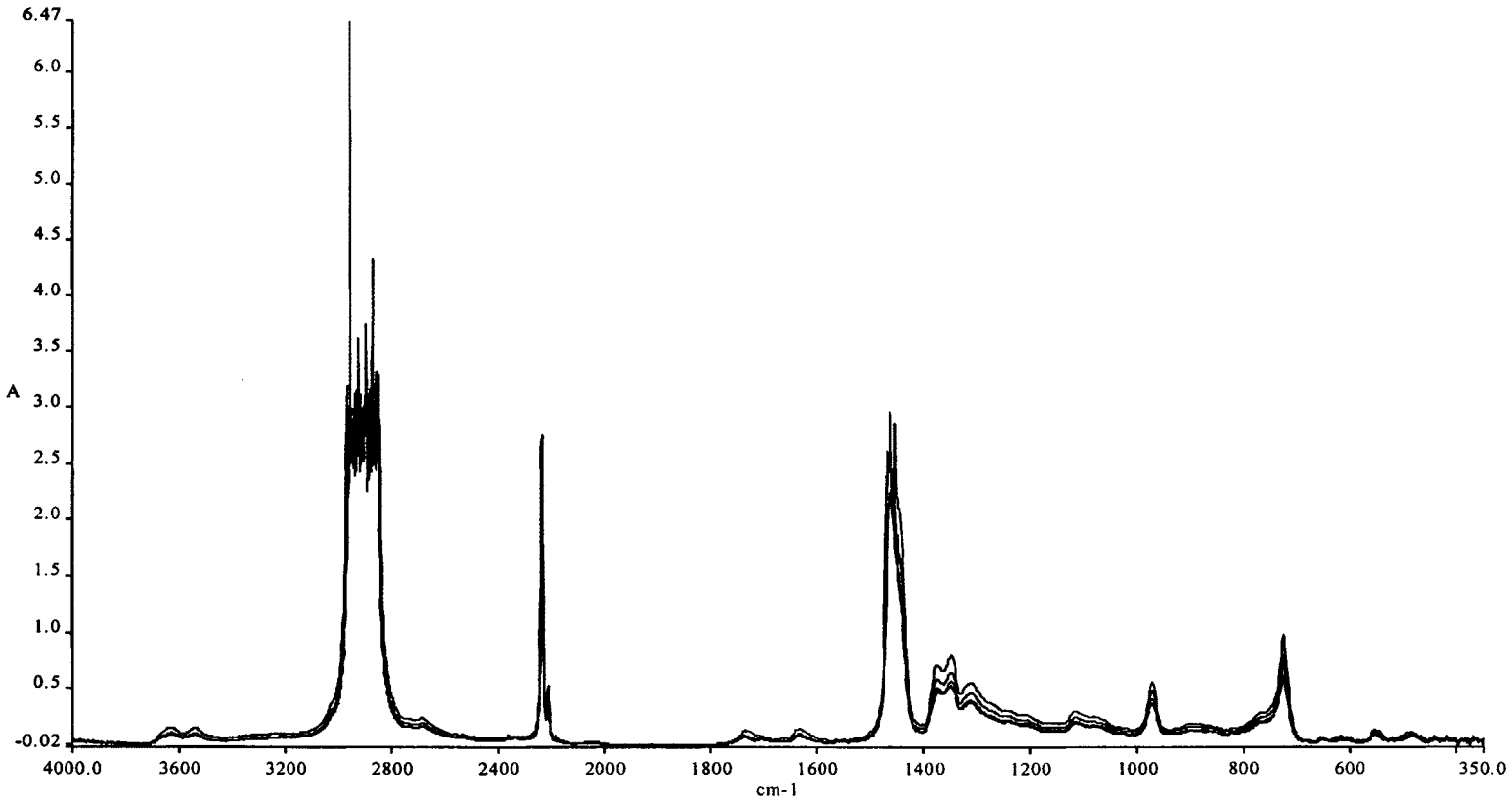

Figure (4.1.11c) Typical spectra in Absorption mode for the Hydrogenated-Butadiene-Acrylonitrile copolymer

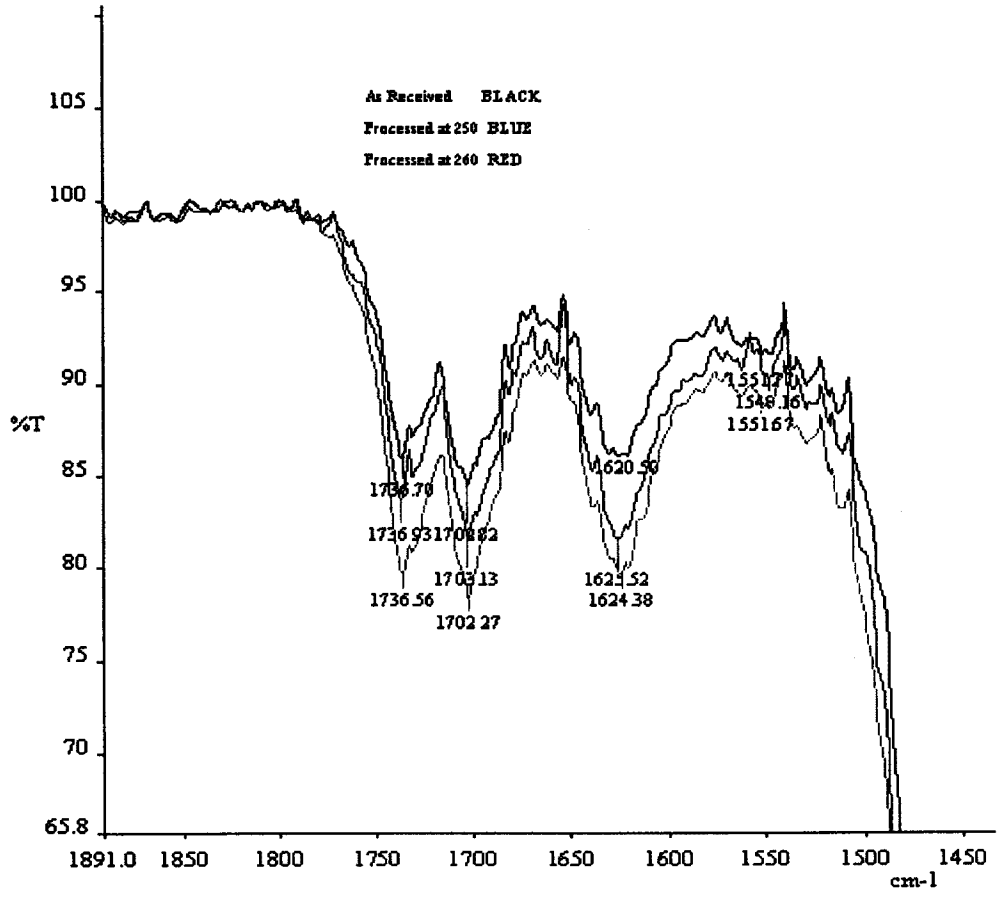

Figure (4.1.12) Carbonyl region in transmission mode of spectra for Z-1.

(-C=O) functionality that stays stable as far as the frequency is concerned. Although the height of these peaks change (increase) with increase in processing temperatures, indicating more generation of these functionalities and hence degradation, but as parameters such as impurities and sample thickness can cause these fluctuation, so we will stick to quantitative interpretation. This wave number characteristic to ester functionalities is accompanied by a companion peak at 1703 cm-1 which may be explained by the presence of carboxyl group. Generation of booth of these functionalities has been reported in previous literature 8,31 Figure 4.1.13 shows spectrums for sample Z-3 , Here we can see that in case of 290 and 250 processed sample there is a new peak at 1665.72 cm-1 that disappears at 260oC. The origin of this peak may be (C=NH) group. As relatively lower saturation level for this brand along with high ACN content (44%) can give rise to the following functionality (C=NH) hence providing a mean of cross linking. Presence of this group was verified by the presence of the absorption peaks at 2240 cm-1(Figure 4.1.11(c)) which moves toward the lower frequencies (Figure 4.1.14) pointing out the destruction of –CN and appearance of >C=NH 31 . The mechanism for this reaction has been reported in many studies found in the literature8,31.

Figure 4.1.15 depicts spectrums of Z-6, Here we observe the appearance of a peak at 1709.76 cm-1 that is absent from the as received sample. This peak merges to the one at

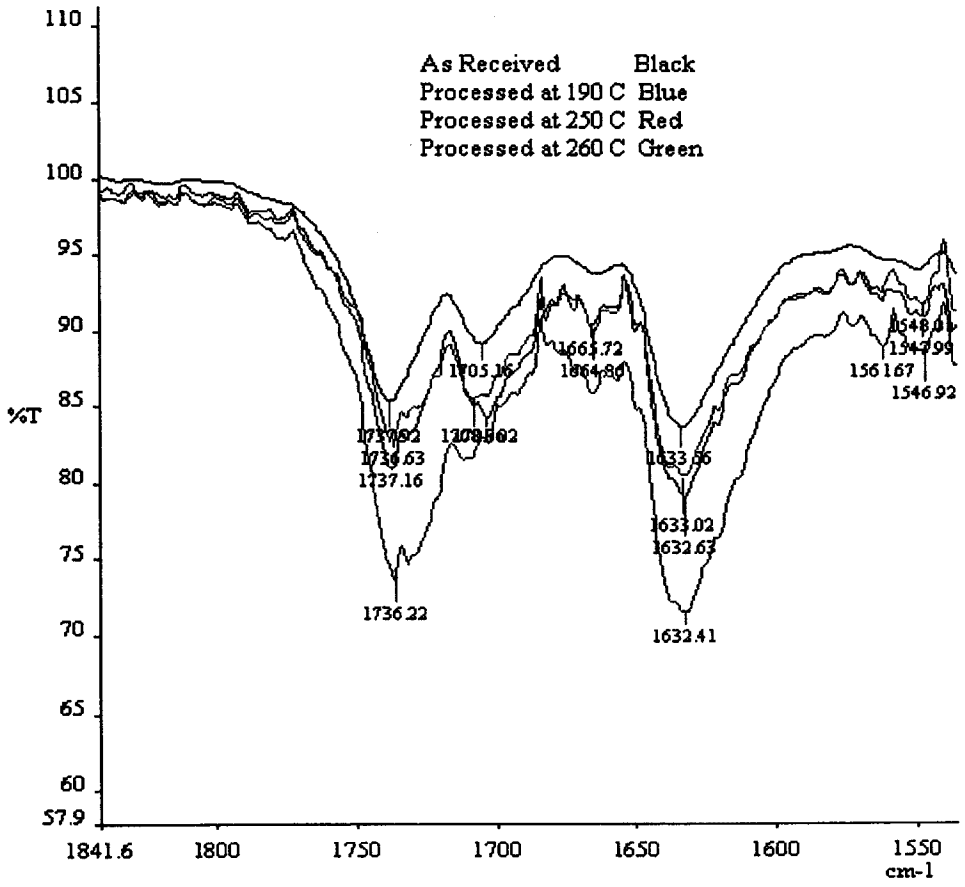

Figure (4.1.13) Transmission spectrum for Z-3. carbonyl region shown.

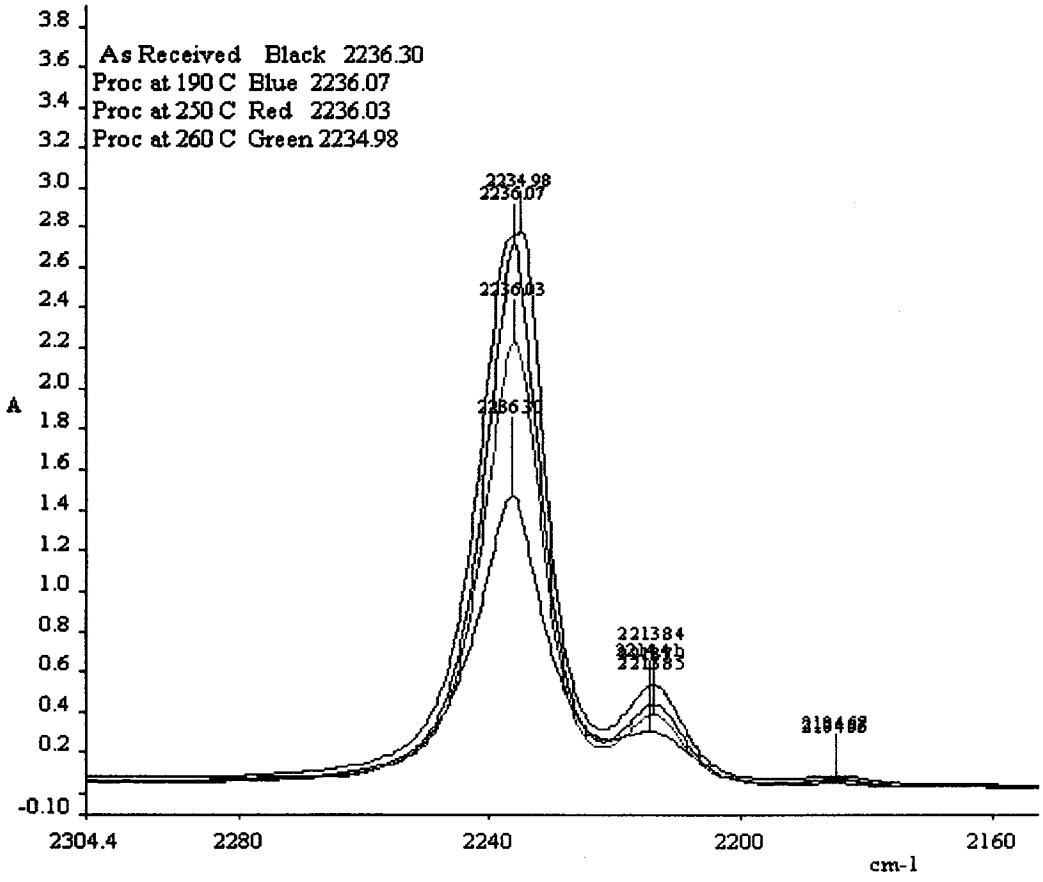

Figure (4.1.14) Transmission spectrum for Z-3. carbonyl region shown.

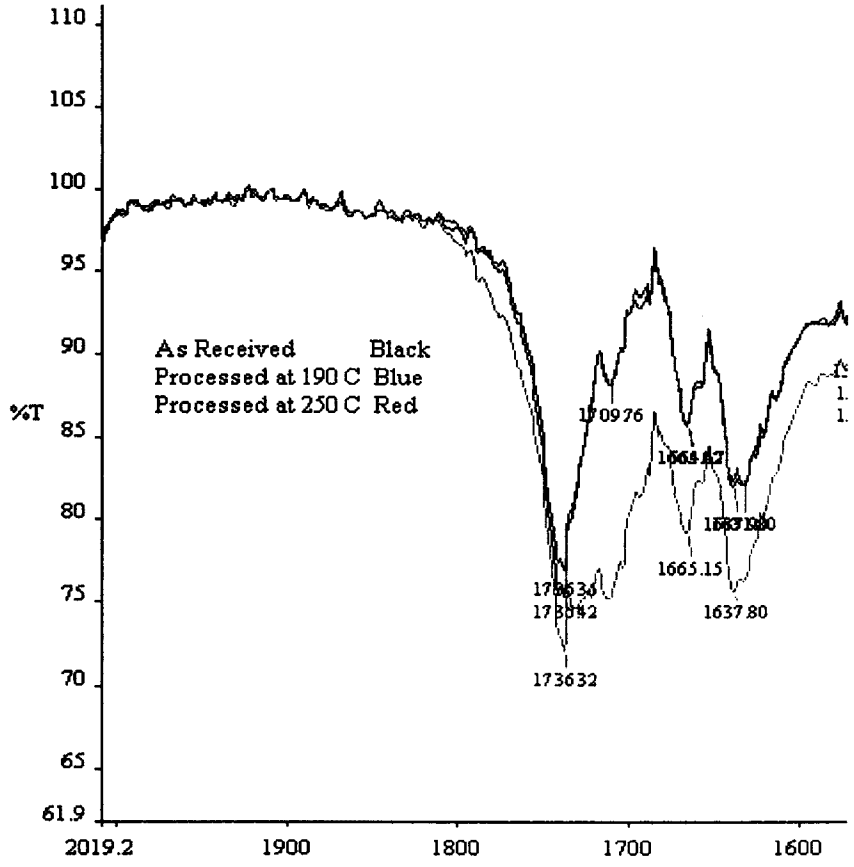

Figure (4.1.15) Transmission spectrum for Z-6. carbonyl region shown.

1736 cm^{-1} for the sample processed at 250oC. The carbonyl group present as fractional impurities in polymers are well distributed among the aldehyde , acid, esters and ketone forms. FTIR analysis showed that the degradation peaks of the spectrum was undergoing changes for these samples, apart of variations in height of different (C=O peaks), new functionalities were appearing and disappearing with temperature.

4.1.4.4 Thermal vs Thermomechanical Degradation

Furthermore, to investigate thermal vs. thermomechanical effects the highly thermomechanically degraded HNBR, Z-6, was selected. Thermomechanical conditioned Z-6 was compared to oven heated sample. The polymer was placed in an oven at 250°C for 10 minutes (same conditioning time and temperature as in the Haake blender). A temperature of 250°C was chosen for the comparison as most samples showed marked degradation at this temperature. Also, Z-2 was selected as a brand degrading to normal extent. In addition, Z-6 degrades through cross-linking, while Z-2 undergoes chain scission. Results of η' and G' for oven heated and conditioned Z-6 and Z-2 are shown in Figure 4.1.16a and Figure 4.1.16b, respectively. In Figure 4.1.16a, some thermal degradation was detected in Z-6; however, thermomechanical degradation is much stronger. This suggests that it is the combined effect of heat and stress that leads to degradation in these blenders. Thermal effects alone contributed ~¼ th of the overall degradation of Z-6 (measured as enhancement to viscosity). Marked thermal degradation in Z-2 was detected in G' only (see Figure 4.1.16b)..

The comparison of thermal and mechanical effects of the processing also shows that, in the conditioning process, part from the direct thermal effects (heating) there are two more effects: (a) viscous heating (b) mechanical stretching (due to stresses). In most

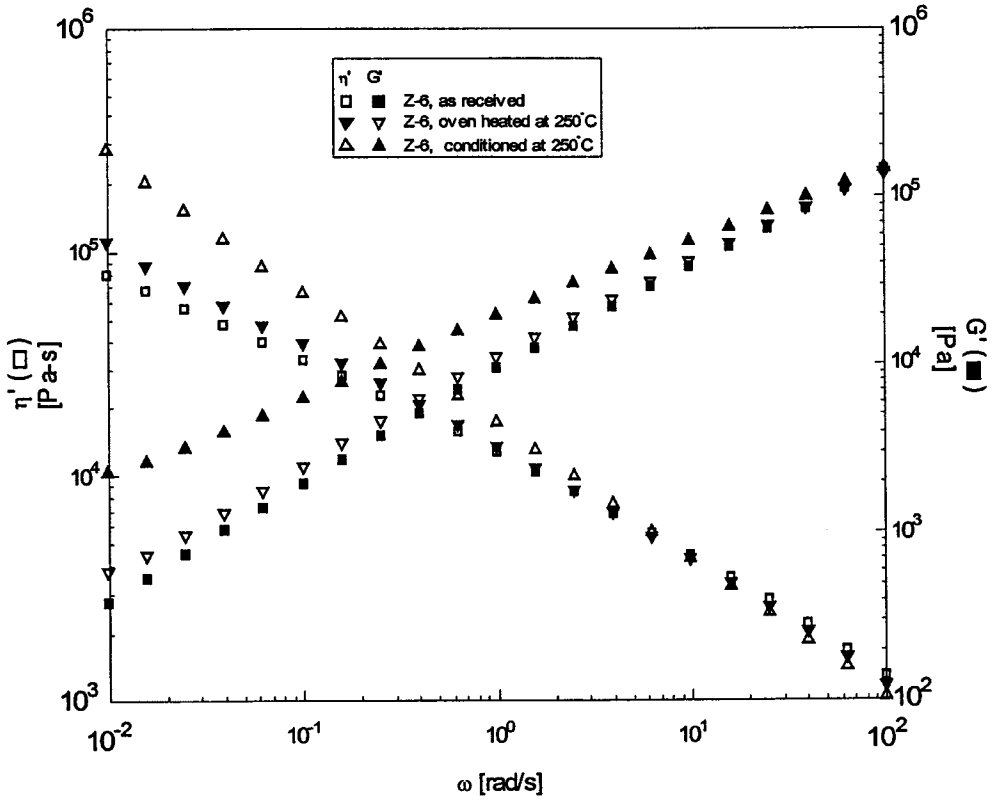

Figure (4.1.16a) Thermal vs Thermomechanical Degradation of Z-6.

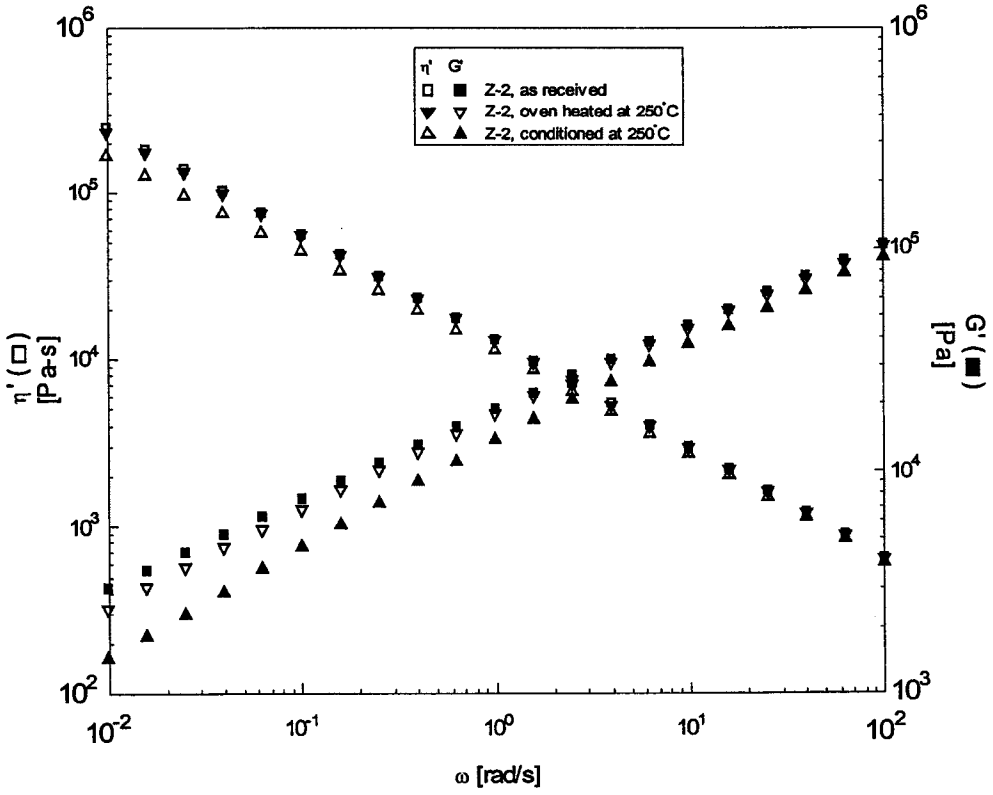

Figure (4.1.16b) Thermal vs Thermomechanical Degradation of Z-2.

of the cases of conditioning, the melt temperature of the material was not more than 4-5°C degrees above the set temperature. So, mechanical effects were a major contributor to degradation. In addition, mechanical mixing might cause the oxygen to access more of the bulk of the rubber, hence accelerating all forms of oxidative degradation.

4.1.4.5 Effect of AO on Degradation

Moreover, the same two samples Z-2 and Z-6 that showed marked decrease and increase in Mw due to degradation were used in another study. Here, the effect of addition of AO on the degradation was examined. Different amounts of AO were added to Z-2 and Z-6 during conditioning. The AO is a 50/50 blend of a primary (Irganox 1010 and a secondary AO, Irgafos 168). This blend of AO is usually used for polyolefins and it is effective against free radical degradation. Figures 4.1.17a and 4.1.17b show the results of viscoelastic properties for Z-6 and Z-2, respectively. The samples were conditioned in the presence of different amounts of AO. For Z-6, where cross-linking dominates, the addition of different amounts of AO was found to be effective in reducing crosslinking. The doses of added AO were 1000, 2000, 4000, and 5000 ppm. As shown in Figure 4.1.17a, the AO succeeded in reducing both viscous and elastic properties of degraded Z-6. Increasing the amounts of AO from 1000 ppm to 5000 ppm shifted the trend towards the as received Z-6 (control sample). At 250°C 5000 ppm of AO was needed to fully save Z-6 from degradation. This amount reduced both η' and G' to that of the as-received resin. This suggests that the AO is effective against crosslinking caused by oxidative degradation of double bonds. On the other hand, Z-2 was conditioned in the presence of

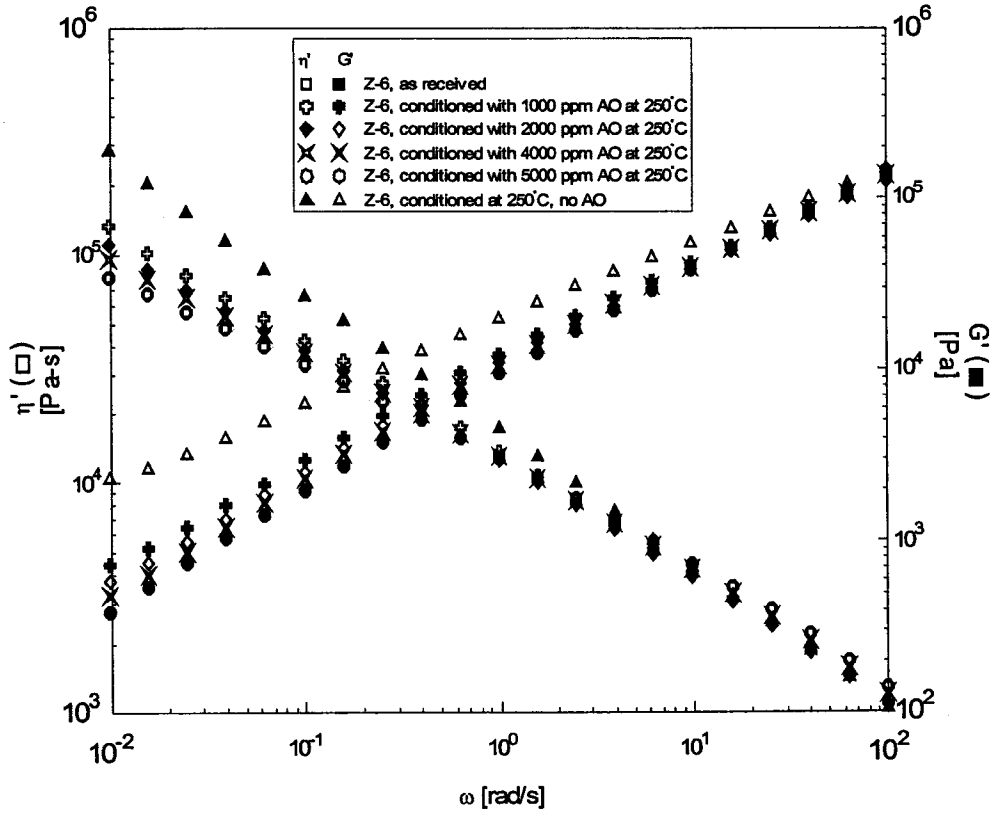

Figure (4.1.17a) Influence of AO on Thermomechanical Degradation of Z-6.

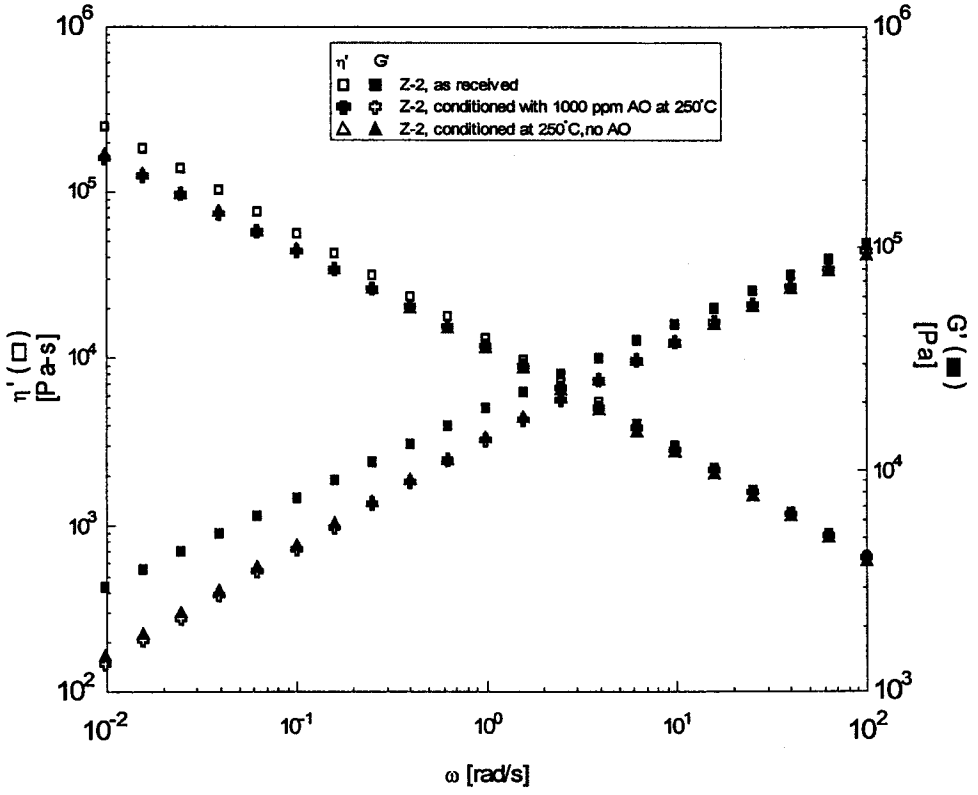

Figure (4.1.17b) Influence of AO on Thermomechanical Degradation of Z-2

1000 ppm of AO. It was shown earlier that dominating mechanism in Z-2 was chain scission. The results of the rheological analysis for Z-2 are given in Figure 4.1.17b. Unlike Z-6, degradation of Z-2 did not slow down with the addition of 1000 ppm, any further addition of AO was also unsuccessful to prevent the degradation to any extent. So, it is likely that the AO used are not effective against alkyl radicals. Other types of additives will be examined in a future study. Also, other methods such as FTIR and SEM will be used to investigate the thermomechanical degradation of these HNBRs. Results will be reported elsewhere[27]. It is worth noting that previous thermogravimetric studies reported onset degradation temperatures for HNBRs that are much higher than those reported in this study[8].

4.1.5 CONCLUSIONS

In this study, different brands of HNBR rubbers were studied for thermomechanical degradation. It was found that thermomechanical treatment does affect these rubbers in the temperature range used in this study i.e 190°C to 260°C and molecular parameters have an effect on the selection of dominating degradation mechanism. From all of the above cases, it is clear that degradation is a combination of chain scission and cross-linking. Also, it was found that a high degree of ACN content and high saturation result in increase in stability. Comparison of Z-1 and Z-3 or Z-6 and Z-7 showed that the stability of HNBRs is strongly influenced by the degree of hydrogenation. Consequently, low degrees of hydrogenation result in high extent of degradation. Relatively unsaturated HNBRs were found to degrade via cross-linking. For highly saturated HNBRs with relatively high ACN content, the Mw plays an important role. In this case, high Mw leads

to degradation through chain scission. In addition, high ACN content shifts the thermomechanical degradation to higher temperatures due to the high activation energy of the C≡N group. However, the net degradation level and mechanism also depends on the level of unsaturation. In the case of low ACN and high degree of hydrogenation, degradation proceeds via chain scission (decrease in Mw). Light scattering confirmed the ability of rheology to detect degradation of HNBR. FTIR results confirmed that carbonyl functionalities were being generated as a result of degradation and HNBR rubbers were crosslinking via C≡N site.

4.1.6 REFERENCES

[1] S. Moss and H. Zweifel, *Polym Degrad Stab.* **25**,217 (1989).

[2] P. Anthony and S.K. De, Rubber Chem. Technol. **74**, 376 (1997).

[3] M. Sarkar, P. Mukunda, P. Prajna,A and Bhowmick, Rubber Chem.Technol. **70**, 856 (1997).

[4] M. Garbarczyk, W. Kuhn, J. Kilnowski and S. Jurga, *Polymer.* **43**, 3169 (2002).

[5] D. Hertz, H. Bussem and T. Ray, "Nitrile Rubber-Past, Present & Future" *Rubber Division, American Chemical Society*, October 11-14, (1994).

[6] S. Bhattacharjee, A. K. Bhowmick and B. Avasthi. Modification of Properties of Nitrile, "*Handbook of Engineering Polymeric Materials*", Cheremisinoff, NP, Editor, Dekker, NY, 555 (1997).

[7] M. Morton, *Rubber Technology*, 3 rd ed . Van Noestrand Reinhold Company, New York (1987).

[8] S. Bhattacharjee, A. K. Bhowmick and B. Avasthi, *Polymer Degrad Stab*, **31**,71 (1991).

[9] S. Saha , *Eur Polym J.* **37**, 2513 (2001).

[10] D.K. Setua, A. K. Bhowmick and G. N. Mathur , *Polym Eng Sci.* **42**,10 (2002).

[11] C. Chaung and C. Han, *J Appl. Polym. Sci.* **29**, 2205 (1984).

[12] C. Ioan, T. Aberle and W. Burchard, *Macromolecules*. **34**, 326 (2001).

[13] S. H. Zhu and C. M. Chan, *Polym Eng Sci*. **39**, 1998 (1999).

[14] J. Clarke, B. Clarke and P. K. Freakley, *Rubber Chem.Technol*. **74**, 1 (2000).

[15] O. Chung and A. Y. Coran, *Rubber Chem.Technol*. **70**, 781 (1987).

[16] C. Sirisinha, S. Limcharoen and J. Thunyarittikorn, *J. Appl. Polym. Sci*. **85**, 1232 (2001).

[17] G. Severe and J. White, *J. Appl. Polym. Sci*. **78**, 1521 (2000).

[18] S. J. Ahn, K. H. Lee, B. K. Kim and H. M. Jeong, *J. Appl. Polym. Sci*. **78**, 1861 (2000).

[19] C. Sirisinha, S. B-Limcharoen and J. Thunyarittikorn, *J. Appl. Polym. Sci*. **87**, 83 (2003).

[20] S. Saha, *Eur Polym J*. **37**, 399 (2001).

[21] S. Schaal and A.Y. Coran, *Rubber Chem. Technol*. **73**, 225 (1999).

[22] S. Schaal and A.Y. Coran, *Rubber Chem. Technol*. **73**, 240 (1999).

[23] I. A. Hussein, K. Ho, S. Goyal, E. Karbashewski and M. Williams MC, *Polym Degrad Stab*. **68**, 381 (2000).

[24] O. Yasuda, T.Ougizawa, T.Inoue and K. Miyasaka, *j. Polym. Sci. Polym Letters Ed*. **21**, 813 (1983).

[25] C. E. Ioan, T. Aberle, and W. Burchard, *Macromol*. **34**, 326 (2001).

[26] C. Boisserie and R. H. Marchessault, *j. Polym. Sci. Part(B)*. **15**, 1211 (1977)

[27] A. W. Pross and R. M. Black, J. Sc of Chem Indus, **69**, 113 (1950)

[28] L. Sharma and T. Kimura, *Polym for Adv Tech*, **14**, 392 (2003)

[29] S. H. Hamid, A. G. Maadhah, F. S. Qureshi and M. B. Amin, *The Arab Journal for Sci and Engg*, **13**, 503,(1988).

[30] S. H. Hamid and W. H. Prichard, *J. Appl. Polym. Sci*. **43**, 651 (1991)

[31] G. Ivan, M. GIRGINCA and S. BASUC, Revue Roumaine de Chimie, **43**,231(1998)

[32] R. A. Chaudhry, MS. Thesis. KFUPM, Dhahran, (2003).

4.2 Study of the Miscibility and Mechanical Properties of NBR & HNBR Blends

4.2.1 ABSTRACT

In this study, hydrogenated acrylonitrile butadiene rubber (HNBR, ZETPOL-2110L) and nitrile butadiene rubber (NBR, NIPOL-DN4555) were blended at different ratios in a Haake melt blender at 130°C. The HNBR and the NBR were of very similar acrylonitrile content and Mooney viscosity. The melt miscibility and solid-state properties were investigated by rheological, thermal and mechanical testing and scanning electron microscopy (SEM) techniques. The dynamic viscosity of the blends followed log additivity rule, while the flow activation energy closely followed inverse additivity rule. On the other hand, the storage modulus showed synergistic effects at all compositions suggesting the presence of emulsion morphology at both ends of the composition range. For the 50/50 HNBR/NBR blend, the SEM micrographs suggest a uniform elongated structure. The thermal analysis showed the presence of two glass transitions, representing the pure components, at all blend ratios suggesting the absence of segmental miscibility of the blends. The small strain mechanical properties such as tensile modulus and yield stress followed linear additivity. However, HNBR and HNBR rich blends were observed to strain harden at a rate higher than that of NBR. Induced crystallization of HNBR was suggested to be the reason for the strain hardening. The different rheological, thermal, and

mechanical testing techniques agree in suggesting that the structurally similar HNBR and NBR are not thermodynamically miscible but mechanically compatible

4.2.2 INTRODUCTION

Nitrile butadiene rubbers (NBR) belong to the class of specialty elastomers that offer a broad range of thermal and oil resistance properties. These elastomers are extensively used in automobile and oil drilling applications [1]. Continuous performance demand by these industries led to the development of hydrogenated nitrile butadiene rubber (HNBR). Removal of double bond in the backbone of the polymer by catalytic hydrogenation results in improved UV and ozone resistance. The two main methods for this catalytic reaction are homogenous and heterogeneous catalytic reactions [2]. Most of the previous literature suggests that homogenous catalytic reactions were preferred over heterogeneous ones. However, the major weakness of homogenous catalytic hydrogenation reaction is the difficulty in removal of the catalyst from the polymer mixture and it is in fact the main reason for the high cost of HNBR [3]

Blending of rubbers is an important route for developing new polymeric materials with tailored physical properties. Blends of butadiene rubbers and other polymers have received wide attention in the literature during the last two decades [4-12,17-19]. The role of NBR as a compatibilizer has also been investigated [5]. Processing conditions, such as mixing speed, blending time, temperature ..etc, were reported to have a strong influence on the ultimate properties of the blend [6,8,15]. Also, blend morphology and compatibility were found to be affected by structural parameters such as acrylonitrile (ACN) content and Mooney viscosity [6,16]. These molecular parameters, characteristic of Nitrile

elastomers, influence blend miscibility as well as the size of dispersed phase [6]. Nitrile rubbers are considered to be polar rubbers [17].

Severe and White [18] studied the miscibility of HNBRs with chlorinated polymers and found that strong interactions between the functional groups are responsible for miscibility. HNBR was suggested to be immiscible with polyisoprene, SBR, and miscible with chlorinated polyethylene. Blends compatibility of NBR and other elastomers such as natural rubber (NR) [6,15] and polystyrene-co-acrylonitrile [16] were studied.

As mentioned earlier that the constraint offered by the difficulty in removal of the catalyst from HNBR is the main cause of its high price. Blending of unsaturated NBR and the more flexible HNBR molecules has its economic and scientific reasons. The available studies indicate that NBR and HNBR have been extensively studied for their blends with other plastics and elastomers. Interestingly, no studies were reported on the blends of NBR and HNBR elastomers.

In the present study, blend miscibility of NBR and HNBR were studied in the complete composition range. A study of the melt miscibility and its implications on the solid-state properties is performed using rheological; thermal analysis; mechanical testing; and scanning electron microscopy (SEM) techniques. This study will mainly highlight the compatibility of NBR/HNBR blends.

Blend morphology is also known to be an indicator of blend compatibility [6,10,15,18]. Generally, smaller phase size of the dispersed phase resulted in better blend compatibility, and improved properties [6,15,17]. For immiscible systems, the state of dispersion and the shape of the dispersed phase greatly influence the rheological responses. Emulsion morphology causes the storage, G′ and loss moduli, G″, to exceed values for the more

viscous component. Scholz et al [19,20], derived a constitutive equation for dilute emulsions of such nature. The two liquids are assumed to be incompressible and totally immiscible. The emulsion was shown to have dynamic moduli given by

$$G'(\omega) = \frac{\eta_m^2 \phi}{80(\alpha/R)} \left(\frac{19k+16}{k+1} \right)^2 \omega^2 \qquad (4.2.1)$$

where η_m, is the viscosity of the matrix liquid; η_d, the viscosity of the dispersed droplets; $k = \eta_d / \eta_m$; R, the radius of the dispersed domains; α, the surface tension between the two liquids; ϕ, the volume fraction of the dispersed phase. In thermal analysis, a single T_g is a proof of segmental mixing of polymer molecules; hence, blend compatibility [21].

4.2.3 EXPERIMENTAL

4.2.3.1 Materials

The NBR and HNBR samples used in this study were commercial samples obtained from Zeon Chemicals, USA. The NBR (NIPOL-DN4555) has an ACN content of 45%, specific gravity of 1, and a Mooney Viscosity of 48-63. On the other hand, the HNBR (ZETPOL-2110L) has an ACN content of 36, specific gravity of 0.95, a Mooney Viscosity of 50-65%, and a 96% degree of hydrogenation. The two polymers represent the best Zeon NBR and HNBR products that closely match the ACN content and Mooney viscosity (Mw) with the degree of hydrogenation as the major difference. Also, the high ACN content NBR was found easy to handle in the Rheological tests, compared to other low ACN content brands. Similarly, the HNBR selected for this study was one with high

level of Hydrogenation. The range of Mooney viscosities of the NBR and HNBR was close enough to reduce the effects of the viscosity ratio on blend miscibility [22]

4.2.3.2 Sample Conditioning and Blend Preparation

The elastomers used in this study were cut into small pieces and ground in a Fritsch Grinding mill. Pure samples as well as blends of 10, 30, 50, 70, and 90 % HNBR (w/w) were conditioned in a Haake Polydrive blender with Cam-type internal rotors. Conditioning was carried out at 130°C for 10 minutes and at 50 rpm. Due to high viscosity of the elastomers, the viscous heating effects were prominent, and in almost most of the cases the melt temperature was ~144°C. Earlier studies of degradation of these elastomers [23] showed that the NBR and HNBR rubbers were stable at this temperature. The agreement of the rheology and light scattering of as-received and conditioned samples suggests no degradation of NBR and HNBR during the conditioning process (23). Air cooled samples were molded in a Carver press at 150°C to form disks and then water cooled. The thermal and mechanical history in the press was the same for all samples. Samples from the press were molded in a form of 25 mm discs (2 mm thick) for later use in rheological and thermal analysis. For mechanical testing, samples were pressed in a form of sheets and dog-bones were later punched out using a hydraulic press.

4.2.3.3 Measurements in ARES

All rheological tests of the pure NBR and HNBR and their blends rubbers were carried out using a parallel plate fixture with a diameter of 25 mm. The use of cone-and-plate geometry was not possible due to loading problems. For all samples, a strain amplitude of 15% was found to be in the linear viscoelastic range following strain sweep

tests. The gap between parallel plates was fixed for all samples as 1.5 mm. The frequency, ω, sweep testing was carried out at 190°C in the range of ω =0.01-100 rad/ s. All measurements were conducted using nitrogen as a convective heating medium to avoid any possible oxidation during the sweep tests. Reproducibility tests were performed for the 50/50 blend. Results are shown in Figure 4.2.1. The agreement of both viscous and elastic properties shows the excellent reproducibility of the rheological measurements. In addition, frequency-temperature sweeps were performed in the range 200°-230°C to obtain the flow activation energy of NBR, HNBR and their blends. A thermal expansion coefficient of 2.5 microns/°C was used.

4.2.3.4 Differential Scanning Calorimetry (DSC)

The thermal properties of the blends were measured calorimetrically at a heating rate of 5 oC/min. A TA Instruments DSC 2910 equipped with Thermal Analyst 2200 software was used for this purpose. A blanket of nitrogen was maintained. Samples from the Carver press were used in this study. Samples of 5 to 10 mg were sliced and then compressed into aluminum pans for testing. Samples were cooled from room temperature to -80oC and then heated at the above mentioned heating rate to 40oC. Thermal transitions were obtained from the heating cycle.

4.2.3.5 Mechanical Testing

For the tensile properties, specimens were stamped out according to ASTM 638 (type V). The tensile tests were performed in an Instron 5567 tensile testing machine at room temperature. The gauge length was kept at 25 mm. The rate of grip separation was

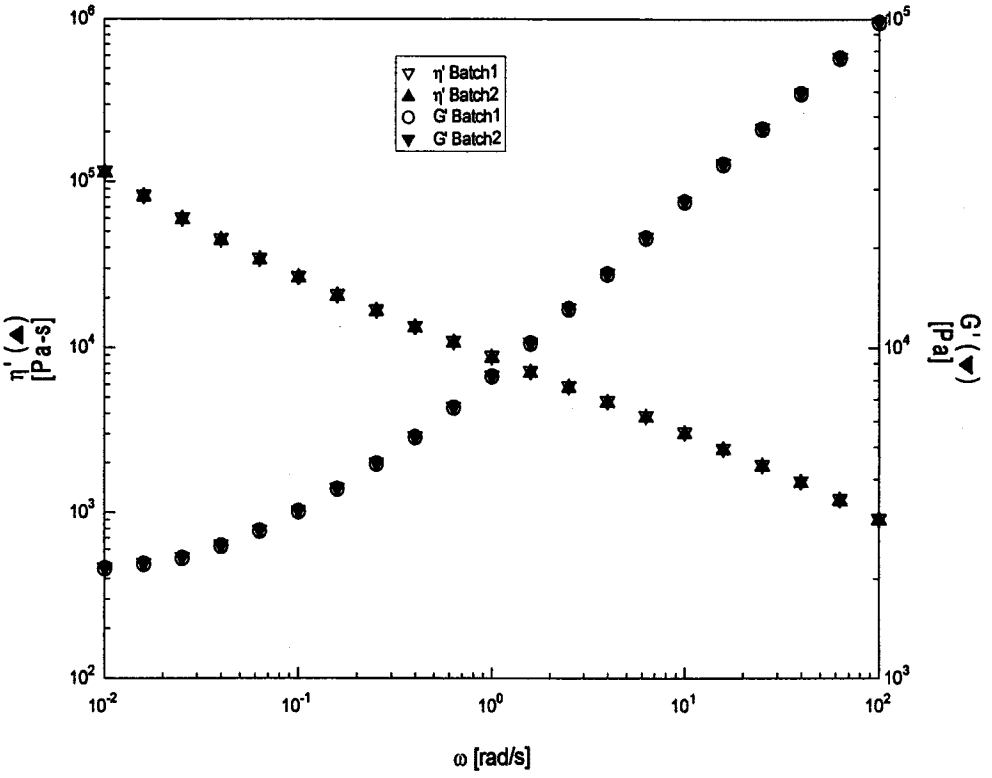

Figure (4.2.1) Reproducibility test. $\eta'(\omega)$ and $G'(\omega)$ for 50/50 blend

520 mm/s [24]. The results reported in this study were based on an average of a minimum of 5 samples.

4.2.3.6 Scanning Electron Microscopy

Scanning electron microscope (JEOL-JSM-T-300) was used for the morphology studies. The objective was to get information regarding the size of the dispersed phase in to the matrix. JEOL-FINE COAT ION SPUTTER was used to coat a thin layer of gold on the specimen to avoid electrostatic charging during examination. The specimens were thereafter mounted on aluminum stub for study.

4.2.4 RESULTS AND DISCUSSION

4.2.4.1 Rheiological Analysis.

Frequency sweep measurements were performed on blends of HNBR/NBR. Results for $\eta'(\omega)$ and $G'(\omega)$ for the 10, 30, 50, 70 and 90% HNBR blends as well as for the pure NBR and HNBR are shown in Figure 4.2.2. At low-ω, $\eta'(\omega)$ data did not show a Newtonian plateau, suggesting a yield behavior. For all blends, values of η' at all frequencies lie between the corresponding values of NBR and HNBR. The HNBR showed the lowest viscosity and the increase in η' of blends was proportional to the weight fraction of NBR. For $G'(\omega)$, results for the 10% HNBR blend were higher than the more elastic component (NBR) over a period of two decades. This positive deviation behavior (PDB) was also observed for other blend ratios. This behavior can easily be observed in

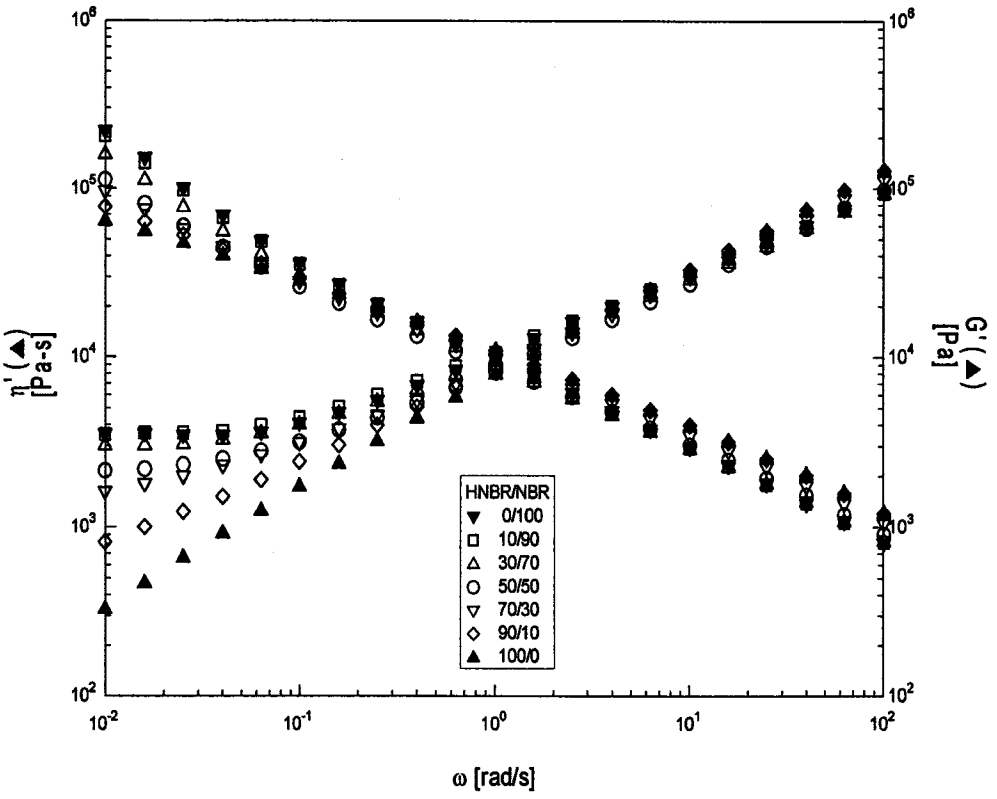

Figure (4.2.2) $\eta'(\omega)$ and $G'(\omega)$ for blends, as well as the pure samples.

Figure 4.2.3, which shows a plot of tan δ (G''/G') vs. ω. Also, it was observed that the cross over modulus for HNBR rich blends followed the linear rule of mixtures.

The increase in G' for the 10, 30, 50 and the 70% HNBR resulted in lower values of tan δ over almost two decades (0.01-1 rad/s). This low-ω range is sensitive to morphology. At high ω (>10 rad/s), values of tan δ were bounded between the pure components. However, such high frequencies are not used for the interpretation of miscibility data [20,25,26]. The described behavior of η' and G' can easily be observed in plots of η'(ϕ) and G'(ϕ) given in Figures 4.2.4a and 4.2.4b, respectively. η'(ϕ) followed log-additivity rule ($\eta'_{blend} = \sum \phi_i \log \eta_i$), while G'(ϕ) showed weak PDB. This is also evident in the wide differences between the predictions of Scholz et al. dilute emulsion model (see Fig. 4b) and the experimental data. The estimated value of α / R, calculated from Scholz et al. model (equation 1), for the 10% and the 90 % HNBR blends was 422 and 384 N/m^2, respectively. These values were in close agreement with previous reports of α / R for compatibilized blends [27]. The small value of α / R is likely not a result of high droplet size since the viscosity data do not support this argument.

Hence, the experimental data of ω-sweep tests and model predictions suggest the presence of emulsion morphology of very small droplet size that did not have a significant influence on the viscosity. However, this emulsion morphology is suggested to have a very weak interface as indicated by the small value of α / R. Hence, these blends are likely to be well dispersed at all compositions with very small droplet size. The suggested good dispersion is later validated by SEM micrographs.

In addition, the activation energy for the blends was calculated from the temperature-

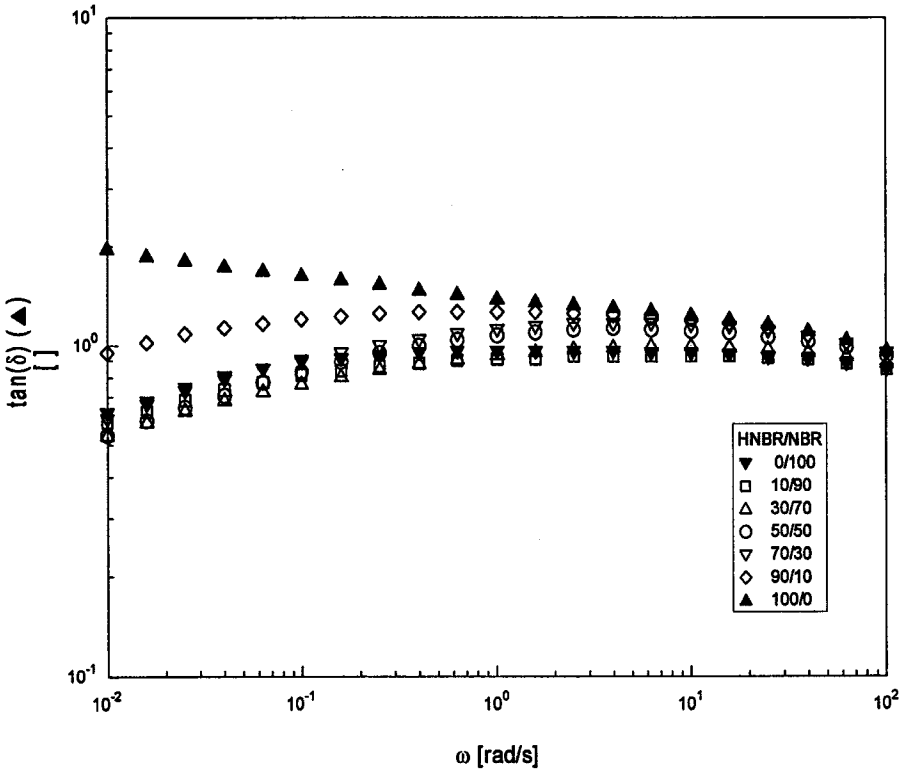

Figure (4.2.3) tan (δ) vs ω for blends. (Ttest =190°C, γ^{o}=15%)

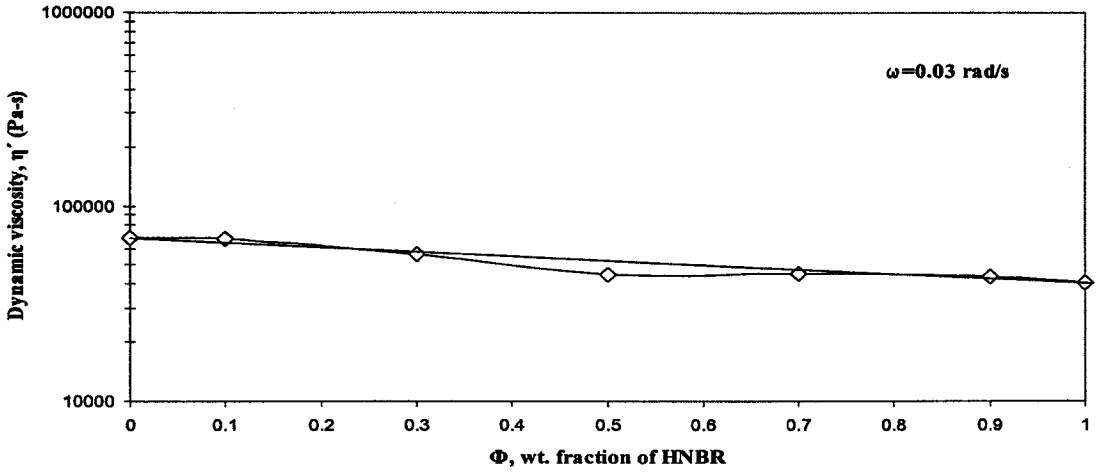

Figure (4.2.4a) Dynamic viscosity $\eta'(\phi)$ as a function of wt fraction of HNBR. (ω=0.03)

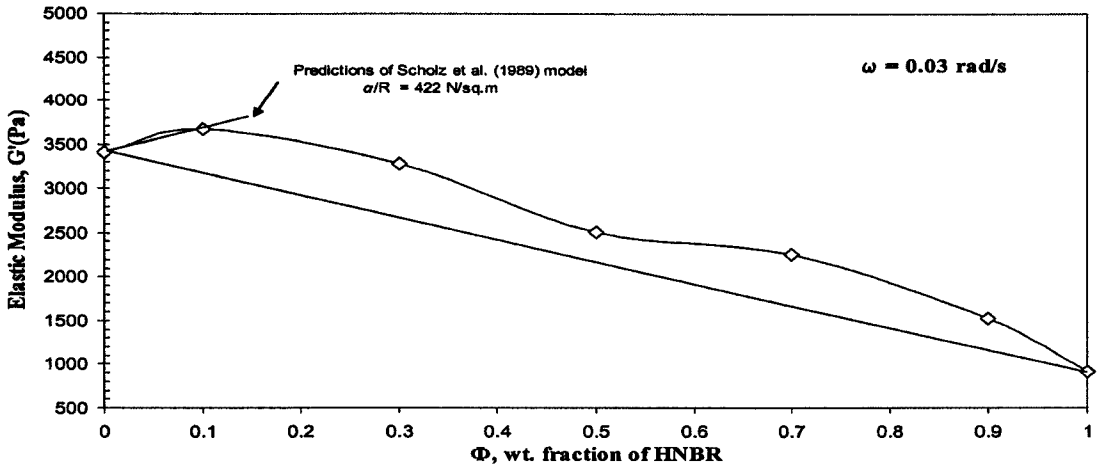

Figure (4.2.4b) Elastic Modulus G′(ϕ) as a function of wt fraction of HNBR (ω=0.03)

frequency sweep tests. Time-temperature superposition (TTS) principle was used to obtain master curves. The temperature was varied from 200° to 230°C at a step of 10°C and the frequency range was 100 to 0.1 rad/s. A typical curve for the 50/50 blend is shown in Figure 4.2.5. The flow activation energy, E, was calculated from the shift factor, a_T, using equation (4.2.2):

$$\log a_T = \frac{E}{2.303R}\left(\frac{1}{T} - \frac{1}{T_o}\right) \qquad (4.2.2)$$

where $a_T = \frac{\omega(T_o)}{\omega(T)}$; T and T_o are the current and reference temperature. The reference temperature was 210°C. Both a_T and E were calculated by ARES Orchestrator software. The flow activation energies for NBR, HNBR and their blends are displayed in Figure 4.2.6. Values of E(ϕ) for HNBR/NBR blends approximately follow the inverse additivity rule ($1/E_b = \sum \frac{\phi_i}{E_i}$).

4.2.4.2 Thermal Analysis.

To investigate the compatibility of NBR/HNBR blends DSC analysis was performed to measure T_g as a function of composition. Samples from the Carver press were analyzed according to the previously mentioned program. The DSC thermograms for the pure components as well as the blends are given in Fig 4.2.7. The glass transition for the flexible HNBR was -25.32°C (T_{g1}), while that of the less flexible NBR was -13.36°C (T_{g2}). It is clear that all blends showed two glass transitions marked as T_{g1} and T_{g2}. Results of T_{g1} and T_{g2} for all blends are given in Table 4.2.1.From the table as well as Fig 4.2.7 it

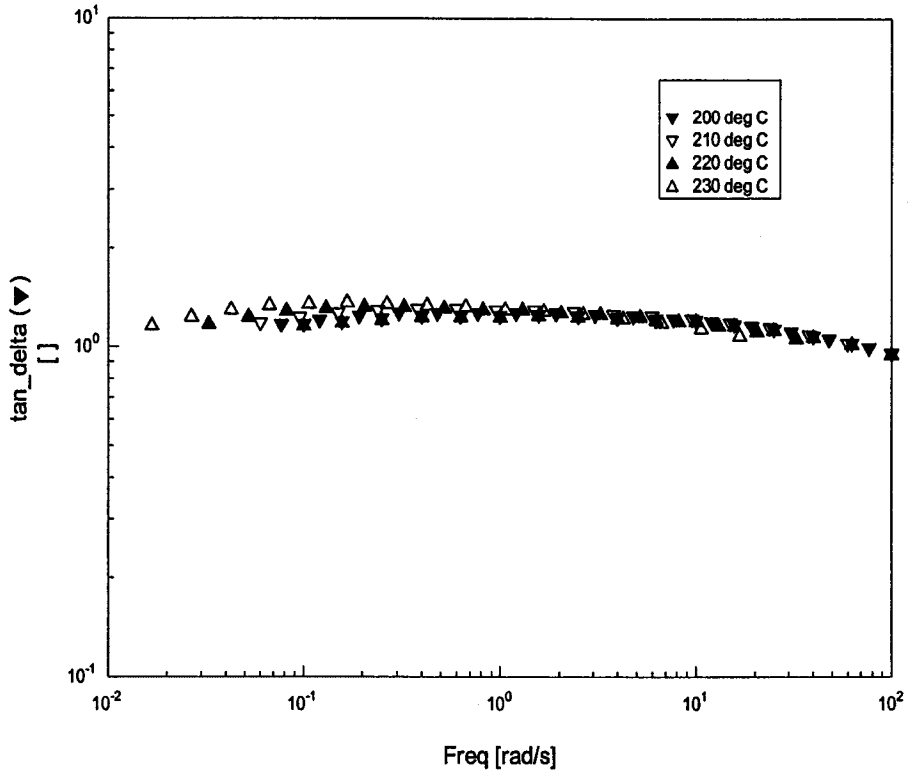

Figure (4.2.5) Master Curve for 90% HNBR blend (T_{test}=190°C,γ^{o}=15%, T_{range}=200°- 30°C)

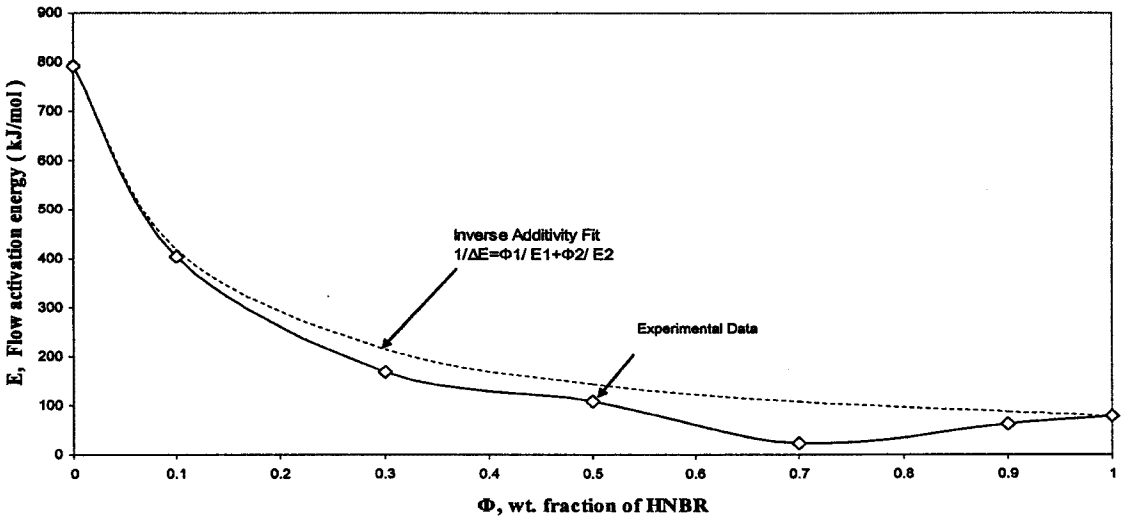

Figure (4.2.6) Flow Activation Energy vs wt fraction (ϕ) of HNBR

Table 4.2.1 Glass Transition Temperatures for blends and the Pure samples.

	5 °C/min		
	File Name	T_{g1} (°C)	T_{g2} (°C)
NBR	B1-5		-13.36
10%HNBR	B2-5	-26.62	-13.23
30%HNBR	B3-5	-25.71	-13.70
50%HNBR	B4-5	-26.27	-14.20
70%HNBR	B5-5	-25.93	-12.82
90%HNBR	B6-5	-26.01	-14.49
HNBR	B7-5	-25.32	

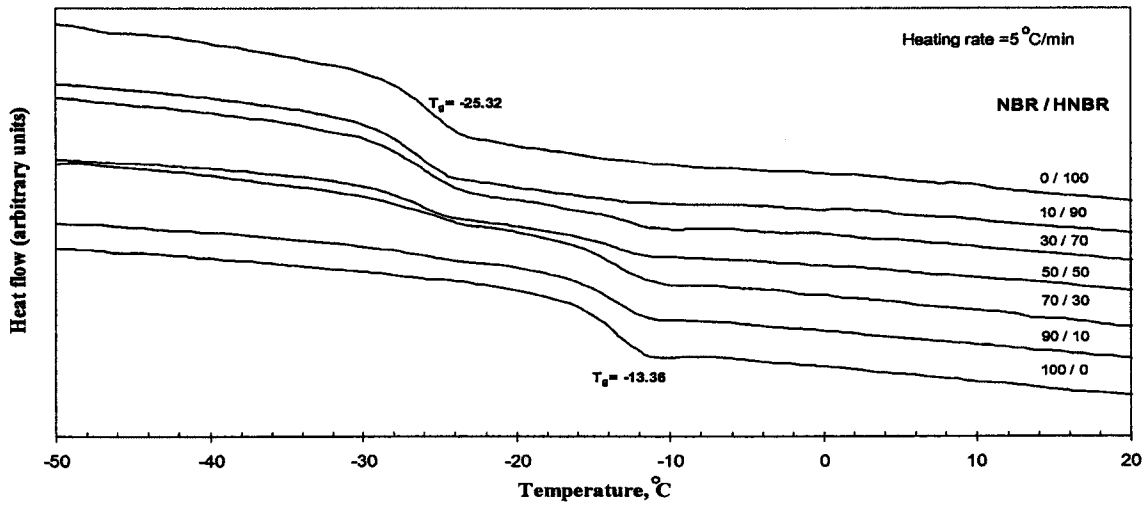

Figure (4.2.7) DSC Thermograms for blends of NBR/HNBR (heating rate =5 °C/min)

can be seen that each brand of rubber has approximately retained its value of T_g in the blend and only slight variations were observed.

These results suggest the absence of segmental mixing; hence, the absence of a single T_g. The fact that the rheological measurements suggested the presence of small droplets supports these observations presence of It seems that the small droplet size suggested by the rheology was not small enough to produce segmental mixing of NBR and HNBR which leads to a single T_g. Hence, these two blends are not thermodynamically miscible at the described mixing conditions. Yet, the blends could be mechanically compatible as discussed in the following section.

4.2.4.3 Mechanical Analysis

Results of the mechanical testing are given in Figures 4.2.8-10. In these figures the displayed mechanical properties represent the average of at least 5 independent measurements and the error bars show the range of these results. The tensile moduli as function of composition for blends of HNBR and NBR are shown in Figure 4.2.8. The modulus for HNBR is 1.37 MPa while that of the NBR is 1.61 MPa. The more flexible HNBR showed the least modulus and the unsaturated NBR was less flexible. In general, the moduli for the blends approximately follow the linear rule of mixtures. Also, results for the stress at yield are given in Figure 4.2.9. Similarly, the yield stress followed the linear rule of mixtures. So, results of Figures 4.2.8 and 4.2.9 suggest that at small deformations the blends show good compatibility.

At high strains, all blends as well as pure NBR and HNBR showed strain hardening . Tests were stopped due to slip and we were not able to break any of the

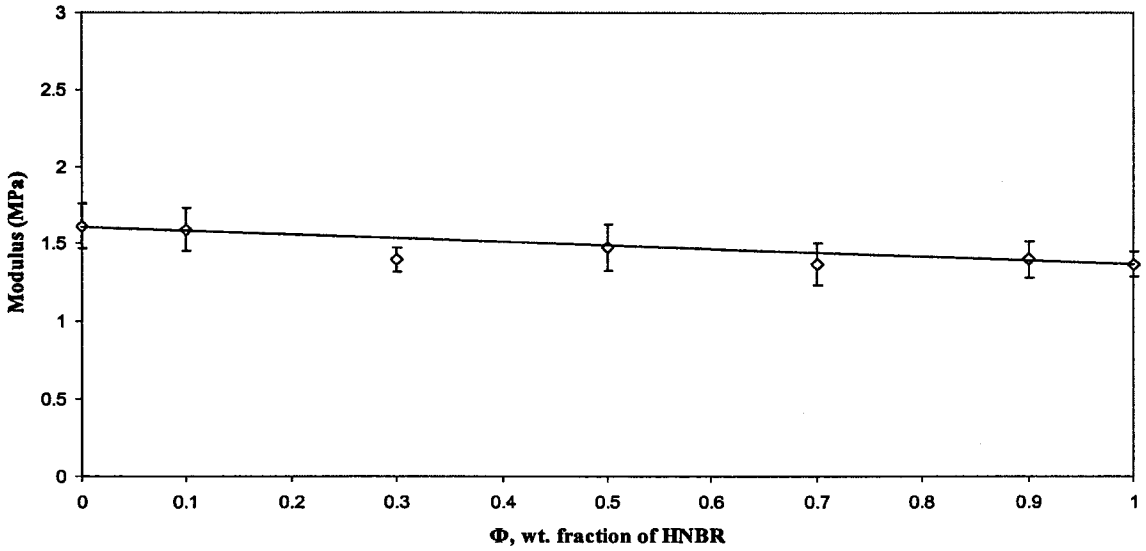

Figure (4.2.8) Tensile Modulus vs wt fraction of HNBR

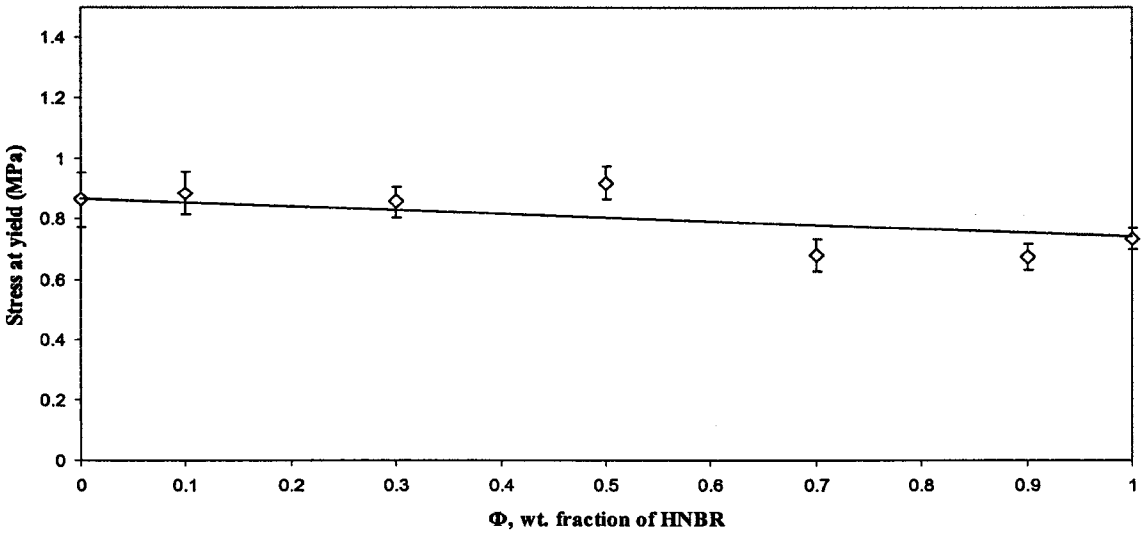

Figure (4.2.9) Tensile Stress at yield vs wt fraction of HNBR

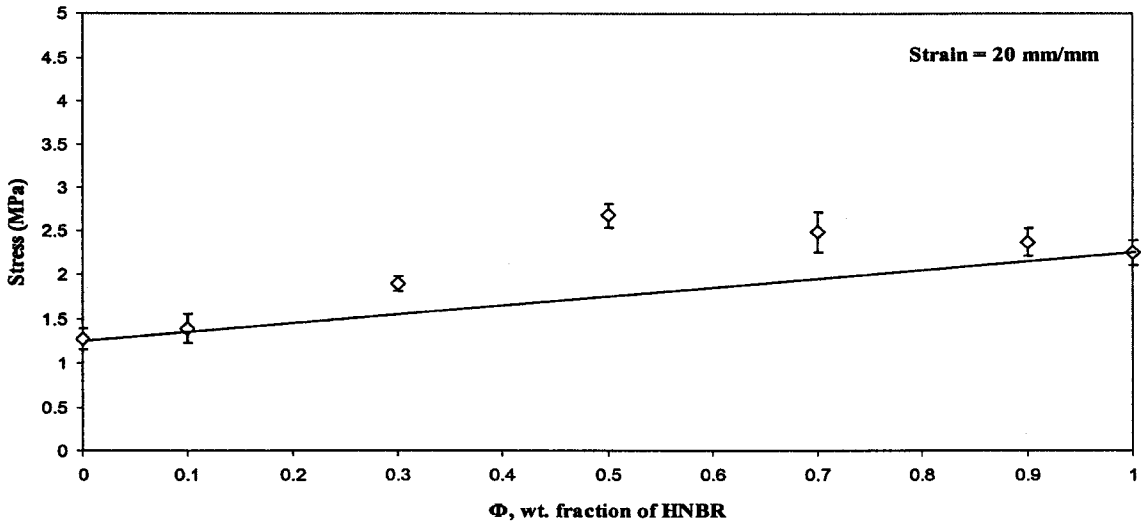

Figure (4.2.10) Tensile Stress at high Strain (200 mm/mm)

samples. Yet, a comparison of the stress at high strain (20 mm/mm) for all blends is given in Figure 4.2.10. In this case, the HNBR (low modulus) showed a stress (2.25 MPa) that is higher than that of NBR (1.27 MPa). This suggests that HNBR undergoes a strain hardening at a rate higher than that of NBR. This strain hardening could be a result of induced crystallization especially for this high ACN content HNBR [18]. For the 10/90 or the 90/10 HNBR blends the behavior of the stress at high strain rubber is linear. However, around the 50/50 composition the stress showed synergistic effects which are likely due to the presence of a different morphology as shown in the following section.

4.2.4.4 SEM

The SEM micrographs for the 10/90; 50/50; and 90/10 HNBR/NBR blends are shown in Figures 4.2.11 a, b and c, respectively. The 10/90 HNBR/NBR blend (Figure 4.2.11a) shows a dispersed and somewhat uniform morphology. The observed small clusters could be a result of the less flexible nature of the NBR which might have inhibited the dispersion of HNBR. These clusters could explain the increase in G′ which resulted tan δ values that are lower than that of the more elastic component (NBR) as shown in Figure 4.2.3. On the other hand, the 90/10 HNBR/NBR blend (Figure 4.2.11c) shows a uniform emulsion-like morphology which could be attributed to the flexible nature of the HNBR matrix. This observation is supported by the previous rheological measurements shown in Figure 4.2.3. There, the value of tan δ for the 90/10 HNBR blend was bounded by the corresponding values of NBR and HNBR. From figures 4.2.11a and 4.2.11c it is clear that the 90/10 HNBR/NBR blend (Figure 4.2.11c) is closer to emulsion morphology than the 10/90 HNBR/NBR blend. For the 50/50 HNBR/NBR blend, the

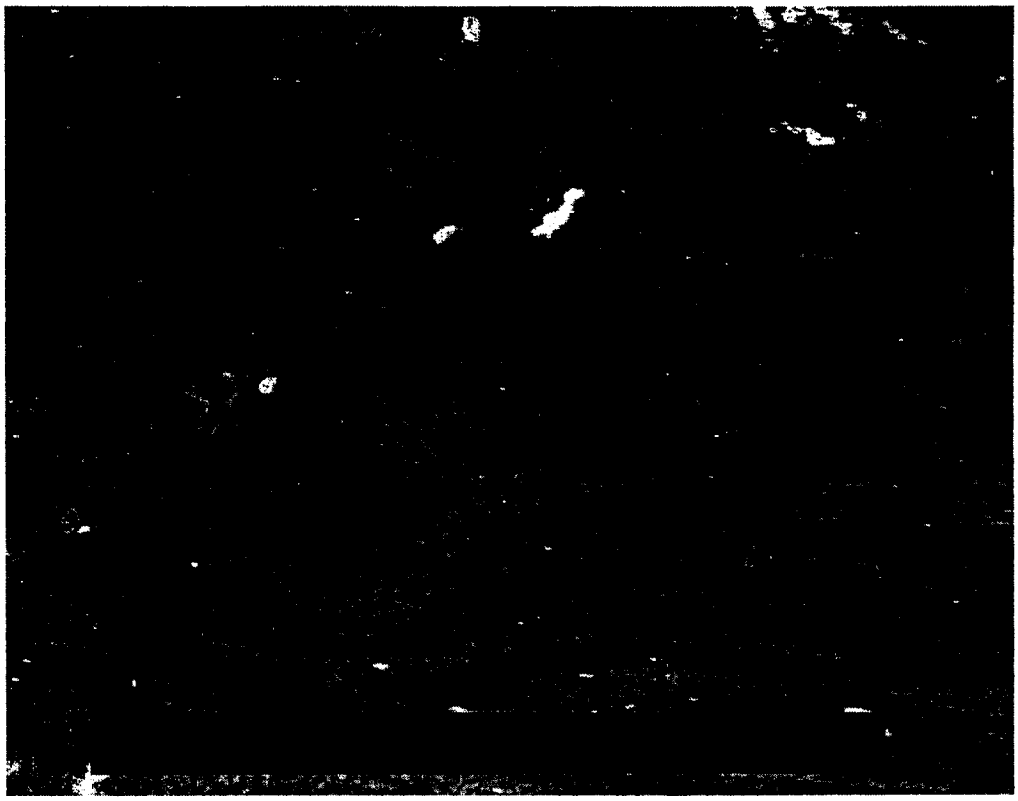

Figure (4.2.11a) SEM micrographs for 10/90 HNBR/NBR blends

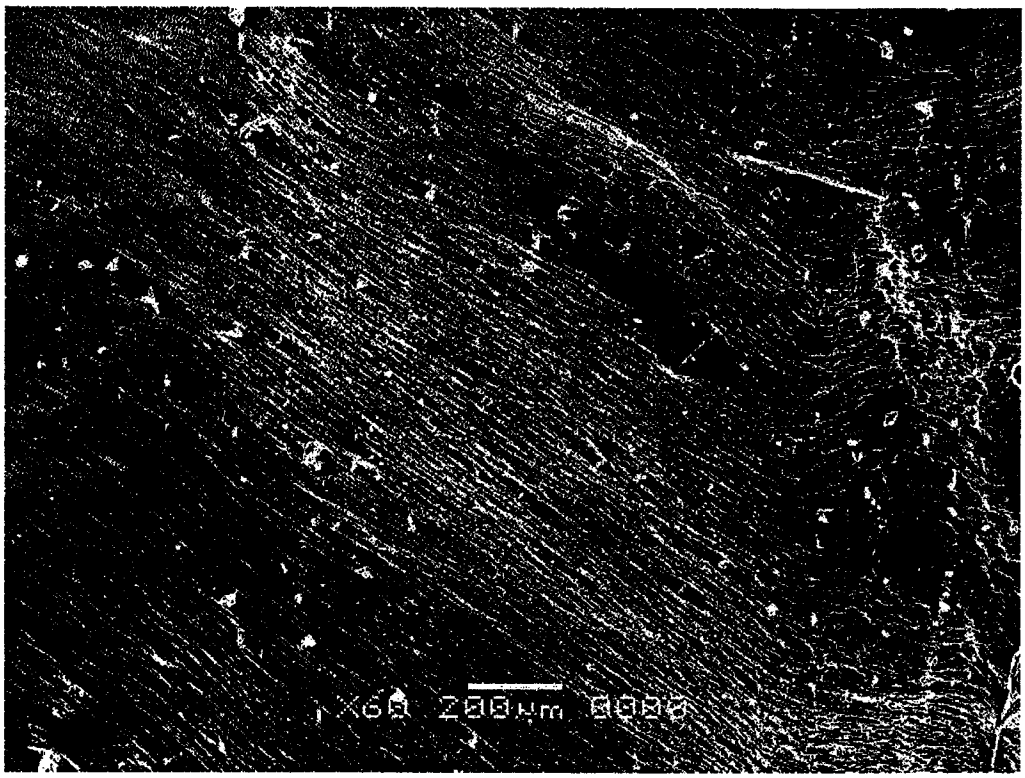

Figure (4.2.11b) SEM micrographs for 50/50 HNBR/NBR blends

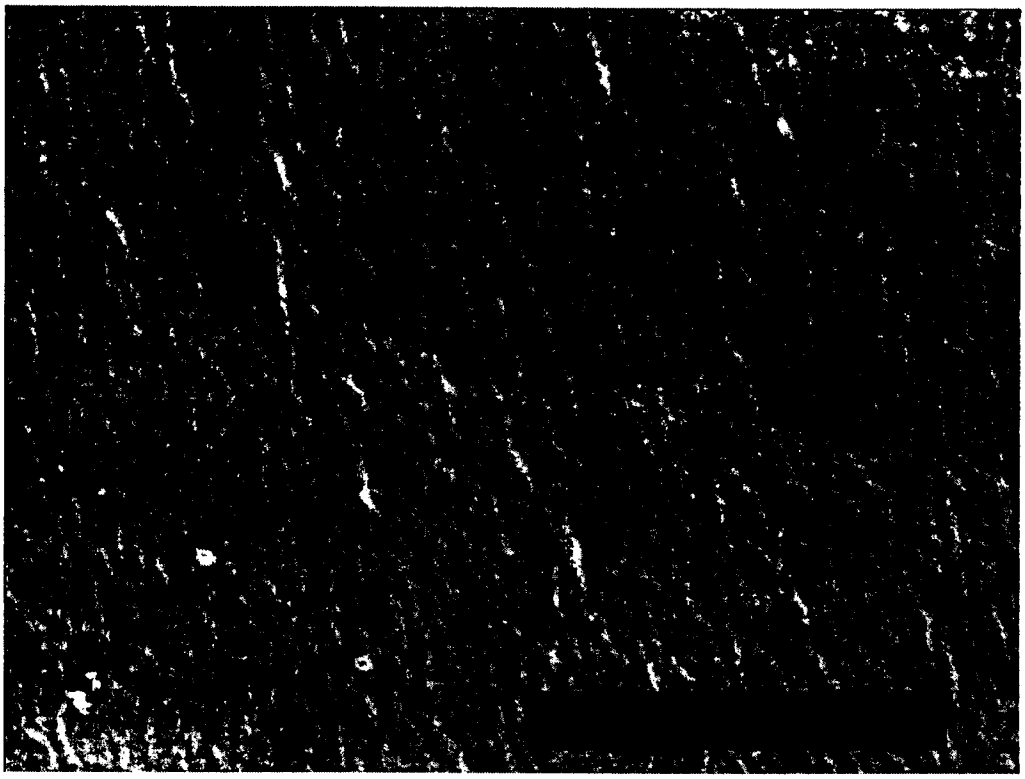

Figure (4.2.11c) SEM micrographs for 90/10 HNBR/NBR blends

SEM micrograph suggests a uniform elongated structure rather than emulsion morphology. This could be due to insufficient shear stress for disrupting these structures. Similar morphology was reported for blends of NBR and natural rubber [6].

4.2.5 Conclusion

In this study, HNBR and NBR of very similar acrylonitrile content and Mooney viscosity were blended at different compositions. The blends of the more flexible HNBR and the less flexible unsaturated NBR show interesting rheological, thermal and mechanical properties. The dynamic viscosity of the blends followed the log additivity rule, while the flow activation energy closely followed inverse additivity rule. On the other hand, the storage modulus showed synergistic effects at all compositions suggesting the presence of weak emulsion morphology at both ends of the composition range. This conclusion is supported by thermal analysis that showed the presence of two glass transitions, representing the pure components, at all blend ratios. For the 50/50 HNBR/NBR blend, the SEM micrographs suggest a uniform elongated structure rather than emulsion morphology. The small strain mechanical properties such as tensile modulus and yield stress followed linear additivity. However, HNBR was observed to strain harden at a rate higher than that of NBR. Induced crystallization of HNBR was suggested as a reason for the strain hardening of HNBR rich blends. In conclusion, the different rheological, thermal, and mechanical testing techniques agree in suggesting that the structurally similar HNBR and NBR are not thermodynamically miscible but mechanically compatible.

4.2.6 References

[1] Hofmann W. Rubber Chem Technol 1963;37:52

[2] Schulz DN, Turner SR, Golub MA. Rubber Chem Technol 1982;55:809.

[3] Bhattacharjee S, Bhowmick AK, Avasthi B. Modification of Properties of Nitrile, "*Handbook of Engineering Polymeric Materials*", Cheremisinoff NP, Editor. Dekker. NY; 1997.

[4] Da Silva AN, Rocha M, Coutinho FM, Bretas R, Farah M. Polymer Testing 2002; 21: 647.

[5] Zhu S-H, Chan C-M. Polym Engng Sci 1999; 39:1998.

[6] Sirisinha C, Limcharoen S, Thunyarittikorn J. J Appl Polym Sci 2001; *85*:1232.

[7] Chee MJK, Ismail J, Kummerlowe C, Kammer H. Polymer 2002; 43: 1235.

[8] Saha S. Eur Polym J 2001; 37: 399.

[9] Saha S. Eur Polym J 2001; 37: 2513.

[10] Boisserie C, Marchessault RH. J of Polymer Sci 1977; 15: 1211.

[11] Setua DK, Soman C, Bhowmick AK, Mathur, GN. Polym Engng Sci 2002; 42: 10.

[12] Lee JH, Lee JK, Lee KH, Lee CH. Polymer Journal 2000, 32, 321.

[13] Coran AY, Patel R, Williams-Headd D. Rubber Chem.Technol 1985;58:1014.

[14] Anthony P, De SK. Rubber Chem Technol 1997;*74*:376.

[15] Clarke J, Clarke B, Freakley PK. Rubber Chem Technol 2000; 74:1.

[16] Ahn SJ, Lee KH, Kim BK, Jeong HM. Appl Polym Sci 2000; 78:1861.

[17] Chung O, Coran AY. Rubber ChemTechnol 1987;*70*:781.

[18] Severe G, White J. J Appl Polym Sci 2000;*78*:1521.

[19] Jha A, Bhowmick AK. Rubber Chem.Technol 1997;*70*:798.

[20] Scholz P, Froelich D, Muller R. J Rheo 1989;33:481.

[21] Paul DR. Polymer Blends, 2nd ed .Academic Press, New York: 2001.

[22] Utracki LA. Polymer alloys and blends: thermodynamics and rheology. NY: Hanser; 1989.

[23] Chaudhry RA. "Degradation of NBR and HNBR: Rheological, light scattering and Molecular Simulation Study", *MS Thesis*, KFUPM, Dhahran, January 2004.

[24] Brown RP. *PHYSICAL TESTING OF RUBBER*, 2 nd ed. Elsevier Applied Science Publishers,NY;1986.

[25] Hameed T, Hussein IA. Polymer 2002;43:6911.

[26] Hussein IA. Macromolecules 2003; 36:2024. Erratum: 36:4667

[27] Brahimi B, Ait-Kadi A, Ajji A, Jerome R, Fayt R. J Rheol 1991;35:1069.

4.3 Miscibility of HNBR and NBR Rubber Blends: A Molecular Dynamics Investigation

4.3.1 ABSTRACT

Binary blend compatibility of a nitrile elastomer blend (NBR/HNBR) was studied for complete range of composition for a single system. An atomistic modeling approach was employed to calculate the classical Flory-Huggins interaction parameterχ, for the pure samples as well as for the blends. High temperature equliberation steps were followed by data collection steps at room temperature. A COMPASS force field was used for the evaluation of cohesive energy density. The results were compared to mechanical testing and rheological results reported by a different study. The blends were generally found to be miscible. Lower values for χ parameter (increased compatibility) were found for all the blends. Values of cohesive energy density were also found to be in linear correspondence with the pure ones. Results were found comparable with those reperted in rheological and mechanical studies. The dispersed and micelle like, and layered morphology ,found in the SEM micrographs for such physical systems was found to be due to processing shortcomings, and high visous nature of these materials rather then molecular and thermophysical interactions.

4.3.2 INTRODUCTION

Different polymers exhibit different advantages and limitations in their properties. For example, natural rubber NR has excellent mechanical properties, but poor thermal and oil resistance, Nitrile rubber NBR on the other hand show the opposite trend. So development of new application specific polymers has always been a hot area. Other widely accepted and used method to obtain products of desirable properties is blending of different polymers. Sometimes we want a material that has the some of the properties of one polymer, and some of the properties of another. Instead of going back into the lab and trying to synthesize a brand new polymer with all the properties we want, we try to mix two polymers together to form a blend that will hopefully have some properties of both. Experimental tests are both time consuming and expensive at times as they require a new polymer actually be synthesized and processed. The ability to predict blend miscibility or degradation by computer aided simulation can be significant as little or no experimental work is required ,that not only saves time but money. Computer simulations have been used to investigate degradation [1] and miscibility [2] in cited literature.

Nitrile rubber (Butadiene-acrylonitrile copolyers) NBR, were first commercialized by I,G Farbindustry, in 1937 as Buna N and later as Perbunan. NBR always had problems with degradaing agents, such as UV light, Ozone, Organic materials, and thermal effects etc, and as the performance demands of the automotive and oil industry increased, another high performance elastomer emerged known as HNBR [3]. The new product Hydrogenated Nitrile rubber as it is known, was just a derivative of NBR, formed by selective hydeogenation of the olefinic unsaturation present in the butadiene of the copolymer. HNBR is an oil-resistent, elsotomer with more thermal stability (resistant to oxidation)

than NBR, polybutadiene, and particularly polyisoprene. Despite of its excellent and broad range of properties, exhibited by a wide variety of brands (varying in three characteristic parameters ACN content, degree of hydrogenation, and Mooney Viscosity) it was reported that the materal undergoes stress-induced crystallization similar to natural rubber. Another weakness of HNBR formed by homogenous catalytic hydrogenation is the removal of the catalyst from the polymer mixture. This is the main reason for the high cost of hydrogenated nitrile rubber. So to improve the final product properties and abtain materials of desired characteristics, extensive blend studies of HNBR with other polymers and elastomers have been found in literature. Most of the basic studies of properties of HNBR have been published by two companies BayerAG and Nippon Zeon, which now manufacture this polymer. In the present study binary blend compatability of NBR and HNBR is studued for a range of composition, by Atomistic and Mesoscopic Simulations. The Flory-Huggins solvent interaction parameter χ is a temperature dependent, dimensionless quantity, which characterizes polymer-solvent interactions. It is a complex parameter, that contains both enthalpy and entropy contributions[5]. The χ parameter was calculated for different compositions to see whether there existed any interactions between these polymers. The χ values obtained from the atmistic simulations were, subsequently supplied into Dissipative particle dynamics (DPD) simulations. The derivation of input parameter (χ) from more detailed atomistic simulation implied that the underlying chemistry of the system was included in the DPD simulations. This way the short scale characteristics were, now, absorbed into large structureless beads.

In the following sections are given the simulation details. The system detail and model construction are given in section 4.3.3.1 and 4.3.3.2 respectively, the atomistic simulation details in 4.3.3.3, and methodology for (DPD) mesoscopic simulation in 4.3.3.4. The results of the atomistic and mesoscopic simulations are discussed in 4.3.4.

4.3.3 COMPUTATIONAL DETAILS

4.3.3.1 System Details

For the NBR and HNBR,s used in this study, an ACN content of 30 % was selected for both brands, For the HNBR ~99.9 hydrogenation was selected. Both of these brands are available commercially (Zeon Chemicals). Values of density were obtained from the Nippon chemicals product information. In this study only one mixture of NBR & HNBR was investigated. The volume fraction of HNBR in the mixture was (0.1666, 0.333, 0.5, 0.666, 0.83) .

4.3.3.2 Model Construction

As a first step the basic structures of the oligomers were constructed. A backbone of 80 C atoms containg four blocks of ACN and Butadiene. The block representation can be shown as A-B-A-B, where (A:Acrylonitrile, B:Butadiene). Having a quick look at the structurer of NBR shows, that it is a complex structure .Being a copolymer of butadiene and acrylonitrile, it contains blocks of these structures. The ACN part of the oligomer is known to be the more charged or polar part of the chain. Hofman attributed this to the withdrawal of electrons from the α-methylenecrbon by the nitrile group, as shown:

$$\begin{array}{l} \delta- \quad \delta++ \qquad \delta- \\ -CH-CH_2-CH=CH- \\ \quad | \\ \quad C\equiv N \end{array}$$

Butadiene monomer copolymerizes into three distinct structures i.e: trans, cis and 1,2.

In a typical nitrile rubber, the following recipie for the structure was reported in literature. Trans configuration is ~78%, cis configuration ~12 %, and ~10% is free vinyl groups[4]. ACN groups are inserted in a statistical pattern ranging from head-tail, head-head and tail-tail, while butadiene is added in the % that was mentioned earlier. The distribution of different isomers into the main structure was taken care of. To convert the NBR to HNBR, all the double bonds present in the butadiene part were saturated. Values of densities of these structures were taken from commercially available brands of Zetpol HNBR having similar Mooney Viscosity range. The respective densities were, NBR=0.975 g/cm^3, and HNBR=0.95 g/m^3. These values were assumes independent of chain length, and equal to the densities of the high MW homologues.

The amorphous phases were constructed by Amorphous-Cell construction program of the Materials Studio (Accertrys Inc). Each cell contained 6 oligomers in total in all the simulations both for pure or for blends.

4.3.3.3 Atomistic Simulations

This study focused the binary blend compatability of NBR ,and highly saturated HNBR. Three systems of each pure NBR and HNBR were constructed at room temperature and equiliberated at various high temperatures (500,600,650°K) for 200 ps (pico second). A time step of 1 fs (femto second) was used in these Atomistic simulation. COMPASS force field was used to model the interatomic interactions between the chains.

This is the force field used to predict structural and thermophysical properties of most organic molecules including polymers. Its energy expression is a combination of valence terms, bond angles,a Coulombic term for the electrostatic interactions, and a Lennard-Jones function for thee van der Walls interactiona[6] . The simulations were carried out in the NVT ensemble with Periodic Boundary Conditions. Then these were equiliberated at room temperature, for 300 ps. For the blends average density was calculated depending on the fraction of polymer in the blend, and again systems were subjected to high and low temperature equiliberation steps. The criteria for equiliberation was developed by monitoring the energy of the system to make it sure that it fluctuates around an average value. Once equliberation achieved, a number of data collection steps followed, at room temperature. The cohesive energy density (CED) of the pure components as well as the mixtures was calculated, from which the χ parameter was derived as a function of composition of different blends.

4.3.3.4 Mesoscopic (DPD) Simulations

Mesoscopic simulations for the blends were performed using DPD program of Material studio (Accertrys Inc). DPD is a mesoscale dynamic simulation that spans length and time scales due to coarse-grained nature of the potentials. The input repulsion parameter for these simulations was obtained from the χ values obtained earlier in the atomistic simulations. The species NBR and HNBR were defined with their amounts specified according to the blend ratio.

4.3.4 RESULTS AND DISCUSSION

4.3.4.1 Atomistic Simulations.

Atomistic simulations were performed for the two pure elastomers using NVT ensemble, from which the values of CED were calculated. Different initial configurations were used to obtain an arithmetic mean value of the CED for the two pure samples. Similarly for blends various data collection steps were performed after the initial high temp and low temp equiliberation. An amorphous cell for the 2/4 NBR/HNBR blend is shown in Figure 4.3.1, as a typical example of the system being studied. The tendency of the polymer to mix at a specific composition was estimated via the CED values of the mixtures and the pure components [2]. The ΔE_{mix} for a binary mixture is defined as

$$\Delta E_{mix} = \phi_1 \left(\frac{E_{coh}}{V} \right)_{pure1} + \phi_2 \left(\frac{E_{coh}}{V} \right)_{pure2} - \left(\frac{E_{coh}}{V} \right)_{mix} \qquad (4.3.1)$$

where ϕ is the volume fraction and the indices pure and mix denote that CED values refer to pure and binary mixtures. Then the χ parameter was estimated as

$$\chi = \left(\frac{\Delta E_{mix}}{RT} \right) V_{mon} \qquad (4.3.2)$$

Figure 4.3.2 shows the CED values of blends as a function of HNBR fraction. All the values for the blends were almost inbetween the pure components indicating miscibility. This linear additivity trend was also found in the mechanical properties for these blends (reported in another study) [7] .Figure 4.3.3 shows the χ parameter as a function of blend composition. The χ parameter controls the interaction between the polymers,if positive; the two species prefer to phase separate, whereas if it is negative

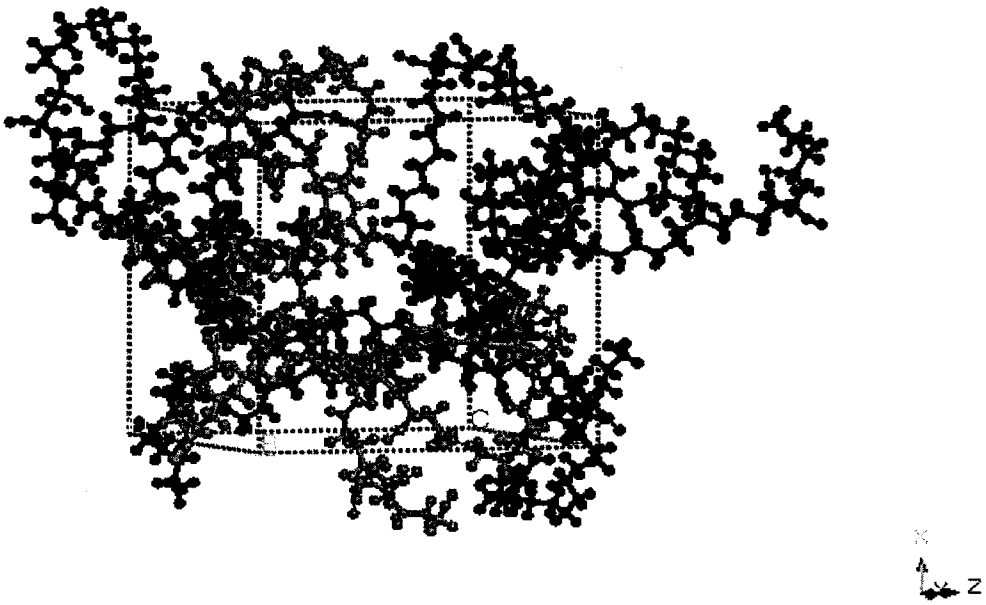

Figure (4.3.1) Amorphous cell of NBR/HNBR in 2/4 ratio. The cell contains 6 chains in total. HNBR chains are black, while the NBR as grey.

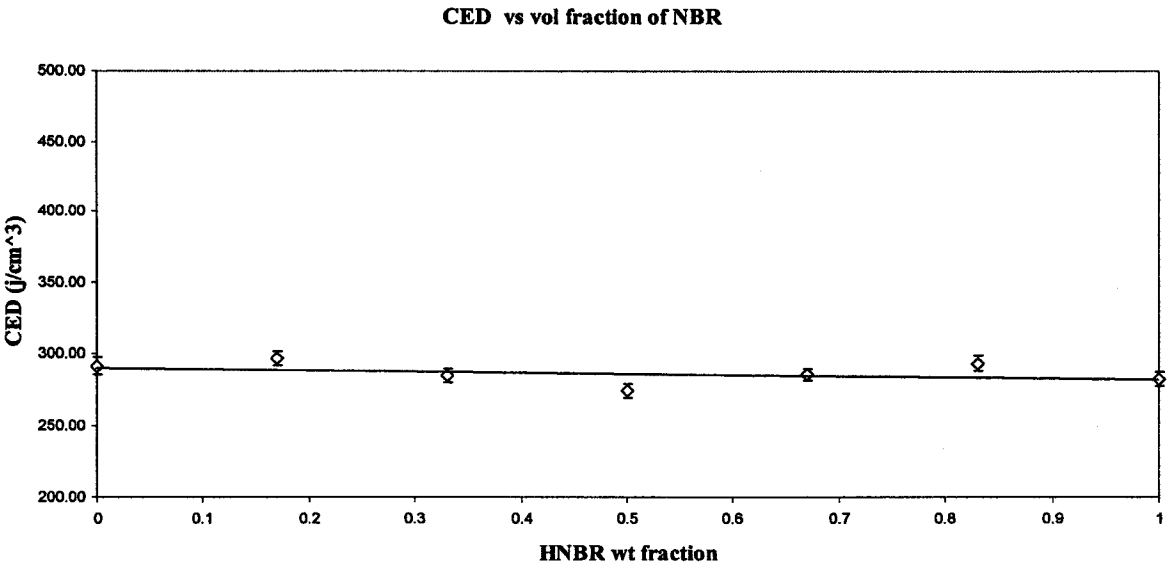

Figure (4.3.2) Cohesive Energy Density as a function of blend composition.

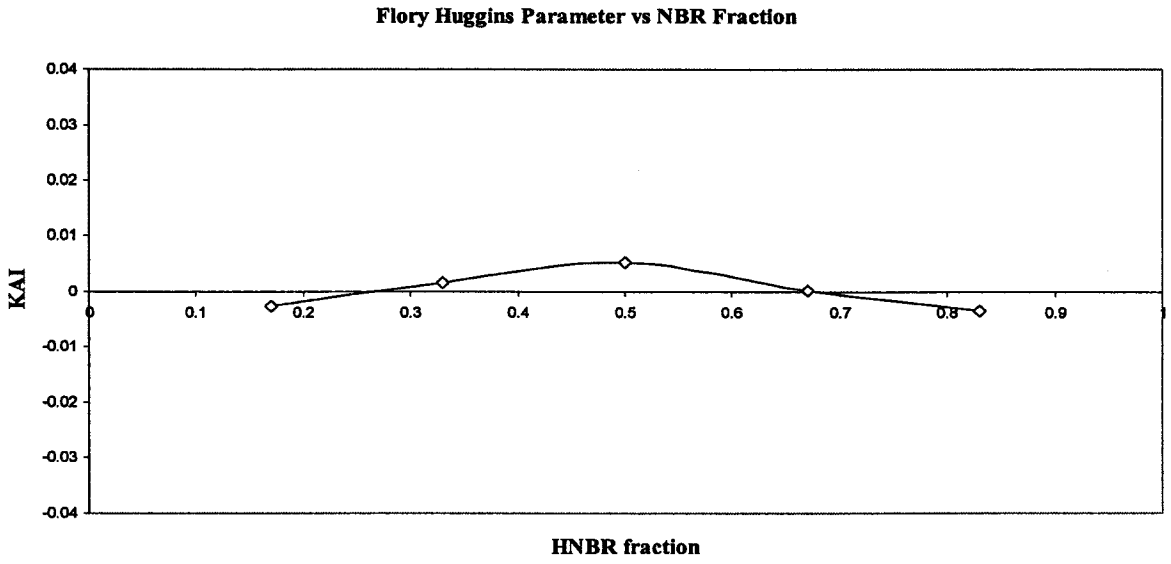

Figure (4.3.3a) χ parameter as a function of blend composition.

they prefer to mix. The χ values for both polymers were almost similar. The blends did not show linear dependence of χ on blend composition rather minor level of incompatibility (positive value of χ) was present especially at high volume fractions (close 0.5). However, the values of χ are so small indicating that misibility is very possible throughout the range of composition. The previous studies[2] showed a χ value of 0.3-0.4 to be high enough to cause incompatibility. While in our present case all values are smaller then 0.01. It is interesting to compare this result to an experimental result of a rheological study made for these blends. Fig (4.3.3b) shows dynamic viscosity as a function of blend composition. The values of dynamic viscosity also show slight deviations from the linear dependence, and especially at (50/50) compositon. Again the effect was very small that generally the materials were considered to be miscible.

4.3.4.2 DPD Simulations.

In the DPD simulations the model beads stood for high Mw polymers. Initial configurations, type and extent of species (NBR/HNBR) were supplied to the program and the systems were let to evolve toward equilibrium (phase separation or mixing). Mixture compatibility was deducted from the final equilibrium morphologies and comparison with SEM micrographs of the actual blends.

Figure 4.3.4 and Figure 4.3.5 show the final morphologies for the 1/9 and 9/1 blends of NBR/HNBR after the DPD simulations. The structures show quite uniform mixing of the two species in booth cases as expected (atomistic simulations), indicating miscibility. No indication of any phase separation or micelle formation was found.

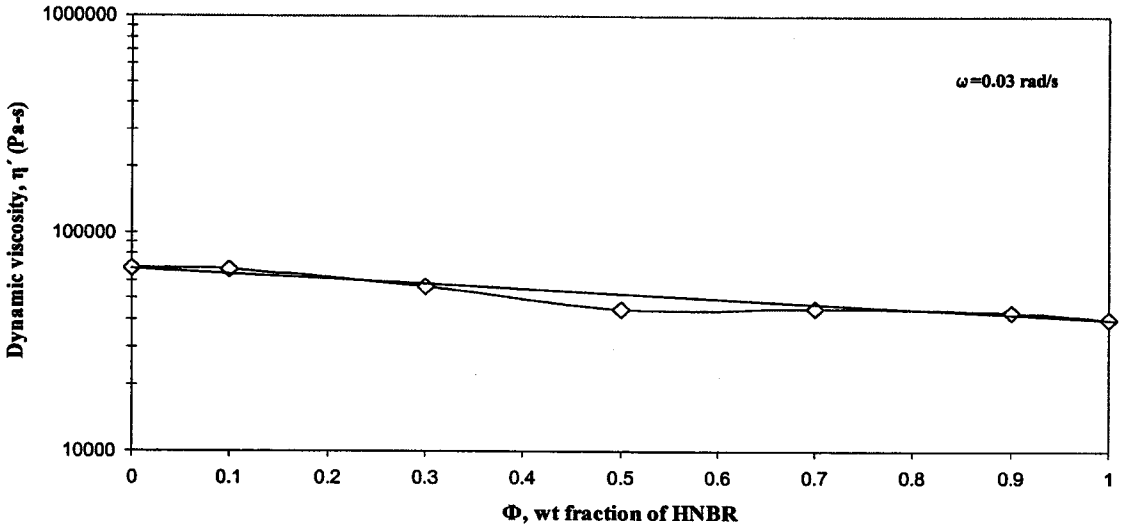

Figure (4.3.3b) Dynamic viscosity as a function of blend composition .

Figure (4.3.4) Profile of 1/9 NBR/HNBR blend after DPD equiliberation

Figure (4.3.5) Morphology of 9/1 NBR/HNBR blend after DPD equiliberation

Figure 4.3.6 shows the SEM micrographs for the 1/9 NBR/HNBR blend. In the picture it is clear that the blend is a uniform mixture of the two rubbers. The overall emulsion like morphology is in well agreement with the results from the simulation for this blend shown in figure 4.3.4. Figure 4.3.7 and Figure 4.3.8 show micrographs for 9/1 NBR/HNBR blend. Looking at the pictures we can see that there existes a dispersed black (HNBR) phase in the matrix of somewhat grey (NBR) phase. However this dispersion is non uniform and shouldent be mistaken as phase separation or micelle formation. As no such evidence was found by the DPD simulations for this sample (Figure 4.3.5) rather the mesoscopic simulations reported perfect mixing and hence compatibility of the two materials. These small clusters of HNBR (black) in the matrix of NBR (white) in figure 4.3.7 and 4.3.8 were infact due to the reason of insufficient mixing of the two materials, the highly viscous nature of the elastomers and relatively leass flexible nature of NBR as compared to HNBR. The blending conditions that were employed (rpm = 50, t= 10 mints) [7] were not sufficient enough to cause the two materials to mix properly resulting in a homogenous phase. The shear stress required to disrupt the molecular structures and cause segmental miscibility was not sufficiently provided during the blending process. Otherwise the DPD results showed no reason for these two materials to result in a single phase and hence be miscible. Its interesting to see a third picture of 1/9 NBR/HNBR blend shown in the Figure 4.3.9. Here again we can see a cluster of black phase in the centre right part of the snap, but the part of interest is the region surrounding this black cluster that shows the mixing of the two species resulting in a hazy blackish grey region joining the black (HNBR) and grey matrix of NBR. This clearly indicates that the two materials

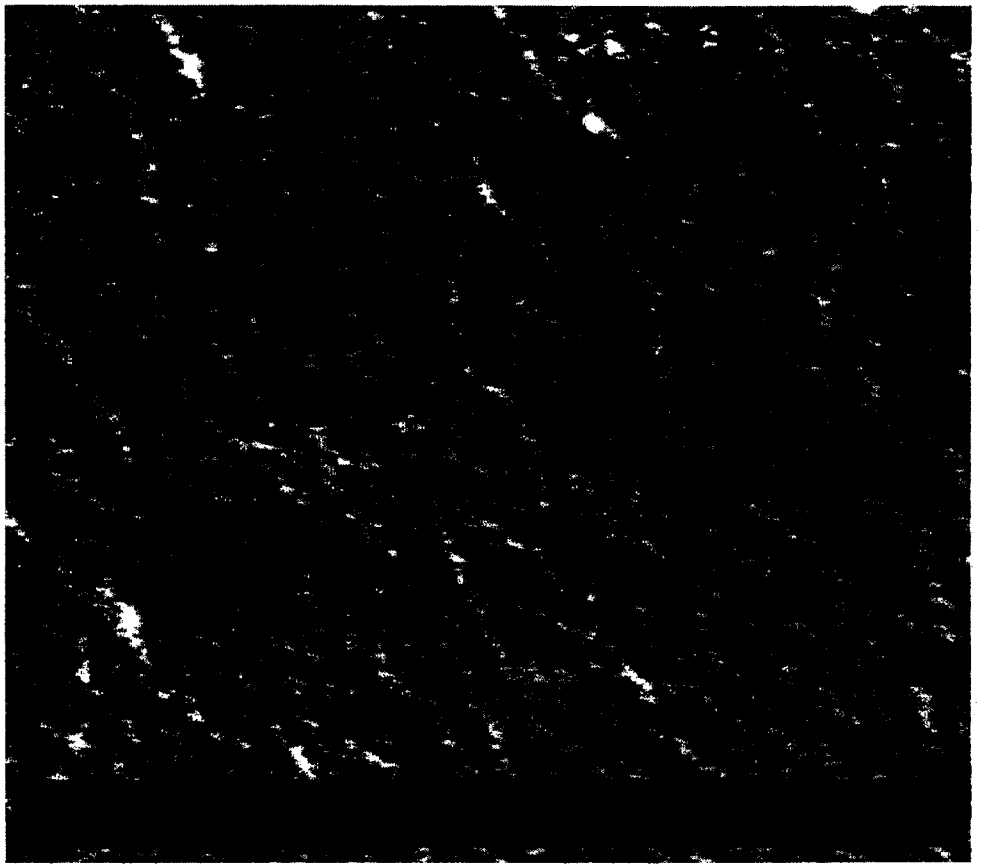

Figure (4.3.6) Micrograph of 1/9 NBR/HNBR blend (The Black line at the base shows the scale of 100 μm)

Figure (4.3.7) Micrograph of 9/1 NBR/HNBR blend (The Black line at the base shows the scale of 100 μm)

Figure (4.3.8) Micrograph for 9/1 NBR/HNBR blend (black line= 100 μm)

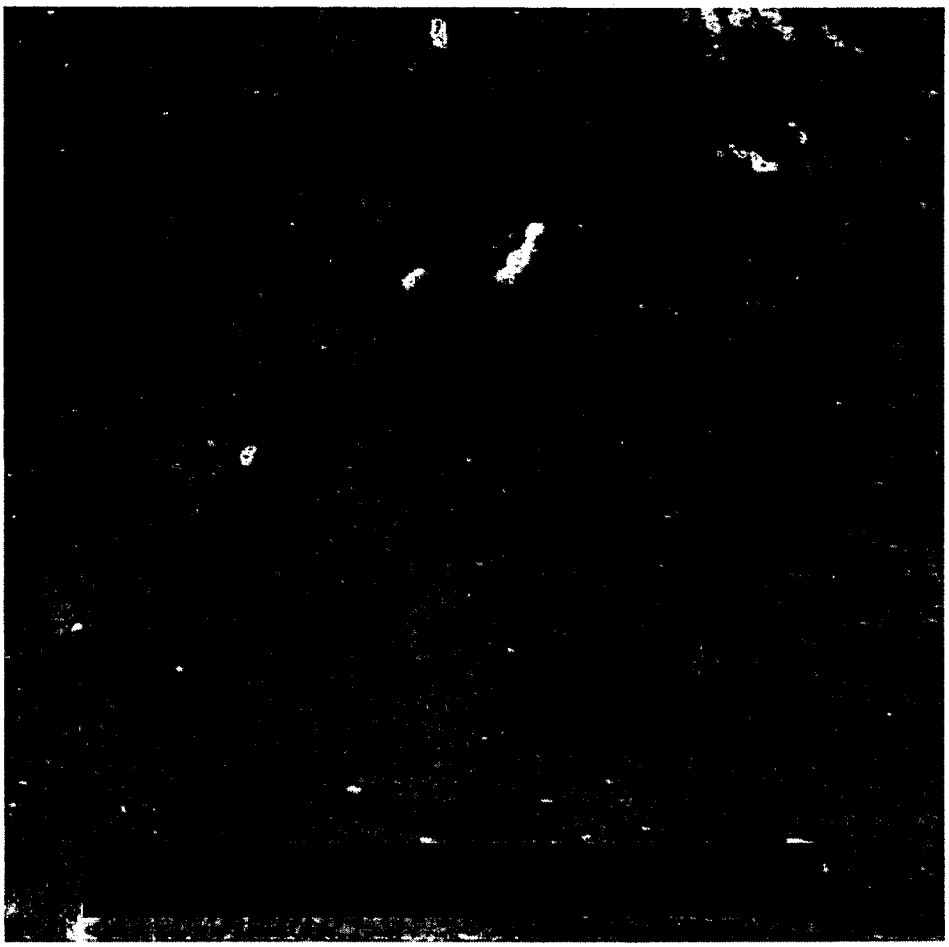

Figure (4.3.9) Micrograph for 9/1 NBR/HNBR blend (black line= 100 μm)

are miscible, and the apparent phase separation or segregated regions of one material into the other are result of mixing conditions rather than thermodynamic interactions.

Figure 4.3.10. shows the micrograph of 5/5 blend that suggests a uniform elongated layered morphology instead of emulsion morphology. The DPD simulation of this blend is shown in figure 4.3.11: which is again a homogenous and well dispersed single phase material, showing absence of any layered region hence indicating that the layered morphology is by the virtue of mixing methodology rather then phase segregation of materials as different layers. It is worth mentioning that two rubbers were ground to small size and were physically mixed before the blending process. Again the blending process can help the layers formation, as the high viscoelastic nature of elastomeric materials inhibit proper melting, and the two materials are infact "masticated" with each other after being soften at elevated temperatures by the constant rotory motion of the blades. The slight positive value of χ (less than 0.1) was far small to produce a layered morphology resulting from molecular interactions. A layered morphology could result, but with a far higher value of χ is shown in figure 4.3.12, which shows a layered system due to high value of χ, but as mentioned earlier this layered morphology was not representative of the actual system i.e the one shown in SEM picture (Figure 4.3.10). In the actual blend the layers were again a physically induced phenomenon and not chemically evolved structure.

4.3.5 CONCLUSION

In this study a combined computational approach (Atomistic and Mesoscopic) was used to investigate blend miscibility of a NBR/HNBR blend. Results were compared to

Figure (4.3.10) Micrograph for 5/5 NBR/HNBR blend (line= 10 μm)

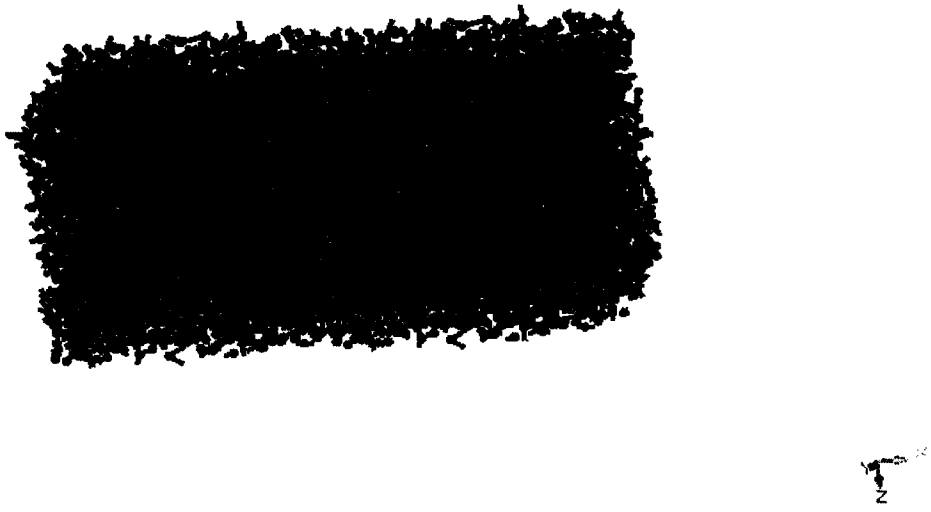

Figure (4.3.11) Morphology of 5/5 NBR/HNBR blend after DPD equiliberation

Figure (4.3.12) Morphology of 5/5 obtained with a high value of χ supplied in DPD simulation

SEM micrographs for similar physical systems. The Atomistic simulations showed that these systems are very much miscible, and to whatever small deviation (at 5/5 blend) from miscibility found, was far from causing any phase separation. Again the mesoscopic simulations showed that the apparent phase separation and layered morphology that was apparent in SEM pictures, was not essentially due to molecular interactions but due to processing conditions, and insufficient mixing to form a homogenous phase. Thermodynamically these systems were miscible and compatible, but the processing difficulties associated with the nature of these elastomers might pose problems to reach the segmental miscibility.

4.3.6 REFERENCES

[1] Gallaher, D.A, Thermal Degradation of Polymers ECAChe Group, Fujitsu,**2002**.

[2] Spyriouni, T.; Vergelati, C. Macromolecules.

[3] Bhattacharjee, S.; Bhowmick, A.; Avasthi. B.; Modification of Properties of Nitrile, "*Handbook of Engineering Polymeric Materials*", Cheremisinoff, NP, Editor, Dekker, NY, **1997**, 555-576.

[3] Sirisinha, C.; Limcharoen, S.; Thunyarittikorn, J. J Appl Polym Sci **2001**, *85*, 1232.

[4] Hertz. D, Bussem. H,; Ray. T, Nitrile Rubber-Past, Present & Future RubberDivision, American Chemical Society, October 11-14, **1994**

[5] Young, R.J,; Lovell, P.A, Introduction To Polymers 2 nd edition, Chapman & Hall, University Press, Cambridge, **1997**

[6] Sun. H, J. Phys. Chem. B **1998**, 102, 7338.

[7] R. A. Chaudhry, MS. Thesis. KFUPM, Dhahran, (2003).

Chapter 5

CONCLUSIONS AND RECOMMENDATIONS

5.1 Conclusions

An investigation of degradation and miscibility of Nitrile elastomers have been investigated in this study. Different brands of HNBR rubbers were studied for thermomechanical degradation. It was found that thermomechanical treatment does affect these rubbers in the temperature range used in this study i.e 190°C to 260°C and molecular parameters have an effect on the selection of dominating degradation mechanism. From all of the above cases, it is clear that degradation is a combination of chain scission and cross-linking. Also, it was found that a high degree of ACN content and high saturation result in increase in stability. Comparison of Z-1 and Z-3 or Z-6 and Z-7 showed that the stability of HNBRs is strongly influenced by the degree of hydrogenation. Consequently, low degrees of hydrogenation result in high extent of degradation. Relatively unsaturated HNBRs and NBR were found to degrade via cross-linking. For highly saturated HNBRs with relatively high ACN content, the Mw plays an important role. In this case, high Mw leads to degradation through chain scission. In addition, high ACN content shifts the thermomechanical degradation to higher temperatures due to the high activation energy of the C≡N group. However, the net degradation level and mechanism also depends on the level of unsaturation. In the case of low ACN and high degree of hydrogenation, degradation proceeds via chain scission (decrease in Mw). Light scattering analysis of the degraded and as received samples showed that variations in Molecular weight and

hydrodynamic radius were in accordance with results of rheology. FTIR results confirmed that carbonyl functionalities were being generated as a result of degradation and HNBR rubbers were crosslinking via C≡N site.

The miscibility investigations comprise of two studies, an experimental and a simulation. In the former study, HNBR and NBR of very similar acrylonitrile content and Mooney viscosity were blended at different compositions. The blends of the more flexible HNBR and the less flexible unsaturated NBR show interesting rheological, thermal and mechanical properties. The dynamic viscosity of the blends followed the log additivity rule, while the flow activation energy closely followed inverse a dditivity rule. On the other hand, the storage modulus showed synergistic effects at all compositions suggesting the presence of weak emulsion morphology at both ends of the composition range. This conclusion is supported by thermal analysis that showed the presence of two glass transitions, representing the pure components, at all blend ratios. For the 50/50 HNBR/NBR blend, the SEM micrographs suggest a uniform elongated structure rather than emulsion morphology. The small strain mechanical properties such as tensile modulus and yield stress followed linear additivity. However, HNBR was observed to strain harden at a rate higher than that of NBR. Induced crystallization of HNBR was suggested as a reason for the strain hardening of HNBR rich blends. In conclusion, the different rheological, thermal, and mechanical testing techniques agree in suggesting that the structurally similar HNBR and NBR are not thermodynamically miscible but mechanically compatible.

In the simulation part a combined computational approach (Atomistic and Mesoscopic) was used to investigate blend miscibility of a NBR/HNBR blends. Results

were compared to SEM micrographs for similar physical systems. The Atomistic simulations showed that these systems are very much miscible, and to whatever small deviation (at 5/5 blend) from miscibility found, was far from causing any phase separation. Again the mesoscopic simulations showed that the apparent phase separation and layered morphology that was apparent in SEM pictures, was not essentially due to molecular interactions but due to processing conditions, and insufficient mixing to form a homogenous phase. Thermodynamically these systems were miscible and compatible, but the processing difficulties associated with the nature of these elastomers might pose problems to reach the segmental miscibility.

5.2 RECOMMENDATIONS

Following are the recommendations as a follow up of this work.

1. Effect of processing parameters, such as rotor speed and processing time on degradation can be studied.

2. Effect of individual parameter (ACN, %Hyd, Mw) on miscibility of HNBR & NBR can be studied booth experimentally and through simulation.

3. Results of Atomistic simulation can be supplied to mesoscale DPD simulations, to have a visual interpretation of the simulation results.

4. Blending of these elastomers with other polymers, such as polyethylene's and polypropylene can be a promising area.

REFERENCES:

Boisserie C, Marchessault RH. J of Polymer Sci 1977; 15: 1211.

Setua DK, Soman C, Bhowmick AK, Mathur, GN. Polym Engng Sci 2002; 42: 10.

Lee JH, Lee JK, Lee KH, Lee CH. Polymer Journal 2000, 32, 321.

Coran AY, Patel R, Williams-Headd D. Rubber Chem.Technol 1985;58:1014.

Anthony P, De SK. Rubber Chem Technol 1997;*74*:376.

Clarke J, Clarke B, Freakley PK. Rubber Chem Technol 2000; 74:1.

Hofmann W. Rubber Chem Technol 1963;37:52

Schulz DN, Turner SR, Golub MA. Rubber Chem Technol 1982;55:809.

Bhattacharjee S, Bhowmick AK, Avasthi B. Modification of Properties of Nitrile, "*Handbook of Engineering Polymeric Materials*", Cheremisinoff NP, Editor. Dekker. NY; 1997.

Da Silva AN, Rocha M, Coutinho FM, Bretas R, Farah M. Polymer Testing 2002; 21: 647.

Zhu S-H, Chan C-M. Polym Engng Sci 1999; 39:1998.

Sirisinha C, Limcharoen S, Thunyarittikorn J. J Appl Polym Sci 2001; *85*:1232.

Chee MJK, Ismail J, Kummerlowe C, Kammer H. Polymer 2002; 43: 1235.

Saha S. Eur Polym J 2001; 37: 399.

Saha S. Eur Polym J 2001; 37: 2513.

Ahn SJ, Lee KH, Kim BK, Jeong HM. Appl Polym Sci 2000; 78:1861.

Chung O, Coran AY. Rubber ChemTechnol 1987;*70*:781.

Severe G, White J. J Appl Polym Sci 2000;*78*:1521.

Jha A, Bhowmick AK. Rubber Chem.Technol 1997;*70*:798.

Scholz P, Froelich D, Muller R. J Rheo 1989;33:481.

Paul DR. Polymer Blends, 2nd ed .Academic Press, New York: 2001.

Utracki LA. Polymer alloys and blends: thermodynamics and rheology. NY: Hanser; 1989.

Chaudhry RA. "Degradation of NBR and HNBR: Rheological, light scattering and Molecular Simulation Study", *MS Thesis*, KFUPM, Dhahran, January 2004.

Brown RP. *PHYSICAL TESTING OF RUBBER*, 2 nd ed. Elsevier Applied Science Publishers,NY;1986.

Hameed T, Hussein IA. Polymer 2002;43:6911.

Hussein IA. Macromolecules 2003; 36:2024. Erratum: 36:4667

Brahimi B, Ait-Kadi A, Ajji A, Jerome R, Fayt R. J Rheol 1991;35:1069.

S. Moss and H. Zweifel, *Polym Degrad Stab.* 25,217 (1989).

P. Anthony and S.K. De, Rubber Chem. Technol. 74, 376 (1997).

M. Sarkar, P. Mukunda, P. Prajna,A and Bhowmick, Rubber Chem.Technol. 70, 856 (1997).

M. Garbarczyk, W. Kuhn, J. Kilnowski and S. Jurga, *Polymer.* 43, 3169 (2002).

C. E. Ioan, T. Aberle, and W. Burchard, *Macromol.* 34, 326 (2001).

C. Boisserie and R. H. Marchessault, *j. Polym. Sci. Part(B).* 15, 1211 (1977)

A. W. Pross and R. M. Black, J. Sc of Chem Indus, 69, 113 (1950)

L. Sharma and T. Kimura, *Polym for Adv Tech*, 14, 392 (2003)

S. H. Hamid, A. G. Maadhah, F. S. Qureshi and M. B. Amin, *The Arab Journal for Sci and Engg*, 13, 503,(1988).

S. H. Hamid and W. H. Prichard, *J. Appl. Polym. Sci.* 43, 651 (1991)

G. Ivan, M. GIRGINCA and S. BASUC, Revue Roumaine de Chimie, 43,231(1998).

D. Hertz, H. Bussem and T. Ray, "Nitrile Rubber-Past, Present & Future" *Rubber Division, American Chemical Society*, October 11-14, (1994).

S. Bhattacharjee, A. K. Bhowmick and B. Avasthi. Modification of Properties of Nitrile, "*Handbook of Engineering Polymeric Materials*", Cheremisinoff, NP, Editor, Dekker, NY, 555 (1997).

M. Morton, *Rubber Technology*, 3 rd ed . Van Noestrand Reinhold Company, New York (1987).

S. Bhattacharjee, A. K. Bhowmick and B. Avasthi, *Polymer Degrad Stab*, 31,71 (1991).

S. Saha , *Eur Polym J.* 37, 2513 (2001).

D.K. Setua, A. K. Bhowmick and G. N. Mathur , *Polym Eng Sci.* 42,10 (2002).

C. Chaung and C. Han, *J Appl. Polym. Sci.* 29, 2205 (1984).

C. Ioan, T. Aberle and W. Burchard, *Macromolecules*. 34, 326 (2001).

S. H. Zhu and C. M. Chan, *Polym Eng Sci.* 39, 1998 (1999).

J. Clarke, B. Clarke and P. K. Freakley, *Rubber Chem.Technol.* 74, 1 (2000).

O. Chung and A. Y. Coran, *Rubber Chem.Technol.* 70, 781 (1987).

Sirisinha, S. Limcharoen and J. Thunyarittikorn, *J. Appl. Polym. Sci.* 85, 1232 (2001).

G. Severe and J. White, *J. Appl. Polym. Sci.* 78, 1521 (2000).

S. J. Ahn, K. H. Lee, B. K. Kim and H. M. Jeong, *J. Appl. Polym. Sci.* 78, 1861 (2000).

C. Sirisinha, S. B-Limcharoen and J. Thunyarittikorn, *J. Appl. Polym. Sci.* 87, 83 (2003).

S. Saha, *Eur Polym J.* 37, 399 (2001).

S. Schaal and A.Y. Coran, *Rubber Chem. Technol.* 73, 225 (1999).

S. Schaal and A.Y. Coran, *Rubber Chem. Technol.* 73, 240 (1999).

I. A. Hussein, K. Ho, S. Goyal, E. Karbashewski and M. Williams MC, *Polym Degrad Stab.* 68, 381 (2000).

O. Yasuda, T.Ougizawa, T.Inoue and K. Miyasaka, *j. Polym. Sci. Polym Letters Ed.* 21, 813 (1983).

VITA

Name	REHAN ANWAR CHAUDRY
Date & Place of Birth	19 August 1976, GUJRAT (PAKISTAN)
Nationality	PAKISTANI
Religion	ISLAM
Educational Qualification	B.Sc in Chemical Engineering from Institute of Chemical Engineering & Technology, Punjab University Lahore (1995-2000). M.S. in Chemical Engineering from King Fahd University of Petroleum and Minerals, Dhahran (2002-2004).